2006

INCREASED OXIDATIVE DAMAGE TO DNA AND THE EFFECTS ON MITOCHONDRIAL PROTEIN IN ALZHEIMER'S DISEASE

Jianquan Wang
University of Kentucky, jianquanwang@gmail.com

ABSTRACT OF DISSERTATION

Jianquan Wang

The Graduate School

University of Kentucky

2006

INCREASED OXIDATIVE DAMAGE TO DNA AND THE EFFECTS ON MITOCHONDRIAL PROTEIN IN ALZHEIMER'S DISEASE

ABSTRACT OF DISSERTATION

A dissertation submitted in partial fulfillment of the
requirements for the degree of Doctor of Philosophy in the
College of Arts and Sciences
at the University of Kentucky

By

Jianquan Wang

Lexington, Kentucky

Director: Dr. Mark A. Lovell, Associate Professor of Chemistry

Lexington, Kentucky

2006

ABSTRACT OF DISSERTATION

INCREASED OXIDATIVE DAMAGE TO DNA AND THE EFFECTS ON MITOCHONDRIAL PROTEIN IN ALZHEIMER'S DISEASE

Alzheimer's disease (AD) is a progressive, irreversible, neurodegenerative disease. The key to understanding AD is to elucidate the pathogenesis of neuron degeneration in specific brain regions.

We hypothesize that there is increased DNA oxidation in AD brain compared to age-matched control subjects, especially in mitochondrial DNA (mtDNA), and that the changes in DNA bases will affect protein expression in mitochondria and contribute to neurodegeneration in AD. To test this hypothesis:

1) We quantified multiple oxidized bases in nuclear DNA (nDNA) and mtDNA of frontal, parietal, and temporal lobes and cerebellum from late-stage AD (LAD), mild cognitive impairment (MCI), and age-matched control subjects using gas chromatography/mass spectrometry with selective ion monitoring (GC/MS-SIM). Also, we quantified oxidized DNA bases in cortex of APP/PS1 transgenic mice. (a) nDNA and mtDNA were extracted from eight LAD and eight control subjects. We found levels of multiple oxidized bases were significantly higher in frontal, parietal, and temporal lobes and that mtDNA had approximately 10-fold higher levels of oxidized bases than nDNA. Eight-hydroxyguanine was approximately 10-fold higher than other oxidized base adducts in both LAD and control subjects. These results suggest that oxidative damage to mtDNA may contribute to the neurodegeneration of AD. (b) Mild Cognitive Impairment (MCI), the phase between normal aging and early dementia, is a common problem in the elderly with many subjects going on to develop AD. Results from eight amnestic MCI and six control subjects suggest oxidative damage to DNA occurs in the earliest detectable phase of AD. (c) Analysis of nDNA from the cortex of four groups (3m, 6m, 9m, 12m) of APP/PS1 and wild type mice showed elevations of 8-hydroxyguanine in 12 month old APP/PS1 mice.

2) To analyze mitochondrial protein changes in LAD, 2D gels were run to separate proteins and MALDI-TOF mass spectrometry was used to identify proteins.

Five mitochondrial proteins were significantly decreased in LAD. This proteomic study provides a proteome map of mitochondria in LAD brain and an insight into the pathogenesis of neuron degeneration in Alzheimer's disease.

Key words: Alzheimer's disease, Mild Cognitive Impairment, Nuclear and mitochondrial DNA oxidation, Proteomics, Mass Spectrometry

Jianquan Wang

October 5, 2006

INCREASED OXIDATIVE DAMAGE TO DNA AND THE EFFECTS ON MITOCHONDRIAL PROTEIN IN ALZHEIMER'S DISEASE

By
Jianquan Wang

Dr. Mark A. Lovell
Director of Dissertation

Dr. Robert B. Grossman
Director of Graduate Study

October 5, 2006

RULES FOR THE USE OF DISSERTATION

Unpublished dissertation submitted for the Doctor's degree and deposited in the University of Kentucky Library are as a rule open for inspection, but are to be used only with due regard to the rights of the authors. Bibliographical references may be noted, but quotations or summaries of parts may be published with only permission of the author, and with the usual scholarly acknowledgements.

Extensive copying or publication of the dissertation in whole or in part also requires the consent of the Dean of the Graduate School of the University of Kentucky.

A library that borrows this dissertation for use by its patrons is expected to secure the signature of each user.

Name
Date

_____
_____
_____
_____
_____
_____
_____
_____
_____
_____
_____
_____
_____
_____
_____
_____
_____
_____
_____
_____
_____
_____
_____
_____

DISSERTATION

Jianquan Wang

The Graduate School

University of Kentucky

2006

INCREASED OXIDATIVE DAMAGE TO DNA AND THE EFFECTS ON MITOCHONDRIAL PROTEIN IN ALZHEIMER'S DISEASE

DISSERTATION

A dissertation submitted in partial fulfillment of the
requirements for the degree of Doctor of Philosophy in the
College of Arts and Sciences
at the University of Kentucky

By

Jianquan Wang

Lexington, Kentucky

Director: Dr. Mark A. Lovell, Associate Professor of Chemistry

Lexington, Kentucky

2006

ACKNOWLEDGEMENTS

I would like to acknowledge many people sincerely for helping and supporting me during my doctoral research. Thanks and appreciation especially go to my advisor, Dr. Mark A Lovell, who has helped me on every step: financial support, scientific thinking, speaking, and writing. The inspiration for doing my research is that Dr. Lovell provided me an outstanding research environment and excellent program. I could not count how many times he revised my paper and dissertation drafts to better my work.

I am very grateful for having this exceptional committee, Dr. Steve Estus, Dr. Bert Lynn, and Dr. Edward DeMoll, and wish to thank them for their support and contribution. I appreciate the opportunity to operate mass spectrometries Dr. Lynn has provided.

I would like to extend many thanks to Dr. William Markesbery, Director of Sander-Brown Center on Aging, who provided excellent human tissue for my research. Also many thanks go to Dr. Daret K St Clair, who provided transgenic mice for my animal studies.

My thanks also must go to my colleagues and friends: Shuling Xiong, Chengsong Xie, Jennifer Smith, Changxing Shao, etc, who have helped me over the years.

Finally, I would like to thank my family for their encouragement, enthusiasm, and constant support.

TABLE OF CONTENTS

LIST OF TABLES

LIST OF FIGURES

LIST OF FILES

jwangETD.pdf 3,502 KB

CHAPTER ONE
Introduction

1.1 Alzheimer's disease

1.1.1 Overview of Alzheimer's disease

Alzheimer's disease (AD) is a progressive, irreversible, neurodegenerative disorder. In 1907, Alois Alzheimer, a German psychiatrist and neuropathologist, published a paper that described a 51-year-old woman with a 4 ½ year course of progressive dementia which subsequently bears his name (Alzheimer 1907). The patient died in a completely demented state. Autopsy revealed an atrophic brain with cortical neuron loss and the presence of silver-positive intracellular tangled bundles of fibers (now called neurofibrillary tangles (NFTs)) and extracellular deposits (now called senile plaques (SPs)), two main hallmark pathological features of AD.

AD is the most common form of dementia in the elderly. Current data suggest AD affects 4-5 million people in the US and 20-30 million people worldwide with a prevalence of 3% for the persons 65-74 years old, 18.8% for those 75-84 years old, and 47.2% for those over 85 years old (Katzman 1976; Markesbery and Carney 1999; Martin 1999). Without efficient preventative methods, it is estimated that by 2050 ~45 million individuals worldwide could develop this disorder with increasing life span (NIA 1995; Selkoe and Schenk 2003).

1.1.2 Clinical characteristics of AD

AD is characterized by memory loss, behavior changes, and impaired cognitive ability. At the very early stage, the only symptom is mild forgetfulness. Patients can not recall the names of recent activities or events. Most people with mild forgetfulness likely do not develop AD. It is easily confused with normal aging forgetfulness, which is not progressive (Sclan and Kanowski 2001). As the disease goes on, progressive worsening of memory is more noticeable. AD patients have trouble learning, speaking or thinking, and cannot carry out daily activities, such as combing their hair, brushing their

teeth, or recognizing familiar people around them. At later stages of AD, patients can become aggressive or wander away from home (Selkoe and Schenk 2003).

1.1.3 Pathological features in AD

Two hallmark pathological features of AD are the presence of neurofibrillary tangles (Figure 1-1) and senile plaques (Figure 1-2). NFTs are intracellular and are composed of paired helical filaments (PHF), which consist of hyperphosphorylated tau, a neuron-specific phosphoprotein that is the major constituent of neuronal microtubules and predominantly located in the axon (Trojanowski and Lee 1995). NFTs are generally present in neurons of the cerebral cortex and are mainly found in temporal lobe structures of the AD brain, such as hippocampus and amygadala (Pappolla et al. 1992; Wang et al. 2006).

Senile plaques are extracellular deposits composed of β–amyloid (Aβ) polypeptides (39 to mainly 42 amino acids) derived from the amyloid precursor protein (APP), a transmembrane glycoprotein precursor, synthesized in endoplasmic reticulum, and transferred to secretory vesicles and cell surface through Golgi apparatus (Weidemann et al. 1989). APP is cleaved by β-secretase to release N- terminal Aβ-42. γ-secretase cleaves APP to release the C- terminal of Aβ-42. Due to the different cleavage sites of β-secretase, Aβ-40 is also produced (Citron et al. 1996). These peptides aggregate easily and form plaques. Traces of transition metals, such as copper, zinc, and iron, may accelerate this aggregation (Lovell et al. 1998). However, Aβ-40 is more soluble and less neurotoxic than Aβ-42. Numerous studies show that Aβ-42 may play an important role in the pathogenesis of AD (Citron et al. 1996; Selkoe and Schenk 2003). Senile plaques are present in the brain in normal aging and Alzheimer's disease, although the AD brain has higher numbers of senile plaques compared to normal aging.

Besides NFTs and SPs, synapse loss and neuron dysfunction occur in AD. Histological examination of AD brain shows pyramidal neuron loss in the hippocampus, which may be caused by accumulated amyloid plaques (DeKosky and Scheff 1990; Scheff and Price 1993; Kril et al. 2002; Kril et al. 2004; Schmitz et al. 2004; Simard et al. 2006). Pyramidal neurons are the primary cell type in cortex and hippocampus.

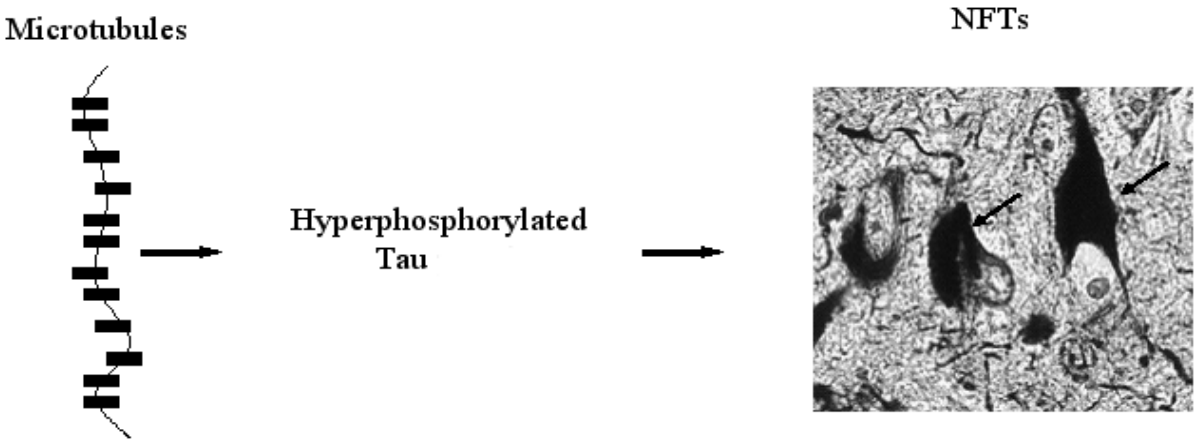

Figure 1-1. Schematic of the formation of neurofibrillary tangles in neuron

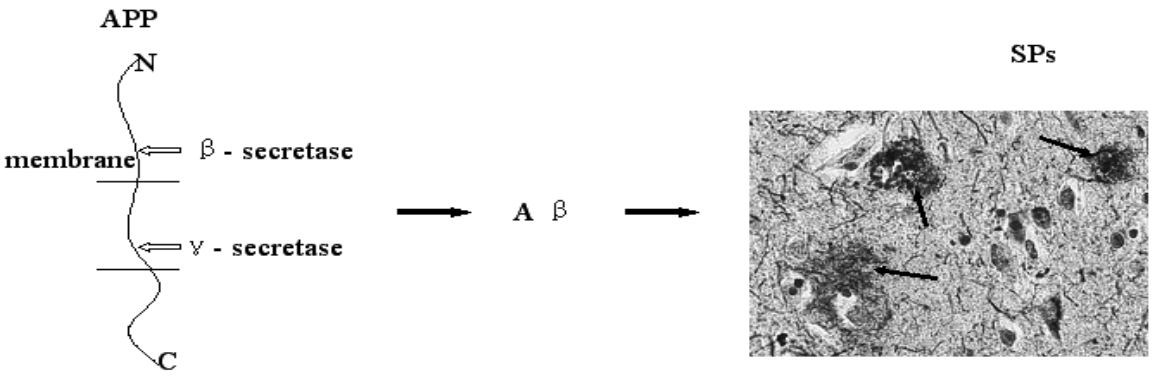

Figure 1-2. Formation of senile plaques from cleavage of APP by β and γ−secretases

Pyramidal neurons are composed of a pyramid-shaped cell body, a tree-like dendrite, and axons. In addition, glia function as supporting cells in CNS. Previous studies show more than half of large pyramidal neurons are damaged in the late stage AD in prefrontal cortex and hippocampal CA1 region (West et al. 1994; Gomez-Isla et al. 1997; Bussiere et al. 2003).

1.1.4 Risk factors of AD

The cause of AD is not fully understood. It probably is not a single cause, but a consequence of several factors. These risk factors may interact with each other and affect each person differently. Age is the most well known factor in AD. The number of people with AD doubles every five years beyond age 65 (Evans et al. 1989; Floyd 1999).

Genetic factors (Henderson 1986), education, diet, environment (Zhang et al. 1990; Zawia and Basha 2005), and head injury (Heyman et al. 1984; French et al. 1985; Sullivan et al. 1987; Borenstein et al. 2006) also play important roles in the development of AD. Early-onset familial AD (FAD), a rare form of AD that usually occurs before age 60, is associated with several genetic mutations, including mutations of APP, Presenilin 1 (PS1) and Presenilin 2 (PS2) (Hardy 1997). Presenilins are transmembrane proteins with six to nine transmembrane domains (Sherrington et al. 1995; Li and Greenwald 1996). Studies show that PS1 and PS2 mutations alter APP processing in favor of Aβ production (Borchelt et al. 1996; Scheuner et al. 1996). Presenilins are also substrates for a caspase-3 family, and mutations in presenilins may make cells vulnerable to apoptotic cell death (Kim et al. 1997; De Strooper et al. 1998).

However, the more common form of AD known as late-onset accounts for 90-95% of total AD cases (Harman 2006). Apolipoprotein ε4 (ApoE4) is the only risk gene identified so far for late-onset AD (Travis 1993; Markesbery 1997; Selkoe 1999). ApoE is encoded by a gene on chromosome 19 and has three isoforms: ε2, ε3, and ε4. The risk of AD increases three fold with one ε4 allele and eight fold with two ε4 alleles compared to non-Apo ε4 carriers (Strittmatter et al. 1993; Evans et al. 1997).

1.2 Mild Cognitive Impairment

Recent emphasis in adult dementing disorders is on early detection with the hope of early treatment to slow disease progression. Mild Cognitive Impairment (MCI) is generally considered to be the transitional zone between normal aging and early dementing disorders, especially AD (DeCarli et al. 2001; DeCarli 2003; Wolf et al. 2004). In general, most MCI subjects eventually convert to AD or other dementias with ~15% of MCI subjects converting to AD per year (DeCarli 2003). Several studies of MCI show elevated levels of tau (Okamura et al. 2002), Aβ (Andreasen et al. 1999), and isoprostanes (Pratico et al. 2002) in ventricular cerebrospinal fluid (CSF), and more recently significant elevations of DNA damage in peripheral leukocytes of MCI and AD (Migliore et al. 2005). Additionally, several gene mutations associated with AD have been observed in subjects with MCI including mutations in apolipoprotein E, PS1, and APP (de Leon et al. 2001; Traykov et al. 2002; Lopez et al. 2003; Nacmias et al. 2004).

1.3 APP/PS1 transgenic mice

Although the majority of AD cases are sporadic, ~ 5% of cases, are linked to specific mutant genes that encode the amyloid precursor protein (APP) or the presenilins (PS1 or PS2) (Selkoe 2001; Selkoe and Schenk 2003; Esposito et al. 2004).

APP is encoded by a gene on chromosome 21, which can be cleaved by β- and γ-secretases to produce amyloid-β peptides (Aβ) mainly containing Aβ40 and Aβ42 (Haass and Selkoe 1993; Xu et al. 1997; Storey and Cappai 1999). Studies show that Aβ42 aggregates faster than Aβ40 and is more toxic to cultured neurons (Pike et al. 1993; Roher et al. 1993; Watt et al. 1994; Lemere et al. 1996; Lovell et al. 1999b; Lovell et al. 2003). Why Aβ is neurotoxic is not clear. The possible reason is that Aβ may lead to the production of free radicals which result the oxidation of protein, lipid, and DNA (Loo et al. 1993; Hensley et al. 1994; Watt et al. 1994).

PS1 and PS2 are encoded by genes on chromosomes 14 and 1 respectively. More than 50 mutations have been identified in PS1 gene, much more than those of in PS2 (Hardy 1997; Cruts et al. 1998). Studies show increased Aβ42 production in PS1 transgenic mice (Duff et al. 1996). APP/PS1 mice have higher levels of Aβ42 compared to single transgenic mice (Blanchard et al. 2003; Wirths et al. 2006).

The amyloid cascade hypothesis suggests that Aβ processing and aggregation may contribute to the pathogenesis of AD. Transgenic mouse models offer opportunities to investigate the molecular mechanisms of Aβ production. APP transgenic mice show early-onset deposition of Aβ in neocortex and hippocampus by 12 month of age (Games et al. 1995; Hsiao et al. 1996; Chishti et al. 2001). Water maze tasks showed increased age-related memory deficit in APP mice. Also, these mice show electrophysical pathology and functional disruption in cortex and hippocampus (Hsiao et al. 1996; Chapman et al. 1999; Stern et al. 2004). In the mouse model coexpressing APP and PS1, the deposition of senile plaques is accelerated at early ages by 12 month of age and the ratio of Aβ42/ Aβ40 was increased in brain (Borchelt et al. 1997; Holcomb et al. 1998; Wengenack et al. 2000). Mutations in presenilins may accelerate the Aβ42 production by altering APP processing (Duff et al. 1996).

1.4 Oxidative stress and AD

1.4.1 Free radical theory of aging

Current evidence indicates that oxidative stress is associated with aging. In 1956, Denham Harman proposed the free radical theory of aging. It says that aging is due to the cumulative damage from free radical mediated reactions. Reactive oxygen species (ROS) are the byproducts of enzymatic redox chemistry. Traces of metal ions may catalyze these reactions (Harman 1973; Smith et al. 2000a; Smith et al. 2000b; Harman 2003).

1.4.2 Mitochondria – power house of cells and source of ROS

Mitochondria are considered the "power house" of cells (Boyer et al. 1954), and are composed of an outer membrane, inner membrane, and matrix (Figure 1-3). ATP (adenosine triphosphate) is produced at the inner membrane through coupling of oxidative phosphorylation with respiration (Boyer et al. 1954; Mitchell 1961). Five enzyme complexes are involved in respiratory chain during energy production. While the enzymes transfer electrons to oxygen in the final step, they pump protons out of the inner membrane, establishing a proton gradient. It is this pH gradient that provides energy to

drive ATP synthesis from ADP and inorganic phosphate (Boyer et al. 1954; Mitchell 1961; Wallace 1999; Jaroszewski et al. 2000; Stock et al. 2000; Eckert et al. 2003).

Mitochondria are then considered a "free radical factory" of the cell because of potential electron leakage from the electron transport chain. Free radicals are atoms or molecules with at least one unpaired electron in the outer shell and are chemically very active (Sampson et al. 1998). In biological systems, free radicals mainly include reactive oxygen species (ROS) and reactive nitrogen species (RNS) (Halfpenny and Robinson 1952; Smith et al. 1998). Oxidative phosphorylation is the major endogenous source of ROS. During respiration, ~2% of the total oxygen consumed by the cell is converted into superoxide radical $O_2^{\cdot -}$ by leaked electrons. Cellular protective enzymes against oxidative stress include Cu/Zn and Mn superoxide dismutases (SOD) that convert superoxide radical to hydrogen peroxide (H_2O_2) , which is either reduced to water or more active hydroxyl radical $^{\cdot}OH$ in the presence of trace metals through the Fenton or Haber-Weiss reaction (Figure 1-4) (Fenton 1894; Harbor and Weiss 1934).

Hydroxyl radicals plus H_2O_2 and singlet oxygen are the ROS we usually talk about. Iron may play an important role in catalyzing and propagating these reactions (Fenton 1894; Harbor and Weiss 1934; Xie et al. 1996; Lyras et al. 1997). Studies have indicated that there is increased iron in AD brain compared to controls (Ehmann et al. 1986). Another potential oxidant is nitric oxide (NO) which is produced in biological reactions from the oxidation of L-arginine. By itself, NO is not very active, although it can react with superoxide radical to from peroxynitrite ONOO-, a very reactive oxidant that can oxidize DNA, protein and lipids (Marletta 1993; Hurshman and Marletta 2002).

Oxidative stress refers to the status when free radicals and their damaged products are beyond the ability of repair systems (Kish et al. 1986; Imlay and Linn 1988; Beyer et al. 1991). Mitochondria are the major source of endogenous free radicals in cells and their DNA and protein may be more easily oxidized than nuclear DNA and protein (Wallace 1992; Ames et al. 1993; Mecocci et al. 1993). Oxidative stress can decrease the mitochondrial membrane potential, which induces cell death through apoptosis (Wadia et al. 1998). Mitochondrial DNA (mtDNA) tends to have higher mutation rates than nuclear DNA (nDNA) because of the lack of histone protection and limited repair mechanisms

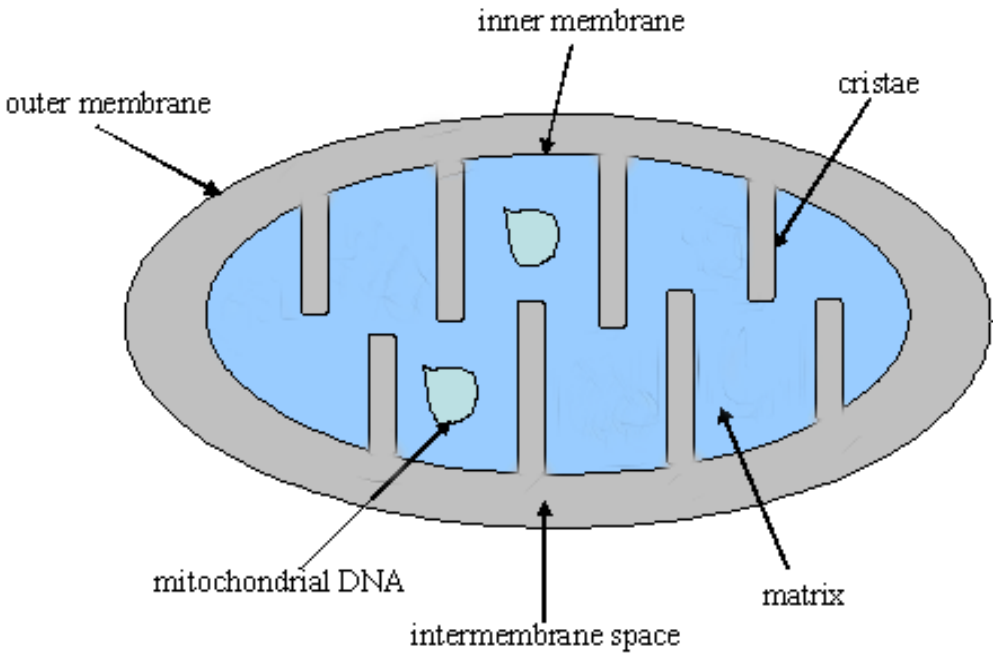

Figure 1-3. Diagram of a mitochondrion. Mitochondria are composed of an outer membrane, inner membrane, and matrix.

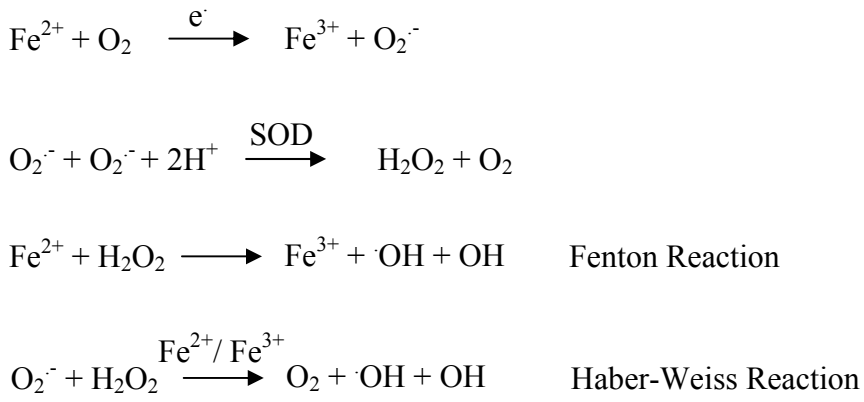

Figure 1-4. Production of reactive oxygen species through Fenton and Haber-Weiss reactions

(Wallace 1992; Ames et al. 1993; Lovell et al. 2000b; Hashiguchi et al. 2004; Stuart et al. 2005). Mutations of mtDNA could cause functional consequences because mtDNA has no noncoding sequences (Wallace 1992). Studies show that there is more than 10 times the damage in mtDNA than is observed in nuclear DNA (Richter et al. 1988; Wang et al. 2005; Wang et al. 2006).

1.4.3 Oxidative stress and AD – protein oxidation and lipid peroxidation

Several lines of evidence indicate that oxidative damage plays an important role in the pathogenesis in AD. Protein oxidation may affect neuron function by damaging enzymes that are critical to neuron metabolism (Smith et al. 1991; Hensley et al. 1995; Poon et al. 2004; Chen et al. 2005). Protein carbonyls have been used to measure damaged protein (Gutteridge and Wilkins 1983; Smith et al. 1991; Youngman et al. 1992). Previous studies show that protein carbonyls are increased in frontal lobe, hippocampus, and parietal lobe in AD compared to control subjects (Smith et al. 1991; Hensley et al. 1995). Studies show that nitrotyrosine is present in NFT in AD brain (Smith et al. 1997).

Lipid peroxidation can cause structural membrane damage leading to cell death and produce secondary bioreactive aldehydes, such as 4-hydroxy-2-nonenal (HNE) and acrolein (Benedetti et al. 1980; Benedetti et al. 1986; Lovell et al. 1997; Bruce-Keller et al. 1998; Markesbery and Lovell 1998; Lovell et al. 2000a, 2001). These two chemicals may form adducts with DNA and protein, which can modify their normal functions. They are both increased in the AD brain and are toxic to cultured neurons (Lovell et al. 1997; Lovell et al. 2000a, 2001). Additionally, HNE is shown to be elevated in cerebrospinal fluid (CSF) of AD subjects (Lovell et al. 1997). Studies also show that the concentration of isoprostanes in the CSF of AD subjects is higher than in the controls (Montine et al. 1998; Musiek et al. 2004). Isoprostanes, a measure of lipid peroxidation, are produced by non-enzymatic, free radical-catalyzed peroxidation from arachidonic acid (Morrow et al. 1992a; Morrow et al. 1992b; Milne et al. 2005).

Studies of antioxidants in AD show varied results. Several studies have shown increased enzyme activities including Catalase, SOD, GSH-Px and GSSG-R, which suggested that elevated enzyme activities reflect a compensatory response to increased

ROS species (Lovell et al. 1995). Some studies show that there is no significant difference or reduced enzyme activity in AD brain (Richardson 1993; Marcus et al. 1998). These inconsistent results suggest that the neuron death in AD brain may not be due to the damages of antioxidant enzymes.

1.4.4 Oxidative stress and AD – DNA oxidation

ROS, especially hydroxyl radicals, can attack DNA bases, leading to more than 20 oxidized base adducts (Steenken 1989a; Cooke et al. 2003). As a consequence of oxidation, DNA may have strand breaks, DNA-DNA and DNA-protein crosslinking, and base modification (Davies 1995; Crawford et al. 2002). Oxidized DNA also may lead to cell death by changing protein expression.

Several biomarkers of DNA damage have been quantified, including 8-hydroxy-2'-deoxyguanosine (8-OHdG), the most useful of several damaged bases (Mecocci et al. 1993; Mecocci et al. 1994; Gabbita et al. 1998; Lovell et al. 1999a). Previous studies show that there is more 8-OHdG in mtDNA than in nuclear DNA and there is a significant increase in aged subjects compared to younger subjects.

The first step in DNA oxidation is to add hydroxyl radical to the double bond of bases. The addition of $^{\cdot}OH$ to the C5-C6 double bond of pyrimidine results in C5-OH or C6-OH adducts (Steenken 1989b, c). The products following these two adducts depend on the absence or presence of oxygen. For purines, the hydroxyl radical is added to C4, C5, or C8 to form the purine-OH radicals. Among them, C8 is the most probable addition position. For guanine-C4 adducts, the elimination of a hydroxyl group leads to the guanine radical cation, which can react with 2'-deoxyribose in DNA causing DNA strand breaks (Steenken 1989c). The guanine-C8 adducts can produce 8-hydoxyguanine with one electron oxidation and produce 2, 6-diamino-4-hydoxy-5-formamidopyrimidine (fapyguanine) with one electron reduction following the ring opening (Steenken 1989c; Dizdaroglu et al. 2002) (Figure 1-6). There are more than 20 damaged bases already described (Cooke et al. 2003). 8-hydroxyguanine has ~1% chance to mispair with adenine resulting in G→T substitution (Cheng et al. 1992). Previous studies show increased levels of some oxidized bases in certain AD brain regions (Lyras et al. 1997;

Gabbita et al. 1998). In our study, we are interested in the following six oxidized DNA bases because they show higher levels compared to other DNA adducts. They are 8-hydroxyguanine, fapyguanine, 8-hydroxyadenine, 4,6-diamino-5-formamidopyrimidine (fapyadenine), 5-hydroxycytosine, and 5-hydroxyuracil (Figure 1-5). The detailed mechanism of the production of these six oxidized bases is shown in Figure 1-6.

1.5 Methods to quantify DNA oxidation

1.5.1 Commonly used methods to detect DNA adducts

Oxidized DNA bases can be measured by various analytical methods. The two most commonly used methods are high-performance liquid chromatography with electrochemical detection (HPLC/ECD), and gas chromatography / mass spectrometry with selective ion monitoring (GC/MS-SIM) (Dizdaroglu et al. 2002). In HPLC/ECD, DNA is enzymically digested into 2'-deoxyribonucleosides before HPLC analysis, while for GC/MS-SIM, acidic hydrolysis is carried out to yield intact and damaged bases that are further derivatized (Herbert et al. 1996; Collins et al. 1997). Artifactual oxidation of DNA bases could be induced during derivatization for GC/MS. Unlike acidic hydrolysis, enzymic hydrolysis only cleaves the damaged nucleosides from DNA backbone. Enzymic hydrolysis method does not induce artifact in the analysis (Dizdaroglu 1998). However, HPLC/ECD can not provide spectroscopic support for structural identification of adducts. Studies also show that acid hydrolysis does not cause any artifacts once the DNA sample is processed under proper experimental conditions (Dizdaroglu 1998). Because enzymes are significantly more costly than formic acid and take a longer time, acid hydrolysis can replace enzymic digestion.

Liquid chromatography / mass spectrometry (LC/MS) and liquid chromatography /tandem mass spectrometry (LC/MS/MS) are also used to quantify DNA adducts (Serrano et al. 1996; Ravanat et al. 1998; Jaruga et al. 2002; Liu et al. 2005; Van den Driessche et al. 2005). However, LC/MS and LC/MS/MS are less sensitive compared to GC/MS-SIM (Dizdaroglu et al. 2002; Jaruga et al. 2002). The sensitivity of GC/MS-SIM is 1-2 fmol for 8-hydroxyguanosine, whereas the sensitivity of LC/MS is ~30 fmol and LC/MS/MS is 10-20 fmol (Dizdaroglu et al. 2001; Jaruga et al. 2002). Because of the

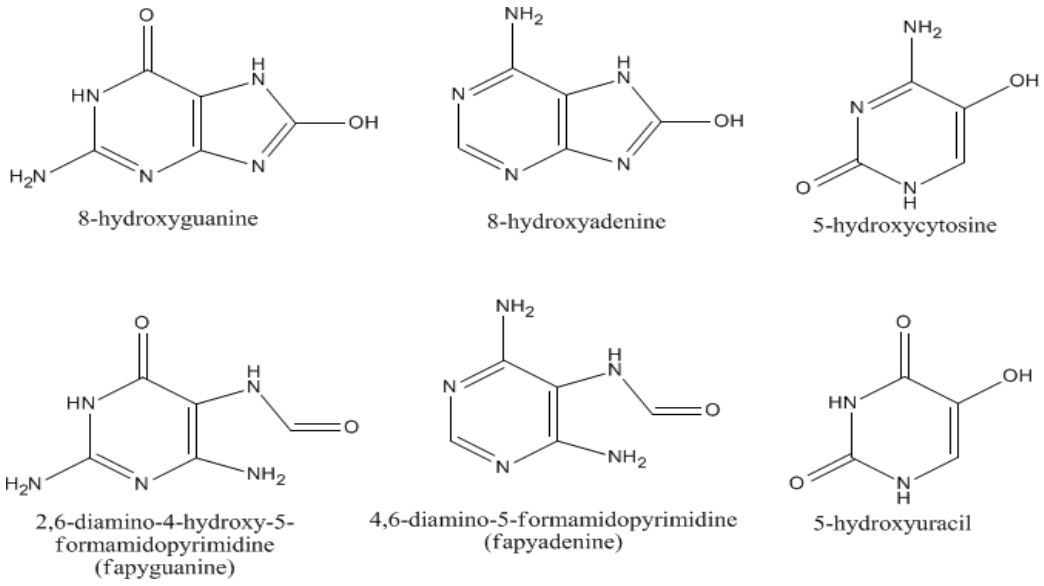

Figure 1-5. Structures of oxidized DNA bases in our study

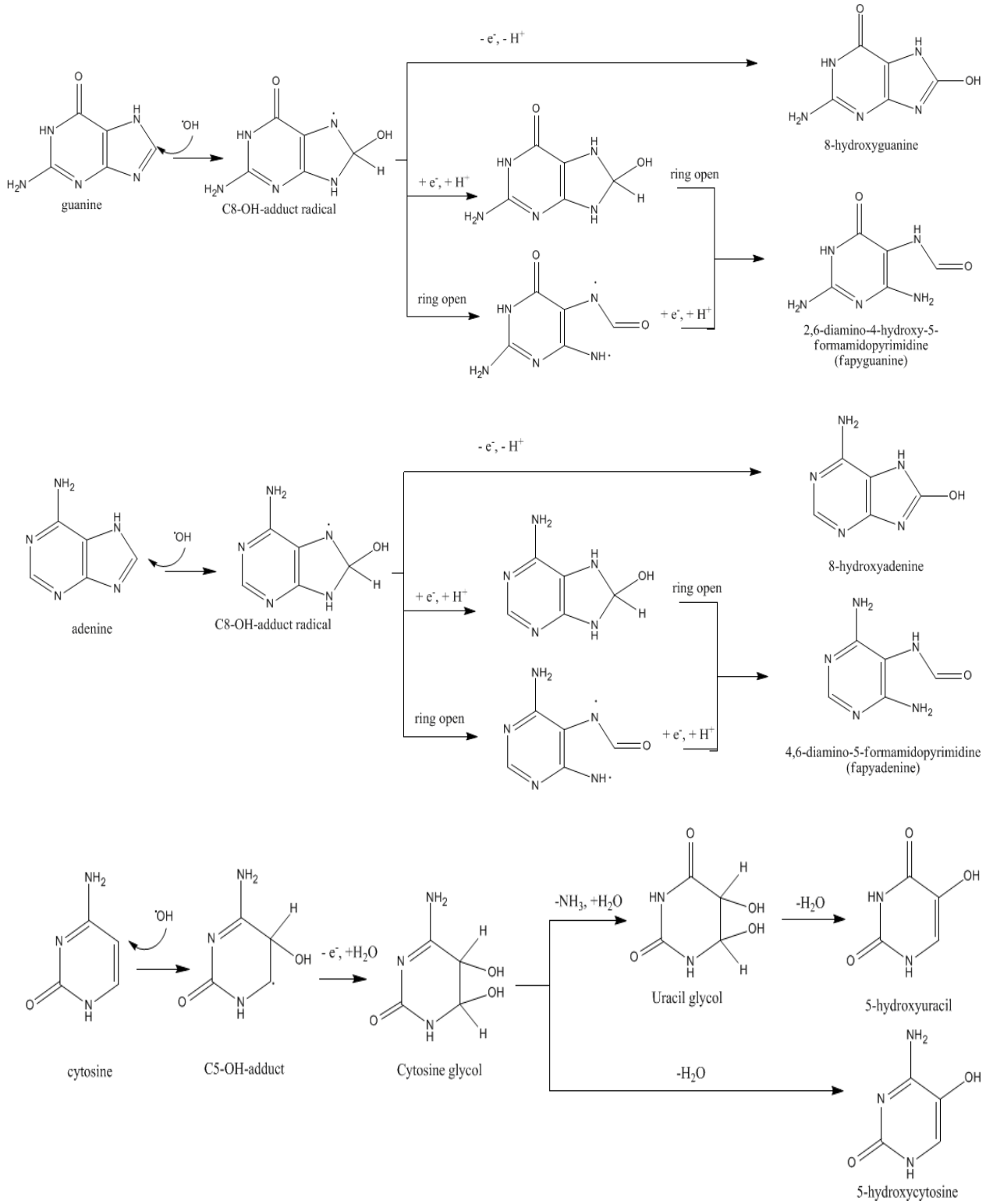

Figure 1-6. Formation of oxidized bases from guanine, adenine, and cytosine

high sensitivity of GC/MS-SIM, this method needs less DNA for analysis. GC/MS-SIM can provide accurate quantification and identification with high selectivity and sensitivity. Using GC/MS, hydrolysates after formic acid are derivatized with silylating reagents containing trimethylsilyl (TMS) groups, such as *N*,*O*-Bis(trimethylsilyl)acetamide (BSA) and *N*,*O*-Bis(trimethylsilyl)trifluoroacetamide (BSTFA). During derivatization, TMS groups will replace the H- in OH, NH, and SH groups. The derivatives are generally less polar, more volatile, and more thermally stable (Halliwell and Dizdaroglu 1992). In selective ion monitoring mode, GC/MS can analyze a wide range of bases in a single run with high sensitivity and selectivity of detection (Halliwell and Dizdaroglu 1992; Dizdaroglu et al. 2002). Stable isotope-labeled internal standards with the exact same chemical and physical properties as analytes are used for quantification of the damaged bases based on the ratio of the peak areas of base adducts versus internal standards.

1.5.2 Principles of GC/MS

GC/MS is one of the most commonly used techniques to analyze volatile organic chemicals. GC/MS is composed of a component for chemical mixture separation (gas chromatograph), a sensitive and qualitative detector (mass spectrometer), and a data collection system (Figure 1-7) (Santos and Galceran 2003). The carrier gas, such as nitrogen, helium, or hydrogen, must be chemically inert to analytes (Parcher 1983; Blumberg 1997). The choice of carrier gas depends on the detector and analytes. In order to shorten analysis time, hydrogen or helium is usually used because of their low viscosity. The carrier gas must be highly pure in order to reduce deterioration of the stationary phase and to limit potential contamination. A constant flow of carrier gas is always desirable to get a constant retention time.

For optimum efficiency and high resolution, a microsyringe is commonly used to inject microliter samples through a rubber septum into a heated chamber with a higher temperature by 20°C to 40°C than column. Once the sample is introduced, it is vaporized rapidly and swept into the column by the carrier gas (Schomburg et al. 1981; Lieshout et al. 1998). For capillary GC, split or splitless injections are used. In the split mode, most of the sample exits with most of the sample lost through the split cutlet. Split ratios vary from 10:1 to 500:1 (Bayer 1986). Because most of the sample in the split injection mode

is wasted, it is generally not suitable for ultra-trace analysis. In the splitless mode, the residence time of sample in the injection port is longer because of the relatively larger sample volume and the lower velocity of carrier gas compared to split injection (Schomburg et al. 1981; Matovská and Lehotay 2003).

Packed or capillary (open tubular) columns are usually used, while capillary columns are more efficient (Grob 1982; Gübitz and Schmid 2000). Column tubing must be chemically inert and thermally stable. Fused silica open tubular column is a new type of wall coated capillary column with much thinner walls than the other glass capillary columns, and provides high sensitivity and reproducibility. The polyimide coating makes the fused silica columns flexible and inert. However, micro cracks might occur in the fused silica because of the differences in thermal expansion of silica and aluminum coating (Michalske and Freiman 1982). Usually, efficiency increases but sample capacity decreases as the internal diameter or film thickness decreases. Column length is another factor that affects resolution. Longer columns improve resolution but increase analysis time (Ettre and March 1974; Matovská and Lehotay 2003).

Temperature control on columns is very important for good reproducibility. Retention time increases as column temperature decreases. In order to get good separation, a temperature slightly above the boiling points of analytes is used for analysis. For the samples with a wide range of boiling points, a temperature program is usually used to avoid poor resolution or long analysis time caused by isothermal analysis (Lieshout et al. 1998).

GC detectors are classified into two categories. One is concentration-sensitive and independent of mass flow of analytes, such as thermal conductivity detectors (TCD) and electron capture detectors (ECD). The other type is a mass-sensitive detector, such as MS and flame ionization detector (FID) (Halász 1964). Once separated analytes flow through the interface between the GC and the MS, they enter the ionization chamber of MS. The interface is maintained at high vacuum ($< 10^{-2}$ Pa) so that no molecular reactions occur. In the MS, electron impact or chemical ionization is used for ion production. Molecular ions (M+) are separated based on different mass/charge ratios by mass analyzer, such as quadrupole analyzer, ion trap， etc. Because of the high sensitivity, a quadrupole analyzer is generally used in GC/MS. The peaks are recorded

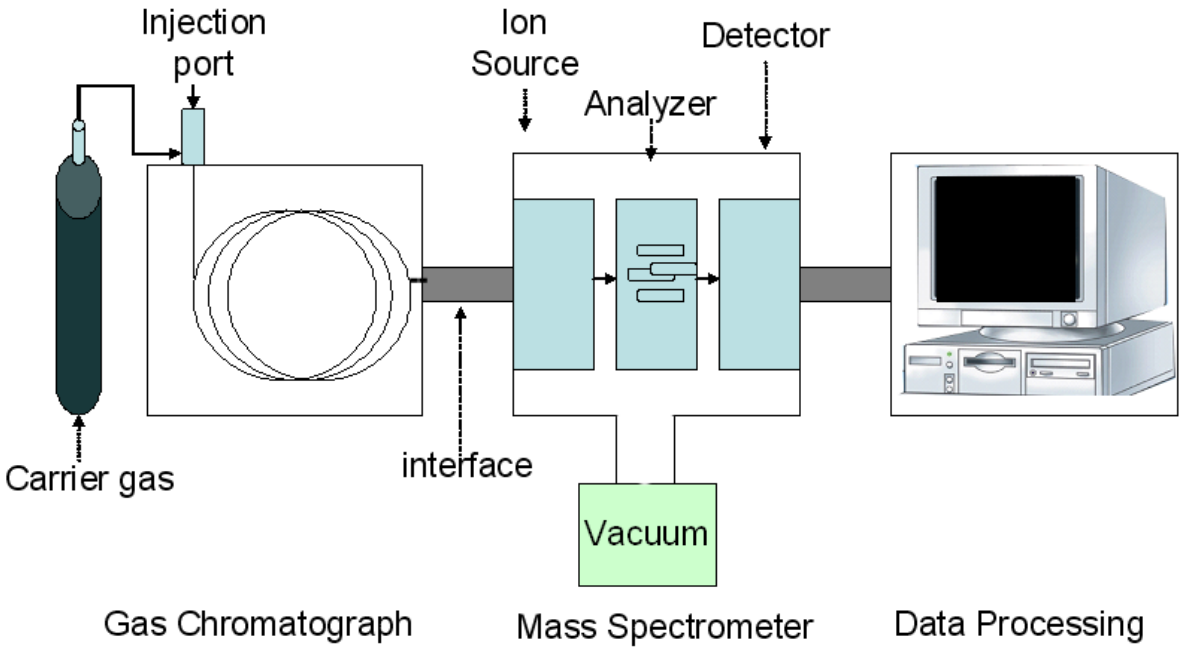

Figure 1-7. Diagram of gas chromatography – mass spectrometry

by a detector and a computer processes the data and converts the electrical signal into a spectrum. The mass spectrum indicates the peaks of molecular ion and other fragments, and the abundances of these ions (Matovská and Lehotay 2003).

Mass spectrometers may be operated in various scanning modes, including full scan and selected ion monitoring (SIM). Analysis in the full scan mode monitors all ions over the full cycle. However, sometimes, only a few selected ions are of interest in an analysis. SIM is used in this case with a higher sensitivity compared to full scan mode, because the selected ions are monitored for a greater portion of the scan time. Detection limits decrease as the number of ions increases (Vékey 2001).

1.6 Proteomics

1.6.1 Background of proteomics

The proteome, the basic sum of "protein" and "genome", is used to describe the entire complement of proteins in a biological system (Wasinger et al. 1995). Proteomics is the field involved with the characterization, quantification, and identification of global proteins in cells, tissue, or organism (Wasinger et al. 1995; Anderson and Anderson 1996; Wilkins et al. 1996; Peng and Gygi 2001; Pedersen et al. 2003). Proteomics was introduced in the 1970s with two dimensional (2D) electrophoresis (O'Farrell 1975; Scheele 1975). Although many proteins were separated at that time, they could not be fully identified because of the limited sequencing techniques. Edman degradation, a method of sequencing amino acids in a small peptide for identification of protein, was a big breakthrough in protein sequencing (Edman 1949). The first protein mapping database was established in 1987 with the methods of 2D electrophoresis and Edman degradation (Celis et al. 1987). However, Edman degradation is low-throughout process and can not sequence peptides over 50-60 residues. One milestone in proteomics was the introduction of mass spectrometry into the analysis of biological molecules, which provides an accurate, sensitive, and high throughput method for protein identification (Andersen and Mann 2000; Pandey and Mann 2000).

1.6.2 Synthesis of mitochondrial proteins

The human mitochondrial genome is much smaller (16.6 kbp) than the nuclear genome (3.3 billion bp). mtDNA encode 13 subunits of complexes involved in oxidative phosphorylation (Wallace 1999) and the necessary RNA machinery (2 rRNAs and 22 tRNAs) (Taylor and Turnbull 2005). The remaining mitochondrial proteins are encoded by nuclear DNA, synthesized at cytoplasmic ribosomes, and transported into the mitochondrial matrix (Figure 1-8). Mitochondrial protein precursors with an N- terminal extension as a targeting signal are recognized by a receptor on the mitochondrial surface. The cleavable signal normally consists of a ~20-60 amino acids residue and an intramitochondrial sorting signal (von Heijne et al. 1989). These precursor proteins are transported by Translocase complexes in the Outer and Inner Membrane (TOM and TIM) (Pfanner et al. 1996). Electrochemical potential and ATP hydrolysis are required during the translocation through membranes (Schleyer et al. 1982; Horst et al. 1997). Then the presequence signal is cleaved off by mitochondrial processing peptidase (MPP) localized in matrix (Schatz 1996; Gakh et al. 2002). This non-native protein is refolded in the matrix and becomes functional in mitochondrial matrix. Unlike proteins in matrix, most outer membrane proteins and carriers proteins on inner membrane do not have a cleavable signal.

1.6.3 Protein separation and isolation

The most efficient way to separate a protein mixture is polyacrylamide gel electrophoresis. In one dimensional electrophoresis, protein mixtures are separated based on molecular weight after denaturation in sodium dodecyl sulfate (SDS). SDS makes proteins negatively charged and run in the electric field in a polyacrylamide gel (Laemmli 1970).

For a whole cell lysate or a very complex protein mixture, 2D electrophoresis is generally used for separation (Figure 1-9). The gel separates proteins based on different isoelectric points (PI) in the first dimension and molecular weight in the second dimension. One single gel can separate complex mixtures of thousands of proteins. One application of 2D electrophoresis is to map proteins from cells or tissues and compare the protein expression between experimental groups.

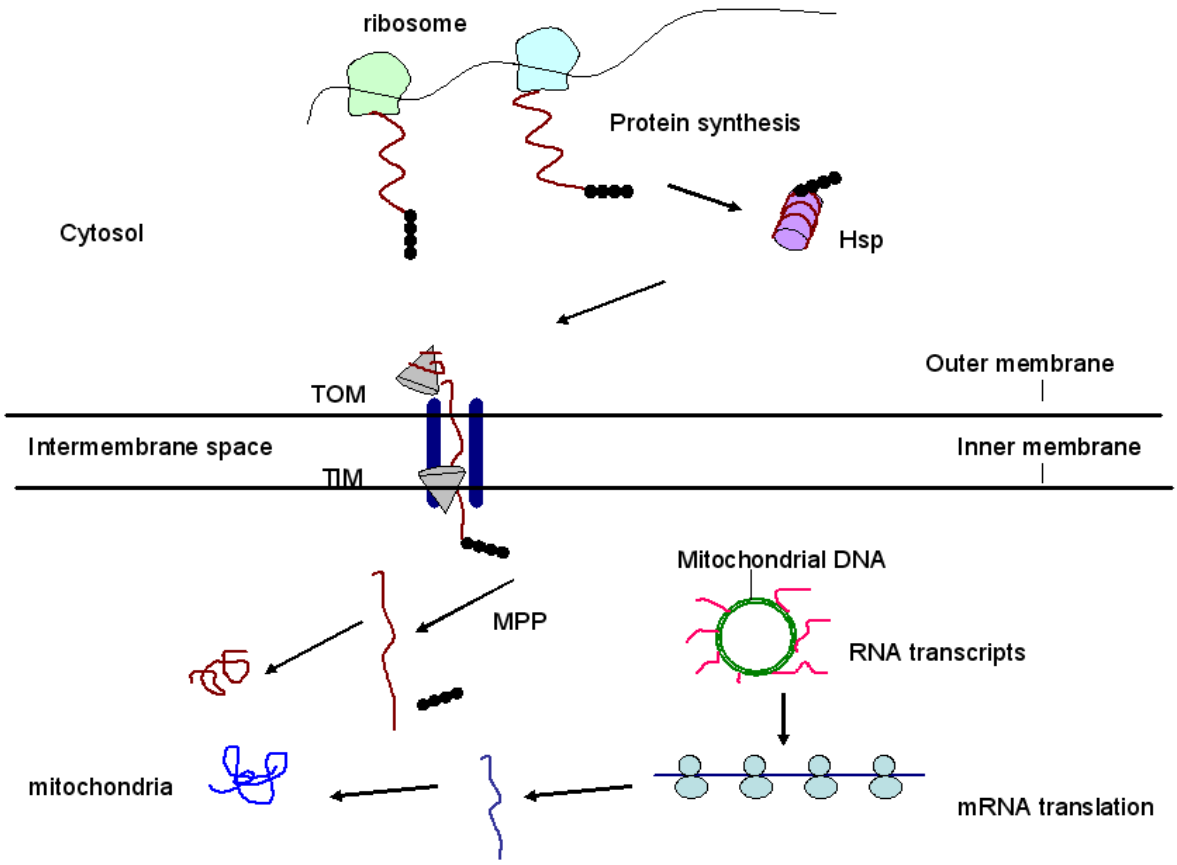

Figure 1-8. Diagram of formation of mitochondrial protein

Several techniques have been developed to resolve the problem of reproductivity in 2D electrophoresis over the years (Anderson and Anderson 1996; Celis and Gromov 1999). The introduction of immobilized pH gradient (IPG) strips to replace tube gels was one of the biggest improvements which increased reproducibility between samples (Bjellqvist et al. 1993; Gorg et al. 2000). In isoelectric focusing (IEF), a high voltage is applied to the ends of strips consisting of polymerized acrylamide gel on a plastic base. After the IEF is complete, the strip is equilibrated with thiol reductant and denaturing reagents and applied to the second dimensional SDS polyacrylamide gel electrophoresis (SDS-PAGE). The other exciting improvement is termed differential gel electrophoresis, which uses different fluorescent dyes to tag different protein samples. Those two samples are run on the same gel and create two images using different fluorescent wavelengths (Unlu et al. 1997).

After isoelectric focusing and SDS-PAGE, a protein spot map is visualized with a proper staining method. Most often, each spot represents a unique protein. The spots of interest are cut out followed by trypsin in-gel digestion. The peptide digest is analyzed using mass spectrometry. The experimental mass spectrum is input into a database containing theoretical protein sequences. Based on the peptide mass fingerprints specific to one protein, the protein is identified (Henzel et al. 1993; Borodovsky et al. 2002; Butterfield et al. 2003; Butterfield and Castegna 2003; Weiler et al. 2003).

To visualize and quantify protein spots, chemical staining such as Coomassie blue G-250/R-250, SYPRO Ruby, fluorescence, and silver are generally used on 2D gels (Urwin and Jackson 1993; Matsui et al. 1999; Berggren et al. 2000). The problem is that low level proteins cannot be detected using this method. Antibody-based detection methods are more specific and more sensitive than the usual chemical stains, although quantification is more difficult because of a limited dynamic range (Jarvik and Telmer 1998).

Although a lot of effort has been devoted to resolve the problems in 2D electrophoresis, it is still a labor and time consuming process. Also, membrane proteins are difficult to detect because of low solubility.

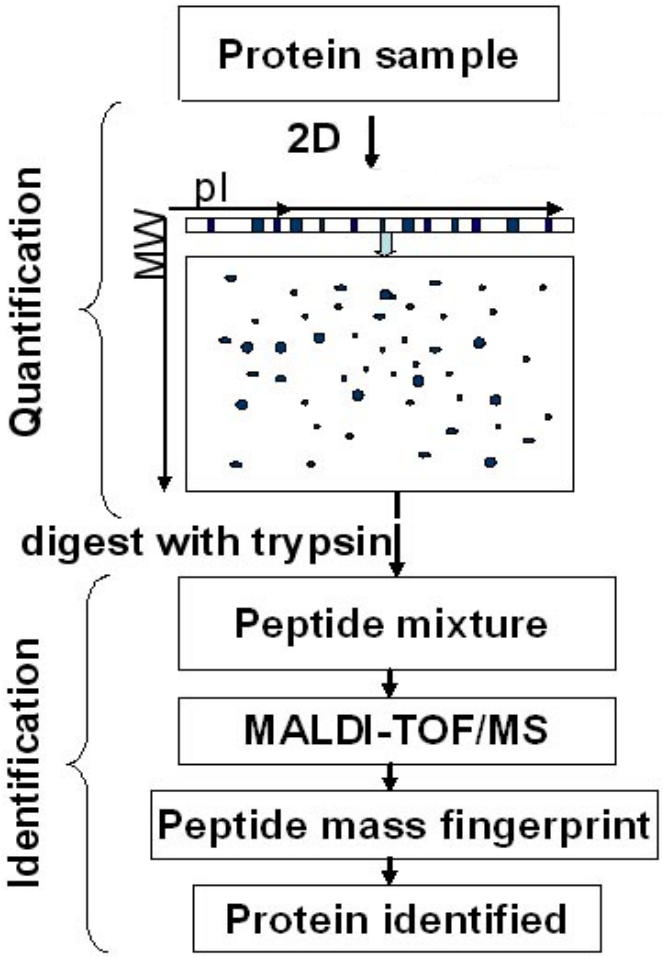

Figure 1-9. Diagram of proteomics with 2-dimensional gel electrophoresis and protein identification based on peptide mass fingerprint

1.6.4 Protein identification and quantification

Two major methods for protein identification are Edman degradation and mass spectrometry. Edman degradation was developed by Pehr Edman for identification of proteins and was a major breakthrough in protein sequencing (Edman 1949). The N-terminal amino acids are cleaved off the peptide without breaking other peptide bonds. The cleaved amino acids are identified through formation of phenylthiohydantoin – amino acid derivatives followed by chromatography or electrophoresis. The procedure is repeated to identify the next amino acid. Peptides longer than 50 – 70 amino acids can not be analyzed reliably by Edman degradation. Long peptides need to be broken up into small peptides and be sequenced individually (Aebersold et al. 1988; Alms et al. 1999). One of the big limitations of Edman degradation is that it does not work if the N-terminal amino acid is chemically modified or concealed in the body of protein.

Mass spectrometry has been widely used in recent years for rapid protein identification. In proteomics, the protein is introduced into the MS in the form of peptides after protease digestion. Electrospray ionization (ESI) and matrix-assisted laser desorption/ionization (MALDI) are two most commonly used methods to ionize peptides. In ESI, fine liquid charged droplets are generated after the liquid sample flows through a microcapillary column into an electronic field (Wilm and Mann 1996; Wilm 2000). As the solvent evaporates, the charged droplet is broken into tiny droplets as the charge reaches a critical point. ESI is a kind of soft ionization method because it does not break the molecules (Fenn et al. 1989). Nanospray ionization was introduced to analyze low abundance proteins at the femtomole level (Wilm et al. 1996; McCormack et al. 1997). Liquid chromatography (LC) has been used to as an automatic sample introduction method recently to replace manual loading methods (McCormack et al. 1997).

MALDI is a laser-based soft ionization method to promote the formation of molecular ions (Karas and Hillenkamp 1988). The analytes are spotted on metal plates with matrix, usually an aromatic acid with chromophore which strongly absorbs laser energy, such as α-cyano-4-hydroxycinnamic acid. The selection of matrix is very important for generation of a good mass spectrum. Matrix materials must be chemically inert, stable in high vacuum condition, and easy to evaporate. As the solvent evaporates, a crystal spot is formed. However, it can not used to analyze peptides bigger than 10

KDa. Koichi Tanaka developed MALDI to be used in the whole range of biological macromolecules in 1988, which allowed him to share the 2002 Noble prize for chemistry with John Fenn.

Once the peptides ions are generated, they are analyzed based on different mass/charge ratios (m/z). The most commonly used mass analyzers are quadrupole, time of flight (TOF), and ion trap mass analyzers. The quadrupole is composed of four parallel metal rods. On one pair, a direct current voltage is applied, while a radio frequency voltage is applied to the other pair. Based on the ratio of given voltages, only ions with a select range of m/z pass through the rods and reach the detector (Miller and Denton 1986; Burlingame et al. 1998). A series of triple quadrupoles can be used in analysis, in which the first and third quadrupoles work as mass filter, and the second one works as a collision cell.

Another commonly used analyzer is TOF, which measures ions based on the time taken to reach detectors through a flight tube. After the ions are accelerated by an electrical field, they have the same kinetic energy (KE):

$$KE = zeV = \frac{1}{2}.m.\left(\frac{d}{t}\right)^2$$

$$\downarrow$$

$$t = d.\sqrt{\frac{1}{2eV}.\frac{m}{z}}$$

Where m is the mass of the ion; z is the charge; V is the acceleration voltage; d is the length of the flight tube & t is the flight time. The velocity of ions depends on their mass/charge ratio. They will fly through the tube at different speeds because they have the same kinetic energy and same charge (Yates 1998). Reflective TOF has an ion mirror which can reflect ions back to reach a detector. It increases the resolution through increasing flight length of ions.

Ion trap analyzer has three electrodes, a ring electrode and two hemispherical electrodes located on two sides. It selectively ejects trapped ions through changing voltages on electrodes (Cooks et al. 1991; Yates 1998).

1.6.5 Database searching

Once mass spectra are generated, database search engines, such as Mascot, provide a speedy way to identify proteins, using the peptide mass fingerprint (PMF) to identify proteins from primary sequence database (James et al. 1993; Yates et al. 1993; Perkins et al. 1999). In PMF, the experimental masses of peptides obtained from proteolytic enzyme digestion are input into the database and are compared with theoretical masses of peptides. Based on the overlap of experimental and calculated masses, a Mowse score is used to describe the match. Rather than the number of the matched peptides, Mowse scores count the match on a probability-based scoring ($-10*\log_{10}P$) (Pappin et al. 1993). However, in PMF, it is hard to identify big genomes because of the peptide mass redundancy. Posttranslational modification of proteins causes another problem in PMF identification, which results in no match in the calculated database. Because of the complexity of peptides, this method cannot be used in the identification of protein mixtures (Clauser et al. 1999).

There are several database search methods available for identification of protein mixtures, such as amino acid sequence database searching (Mann and Wilm 1994; Wilm et al. 1996), *De novo* peptide sequence information (Mackey et al. 2002), and uninterpreted MS/MS data searching (Yates et al. 1995; Perkins et al. 1999). Amino acid sequence searching is more specific than PMF. In this method, a partial amino acid sequence is determined by MS/MS spectra. Combined with the mass of parent peptide and masses of the peptides on each end, the unknown peptide is matched with the theoretical peptide sequence in the database (Mann and Wilm 1994; Wilm et al. 1996). *De novo* peptide sequence databases can provide both sequence information of DNA and protein. It can be used in the organisms that have no well-annotated databases (Mackey et al. 2002). The most commonly used method to interpret MS/MS spectra is uninterpreted MS/MS data searching, such as Mascot, or SEQUEST (Yates et al. 1995; Perkins et al. 1999). Although several improvements have been made in proteomics, especially in protein mixture identification, it is still a big challenge to identify the low-abundance proteins and highly modified proteins.

1.7 Statements of research projects

1.7.1 Increased oxidative damage in nuclear and mitochondrial DNA in Alzheimer's disease

As mentioned above, oxidative stress plays an important role in the development of AD. ROS can attack DNA bases, leading to more than 20 oxidized base adducts. As a consequence of oxidation, DNA may have strand breaks, DNA-DNA and DNA-protein crosslinking, and base modification. Several biomarkers of DNA damage have been quantified, including 8-hydroxy-2'-deoxyguanosine (8-OHdG), the most studied biomarker in DNA oxidation. In 1993, Mecocci et al. reported an age-depended increase of the levels of 8-OHdG in both nDNA and mtDNA in human brain. Subsequently, she observed increased levels of 8-OHdG in brain tissue of AD compared to normal aged subjects (Mecocci et al. 1994). In 1998, Gabbita et al. reported increased levels of multiple oxidized DNA bases in nDNA in AD subjects.

We hypothesized that oxidative damage to DNA, especially mtDNA, may play an important role in the pathogenesis of Alzheimer's disease.

To carry out this study, brain specimens from eight late-stage AD (LAD) (four females, four males) and eight age-matched control subjects (four females, four males) were used for the analysis of oxidative damage to DNA. Four brain regions (frontal lobe, parietal lobe, temporal lob, and cerebellum) were used. Among them, cerebellum was used as a control region compared to the other three neocortical regions.

1.7.2 Increased oxidative damage in nuclear and mitochondrial DNA in Mild Cognitive Impairment

Recent emphasis in adult dementing disorders is on early detection with the hope of early treatment to slow disease progression. Mild Cognitive Impairment (MCI) is generally considered to be the transitional zone between normal aging and early dementing disorders. In general, most MCI subjects eventually convert to AD or other dementias with ~15% of MCI subjects converting to AD per year. Several gene mutations associated with AD have been observed in subjects with MCI including mutations in apolipoprotein E, presenilin 1, and the amyloid precursor protein. Several

studies of MCI show elevated levels of tau, Aβ, and isoprostanes in ventricular CSF, and more recently significant elevations of DNA damage in peripheral leukocytes of MCI and AD (Migliore et al. 2005).

As we saw elevated DNA oxidation in AD brain in our previous study, this study tried to address when the oxidation begins in AD progression. Although increased DNA oxidation is observed in the AD brain, it is unclear when the oxidative damage begins. To determine if DNA oxidation occurs in the brain of subjects with MCI, we quantified multiple oxidized bases in nuclear and mitochondrial DNA isolated from frontal, parietal and temporal lobes and cerebellum of short post-mortem interval autopsies of eight patients with amnestic MCI and six age-matched control subjects.

1.7.3 Increased oxidative damage in nuclear DNA in APP/PS1 transgenic mice

The amyloid cascade hypothesis suggests that Aβ processing and aggregation may contribute to the pathogenesis of sporadic AD. APP is cleaved by β- and γ-secretases to produce Aβ mainly containing Aβ40 and Aβ42. The possible reason why Aβ is toxic is that it may lead to the production of free radicals that result in the oxidation of proteins, lipids, and DNA. More than 50 mutations have been identified in PS1, much more than those of in PS2. Studies show increased Aβ42 production in PS1 transgenic mouse (Duff et al. 1996).

APP transgenic mice show senile plaques in neocortex and hippocampus by 12 month of age. In the mouse model coexpressing APP and PS1, the deposition of senile plaques get accelerated at early ages (Holcomb et al. 1998; Wengenack et al. 2000).

The present study was carried out to measure levels of oxidized nDNA bases in the brain of APP/PS1 transgenic mice using GC/MS-SIM and stable isotope labeled internal standards, and to study the relation of Aβ deposition and DNA oxidation. The bases quantified were 8-hydroxyadenine and 8-hydroxyguanine, the most studied biomarkers of DNA damage.

1.7.4 Proteomic Studies of Mitochondria in Alzheimer's Disease

Mitochondria are the major source of free radicals in cells and their DNA and proteins may be more easily oxidized than in the nucleus. Our previous studies show

increased nuclear and mitochondrial DNA damage in LAD and MCI brain. The DNA damage may lead to the altered protein expression in cells. Numerous studies also showed protein changes in cultured neuron cells and AD brain (Butterfield and Castegna 2003; Choi et al. 2004; Lovell et al. 2005). Protein oxidation may affect neuron function through damaging enzymes that are critical to neuron metabolism.

Proteomics provides an ideal way to study the mitochondrial proteome in AD brain. Two-dimensional gel electrophoresis has the ability to resolve complex mixtures of thousands of proteins in one gel.

Based on our results and previous studies of AD, we hypothesized that DNA damage may alter protein expression in AD brain, especially in mitochondria. In this study, we used proteomics to characterize protein changes in mitochondria in the brain of five LAD and four age-matched control subjects.

CHAPTER TWO
Materials and Methods

2.1 Reagents

N, O-Bis(trimethylsilyl)trifluoroacetamide (BSTFA) and anhydrous pyridine were from Aldrich Chemical (Milwaukee, WI, USA). Molecular biology grade phenol, chloroform, isoamyl alcohol, proteinase K, sucrose, acetonitrile and other standard chemicals for preparation of buffers were obtained from Sigma (St. Louis, MO, USA).

Stable labeled oxidized base analogues were from Cambridge Isotope Laboratories (Andover, MA, USA). These included 8-[8-^{13}C, 7, 9-$^{15}N_2$] hydroxyguanine, 8-[8-^{13}C, 6, 9-diamino-$^{15}N_2$] hydroxyadenine, 5-[2-^{13}C, 1, 3-$^{15}N_2$] hydroxycytosine, 5-[$^{13}C_4$, $^{15}N_2$] hydroxyuracil, [formyl-^{13}C, diamino-$^{15}N_2$] fapyadenine, and [formyl-^{13}C, diamino-$^{15}N_2$] fapyguanine.

The oct-1 antibody was from Santa Cruz Biotechnology (Santa Cruz, CA, USA) and the porin antibody was from Oncogene (San Diego, CA, USA).

The DNA Extractor WB and mtDNA Extractor CT kits were from Wako Chemicals USA, Inc. (Richmond, VA, USA).

IPG strips, Coomassie Blue G-250, Sypro ruby and the 2D starter kit were purchased from Bio-Rad Laboratories (Hercules, CA, USA). Percoll for gradient centrifugation was from Amersham Biosciences (Piscataway, NJ, USA). The density marker beads were from Amersham Pharmacia Biotech AB (Uppsala, Sweden).

2.2 Methods

2.2.1 Brain specimen sampling

Due to the low yield of mtDNA from brain samples, large (15–20 g) specimens of frontal, temporal and parietal lobe and cerebellum were removed at autopsy, immediately placed in liquid nitrogen and stored at −80°C until used for analysis. Although the specimens were primarily composed of cerebral cortex and cerebellar cortex, some gyral and subcortical white matter or folial white matter was present.

All LAD patients were followed longitudinally at the University of Kentucky Alzheimer's Disease Center (UK-ADC) Clinic. All AD subjects met standard clinical diagnostic criteria for probable AD (McKhann et al. 1984) and met accepted neuropathologic criteria for the diagnosis of AD (Mirra et al. 1991, Gearing et al. 1995, Anon 1997).

All MCI patients were followed longitudinally at the UK-ADC Clinic and were initially normal on enrollment but developed MCI during follow-up. The clinical criteria for amnestic MCI were those described by Petersen et al. (1999) and include: (i) memory complaints; (ii) expected memory impairment for age and education; (iii) normal general cognitive function; (iv) intact activities of daily living and (v) the subject does not meet criteria for dementia. Objective memory test impairment was based on a score $\leq$ 1 SD from the mean of controls on the CERAD Word List Learning Task (Morris et al. 1989) and corroborated in many cases with the Free and Cued Selective Reminding Test. Patients with MCI showed a significant increase in neuritic plaques in neocortical regions and a significant increase in neurofibrillary tangles in entorhinal cortex, hippocampus and amygdala (Markesbery et al. 2006).

All control subjects were followed longitudinally in the UK-ADC Clinic and had neuropsychological testing annually which remained in the normal range. Exclusionary criteria included strokes, hemorrhages, history of hypoxia or hypoxic changes, systemic disorders affecting the CNS and psychiatric or other neurological disorders. The most frequent causes of death were myocardial infarcts, pneumonia, pulmonary emboli, cancer (none of the patients had cerebral metastases) and congestive heart failure.

All patients had extensive neuropathological evaluation of multiple neocortical, ventromedial temporal lobe, basal ganglia, brainstem and cerebellum sections using the modified Bielschowsky stain, hemotoxylin-eosin and 10D-5 and alpha synuclein immunostains. Braak staging (Braak and Braak 1991) was determined using the Gallyas stain on sections of entorhinal cortex, hippocampus and amygdala and the Bielschowsky stain on neocortex.

None of the subjects demonstrated significant Lewy body pathology.

2.2.2 Isolation of nuclear DNA

Brain specimens from eight LAD (four females and four males) and eight age-matched control (four females and four males) subjects were used for the analysis of oxidative damage to DNA in the LAD study.

To examine oxidative DNA damage in MCI, brain specimens from eight MCI (four females and four males) and six age-matched control (two females and four males) subjects were used for DNA isolation.

To examine the effects of amyloid deposition on DNA oxidation, brain specimens from APP/PS1 mice and wild type were used for the analysis of oxidative damage to DNA. Four groups of different ages (3m, 6m, 9m, 12m) were used with 8 to 10 mice in each group.

A modified procedure of Mecocci et al. (1993) was used to isolate DNA. Briefly, brain specimens were homogenized on ice using a motor-driven Teflon-coated dounce homogenizer in MSB-Ca^{2+} buffer (0.21 M mannitol, 0.07 M sucrose, 0.05 M Tris-HCl, 3 mM $CaCl_2$, pH 7.5). Disodium EDTA was added to the homogenate with final concentration at 0.01 M, followed by centrifugation at 1,500 x g at 4°C for 20 min. The pellet was resuspended in MSB-Ca^{2+} buffer and centrifuged again. The combined supernatant was kept for isolation of mtDNA and the resulting nuclear pellet was suspended in digestion buffer (0.5% sodium dodecyl sulfate, 0.05 M Tris-HCl, 0.1 M Na_2EDTA) and incubated with 400 µg/mL proteinase K in a 55°C water-bath overnight. Then, 160 µL of 5 M NaCl per 10 mL solution was added, followed by extraction three times with buffer-saturated phenol containing 5.5 mM 8-hydroxyquinoline and three times with chloroform/isoamyl alcohol (24 : 1). 8-hydroxyquinoline was used to limit artifactual DNA oxidation. For the resulting clear solution, 800 µL 5 M NaCl per 10 mL and an equal volume of chilled absolute ethanol were added to precipitate DNA. After centrifugation, the DNA pellet was washed three times with 60% ethanol and air-dried. The pellet was dissolved in autoclaved water and a Genesys 10UV spectrometer (Rochester, NY, USA) used to measure concentration and purity of DNA samples at 260 and 280 nm. The ratio of A260/A280 was used to verify DNA purity.

Due to the large sample size, DNA isolated in theses studies is probably from a mixture of glia and neurons and represents a global measure of DNA oxidation. The DNA was stored at −80°C until used for GC/MS-SIM analyses.

2.2.3 Isolation of mitochondria

The combined supernatant from above was centrifuged at 20,000 x g for 20 min. The pelleted crude mitochondrial fraction was washed with MSB-Ca^{2+} buffer once. This raw pellet still contained contaminants, including cytosolic proteins.

To further purify the mitochondria, it was resuspended in 2 mL MSB-Ca^{2+}, loaded onto the percoll/MSB-Ca^{2+} buffer (1 : 1), and centrifuged at 50,000 x g for 1 h. Several bands were observed after centrifugation and the light brown band (1.035 g/ml) was separated. This fraction was primarily composed of intact mitochondria.

The pelleted mitochondria were resuspended and centrifuged a second time through a percoll gradient leading to highly purified intact mitochondria. The mitochondria were centrifuged and washed three times with MSB-Ca^{2+} buffer. The resulting pellet was used for isolation of mtDNA or protein.

To verify the purity of mitochondria, representative samples were fixed with 2.5% glutaraldehyde, post fixed in 1% osmium tetroxide, dehydrated through graded ascending alcohols and propylene oxide, and embedded in Spurr's low viscosity embedding media. Sections were cut and analyzed by electron microscopy (EM) by the UK Electron Microscopy Facility.

2.2.4 Isolation of mitochondrial DNA

For DNA isolation, the mitochondrial pellet from above was lysed by addition of 2% sodium dodecyl sulfate solution and 400 μg/mL proteinase K for 4 hr in a 37°C water bath. After addition of 160 μL 5 m NaCl per 10 mL, the solution was extracted three times with buffer-saturated phenol (5.5 mm 8-hydroxyquinoline) and chloroform/isoamyl alcohol (24 : 1) as described above. mtDNA was precipitated with 800 μL 3m sodium acetate and two volumes of absolute ethanol at −20°C overnight. mtDNA was pelleted at 14,000 x g for 20 min, washed with 60% alcohol, dried, then resuspended in 200 μL

autoclaved water. The concentration was calculated based on the absorbance at 260 nm measured by UV-Vis spectrometry.

2.2.5 Western blot analysis

To verify the purity of nuclear and mitochondrial fractions, nuclear and mitochondrial proteins from representative AD and control subjects were dissolved in distilled water. Protein concentrations were determined using the Pierce BCA method. Protein (50 µg) was separated on a 4–20% sodium dodecyl sulfate–polyacrylamide gel electrophoresis gradient gel and was transferred to nitrocellulose. The blot was blocked in 5% milk in 0.5% Tween-20/Tris-buffered saline (TTBS) overnight at 4°C. Primary antibodies (rabbit anti-porin [1 : 1000] and rabbit anti-oct-1 [1 : 500]) were added and blots were incubated for 3 hr at room temperature. The blots were washed three times for 10 min each with TTBS and incubated in horseradish peroxidase conjugated secondary antibody for 1 h. The blots were rinsed three times with TTBS and the bands visualized using enhanced chemiluminescence per manufacturer's instructions (Amersham Pharmacia Biotech, Piscataway, NJ, USA).

2.2.6 Polymerase chain reaction amplification of mitochondrial DNA and neural DNA

To further verify that mtDNA was not contaminated by nDNA, PCR was performed with 500 ng mtDNA and nDNA using primers for APOE, a nuclear-coded protein. PCR reaction mixtures of 50 µL contained 1 × PCR buffer, 250 µm dNTPs, 0.625 U Taq polymerase, 1.5 mm $MgCl_2$, and 500 ng DNA. Primer sequence were as described by Tsukamoto et al. (1993); and were 5'-GGCGCTCGCGGATGGCGCTGAG-3'(sense primer) and 5'-GCACGGCTGTCCAAGGAGCTGCAGGC-3' (reverse primer) (Integrated Device Technology, Santa Clara, CA, USA) PCR products were separated on a 2% low-melt agarose gel containing ethidium bromide as previously described (Addya et al. 1997).

PCR amplification showed no cross-contamination between nDNA and mtDNA (Wang et al. 2005).

2.2.7 Isolation of nuclear DNA and mitochondrial DNA using NaI method

To ensure that phenol extraction did not lead to artifactual DNA oxidation, nDNA and mtDNA were isolated from four representative frontal lobe specimens using DNA Extractor WB and mtDNA Extractor CT kits (Wako Chemicals USA, Inc.) following the manufacturer's instructions. To isolate nDNA, tissue specimens were homogenized in the lysis buffer provided in the DNA Extractor WB kit. The homogenate was centrifuged at 1,500 x g and 4°C for 15 min and the pellet resuspended in enzyme reaction solution. Proteinase K was added to a final concentration of 10 μg/mL and the solution was incubated in a 55°C water-bath overnight. RNase was added to the solution at a final concentration of 20 μg/mL and incubated for an additional 10 min. The supernatant was collected after centrifugation at 10,000 x g and 25°C for 2 min. nDNA was precipitated by the addition of 0.6 mL NaI solution from the kit and an equal volume of 100% isopropanol.

For mtDNA isolation tissue specimens were homogenized in ice-cold homogenization buffer provided in the mtDNA Extractor CT kit. The homogenate was centrifuged at 1,500 x g and 4°C for 15 min. The supernatant was collected and centrifuged at 20,000 g at 4°C for 20 min and solutions I, II and III from the kit were added to the pellet as in the manufacturer's instructions. mtDNA was precipitated by the addition of 0.3 mL NaI and an equal volume of 100% isopropanol. DNA concentrations were measured by the absorbance at 260 nm.

2.2.8 Sample preparation for gas chromatography/mass spectrometry

nDNA (200 μg) and mtDNA (20 μg) were used for analysis by GC/MS-SIM. Individual bases were prepared by acid hydrolysis and derivatization with BSTFA. The DNA samples were added to 5-mL conical glass tubes with a Teflon disc screw cap. Isotope-labeled internal standards were added for quantification of oxidized bases. Two hundred and fifty microliters of 90% formic acid was used to hydrolyze DNA at 145°C for 30 min in evacuated tubes. Acid hydrolysis releases intact and modified bases by cleaving the bonds between bases and sugar moieties. After hydrolysis, the samples were lyophilized and derivatized with a mixture of BSTFA/pyridine (1 : 1) at room temperature for 2 h in evacuated tubes.

The derivatized products were lyophilized again and dissolved in 20 μL BSTFA immediately before analysis and 2 μL injected into the GC/MS-SIM for analysis.

2.2.9 Gas chromatography/mass spectrometry analysis

A Hewlett-Packard model HP6890 gas chromatograph interfaced with an MS detector was used. The injection port was maintained at 250°C. A 5% phenylmethylsiloxane capillary column (30 m, 0.25 mm i.d., 0.25 μm film thickness; HP-5MS) was used for separation. Ultra-high-purity helium was used as a carrier gas at an inlet pressure of 11.8 psi using constant flow and a splitless mode. The glass liner in the injection port was filled with silanized glass wool, which allowed homogeneous vaporization of injected samples. The initial temperature was held 2 min after sample injection with the following ramps: ramp 1: 100–178°C at 3°C/min; ramp 2: 178–181°C at 0.3°C/min; ramp 3: 181–208°C at 3°C/min; ramp 4: 208–280 at 10°C/min. The final temperature was maintained for 2 min. The run time was 56.2 min for each sample. The temperature of the ion source inside mass spectrometer was ~180°C.

2.2.10 Amyloid plaque counts

APP/PS1 mice were sacrificed by halothane overexposure using procedures consistent with the Panel on Euthanasia of American Veterinarian Association. The brains were quickly removed and a single hemisphere without cerebellum was placed in 4% phosphate buffered paraformaldehyde. The hemisphere was dissected after paraformaldehyde fixation for 7 days and embedded in paraffin. 10 μm sections were cut using a Shandon Finesse microtome and placed on Plus slides. Sections were stained using a monoclonal antibody against Aβ17-34 (Vector Laboratories, Burlingame, CA) using standard protocols. Briefly, sections were deparaffinized through xylene and graded descending alcohols to water, incubated 30 min at room temperature in 3% H_2O_2/methanol, washed in distilled/deionized water, followed by 3 min incubation at room temperature in 90% formic acid. The sections were washed 5 min in running distilled/deionized water, pretreated 10 min at room temperature with 2 mg/ml pepsin (Biomedia, Foster City, CA), blocked in 15% normal goat serum in automation buffer 1 hr at room temperature after 3 times (2 min each) washes in automation buffer. Sections

were incubated in a 1:100 dilution of anti-Aβ at 4 ^{o}C overnight and washed 3 times (5 min each) with automation buffer. The sections were incubated 1 hr at room temperature in horse anti-mouse IgG (1:2000) in 1.5% horse serum/automation buffer. The sections were washed 3 times (5 min each) in automation buffer, incubated 30 min in Vector laboratories ABC reagent, washed 3 times (5 min each) in automation buffer, and color developed using DAB. Sections were counterstained using hematoxylin/ecosin, dehydrated, cleared in xylene and coverslipped. This work was done by Dr. Markesbery's neuropathology laboratory.

Aβ deposits were counted semi-quantitatively by taking serial micrographs of the entire hemisphere of each animal using a 20X objective on a Nikon Eclipse E60 Microscope. Each Aβ deposit was circled and counted on the printed micrograph with naked eye. Deposits considered as an independent plaque must be discrete and not connected to another. The number of Aβ deposits were normalized to the area of the section measured using Bioquant software. This work was carried out by Dr. WR Markesbery.

2.2.11 Two-dimensional electrophoresis

Five hundred milligram lyophilized mitochondrial protein was dissolved in 300 µl rehydration buffer (8.0 M urea, 4% CHAPS, 100 mM DTT (dithiothreitol), 0.001% bromophenol blue, 0.2% Bio-Lytes) and loaded onto the 17 cm IPG (pI 3-10) strips. The strips were rehydrated for 12 hr at room temperature under mineral oil. A pause is needed after rehydration for inserting paper wicks, adding mineral oil, transferring strips from rehydration tray to focusing tray per manufacture. Then a self-defined program (300 V for 5 hr, 1,000 V for 1hr, 2,500 V for 1 hr, and 5,000 V for 80,000 voltage:hour) was run for total time of about 23 hr.

Before running the second dimension, the strips were equilibrated with equilibration buffer I (6 M urea, 2% SDS, 0.375 M Tris-HCl, 20% glycerol, 130 mM DTT) and equilibration buffer II (6 M urea, 2% SDS, 0.375 M Tris-HCl, 20% glycerol, 130 mM iodoacetamide) for 20 min each. After equilibration, the strips were washed in running buffer and loaded onto 8-16% SDS-PAGE gel. Running conditions were 16 mA/gel for 30 min, then 24 mA/gel for about 5 hr.

2.2.12 Gel staining and image analysis

The gels were stained with Sypro ruby per manufacture's instruction. Briefly, the gels were fixed with 30% methanol/10% acetic acid for one hr. 250 ml of Sypro ruby solution was used to stain the gels overnight in a dark box. The gels were washed with 20% ethanol 3 times (15 min each wash). Gel images were taken using a ChemiDoc XRS system and analyzed with PDQuest software from Bio-Rad.

Spots stained with Sypro ruby can only be visualized under UV light. In order to see spots under white light, the gels were stained with 0.1% Colloidal Coomassie Brilliant Blue G250. Briefly, gels were fixed in fixing solution (1.3% phosphoric acid, 20% methanol), and stained overnight with fresh staining solution (0.1% Coomassie Blue, 1.6% phosphoric acid, 8% ammonium sulfate, 20% methanol). Gels were transferred to neutralization buffer for 1-3 min (0.1 M tris-base, pH 6.5), followed by washing with 25% methanol for less than 1 min. Gels were stored in 20% ammonium sulfate at 4 ^{o}C until the spots were cut for trypsin digestion.

2.2.13 Trypsin digestion for MS analysis

After PDQuest analysis, spots of interest were cut out as close to the edge of spots as possible using glass Pasteur pipette. The gel pieces from single spot were washed with water 3 times. 100 mM NH_4HCO_3 was added followed by addition of an equal volume of acetonitrile. The solution was vortexed for 15 min and centrifuged at 10,000 g for 5 min. The gel pieces were dehydrated with 100 µl acetonitrile until they stuck together. All liquid was removed. If gel particles were still blue (stained with Coomassie Brilliant Blue), this step was repeated until gel became white. The pellet was dried and rehydrated in 1.5 µM modified trypsin for 60 min at 4°C. Excess trypsin was aspirated and the gel digested in a 60°C water bath overnight. 5% formic acid was added to stop the digestion reaction. The supernatant is ready for MS.

2.2.14 MALDI-TOF analysis and database searching

A Bruker Autoflex MALDI-TOF (Matrix assisted laser desorption ionization – time of flight) mass spectrometer (Bruker Daltonics, Billerica, MA, USA) at the University of Kentucky Mass Spectrometry Facility was used to generate mass spectra.

An AnchorChip target (Bruker Daltonics) was used to load trypsin digested samples. 1μl of the supernatant was loaded onto an α-cyano-4-hydoxycinnamic acid (0.3 mg/ml in ethanol: acetone, 2:1 ratio) spot. After the sample spot was air dried, 1 μl of 1% TFA solution was used to wash the spot. The resulting spot was recrystallized with 1μl of a solution of ethanol:acetone:0.1% TFA (6:3:1).

All spectra consist of at least 40 laser shots depending on the intensity of samples. The MASCOT search engine was used to search proteins based on the peptide mass fingerprints. The following parameters were used in database search: homo sapiens; monoisotopic; oxidation (methionine); mass tolerance of 100 ppm; and up to one missed trypsin cleavage.

2.3 Statistical Analysis

Statistical analyses of all the data were carried out using 2-way ANOVA and ABSTAT software (Arvada, CO, USA). $p \leq 0.05$ was considered as a significant difference. All results are expressed as mean ± SEM. Comparison of age and post-mortem interval was by two-tailed Student's t-test. Braak staging scores were compared using non-parametric testing and the Mann–Whitney U-test. Braak staging scores are reported as the median.

CHAPTER THREE

Results

3.1 Increased oxidative damage in nuclear and mitochondrial DNA in late stage Alzheimer's disease

Mitochondrial density was measured using density marker beads. Results show that mitochondria position at a density of 1.035 g/ml during centrifugation through a percoll gradient (Figure 3-1). Electron microscopy of a representative mitochondrial preparation isolated using our procedure showed a highly purified (~95%) mitochondrial fraction (Figure 3-2).

We also carried out Western blot analysis of nuclear and mitochondrial protein samples using Oct-1 and porin antibodies to verify the purity of nuclear and mitochondrial fractions, respectively. Western blot analysis (Figure 3-3) of representative nuclear and mitochondrial fractions probed for Oct-1, an octamer-binding protein specific to nuclei, and porin, a membrane-bound mitochondrial transport protein, showed no cross contamination of proteins between the mitochondrial and nuclear fractions. Figure 3-4 shows the results of PCR amplification of representative mtDNA and nDNA samples for APOE, a nuclear-coded protein, and demonstrates that there was no cross contamination of nDNA in mtDNA.

One representative DNA sample (50 μg) was run with six isotope-labeled internal standards (1μg each). The chromatogram is shown in Figure 3-5. The bases of interest were well separated, as indicated by their different retention times. 5-Hydroxyuracil was eluted at a retention time of 18.4 min. The other oxidized bases were 5-hydroxycytosine (21.7 min), fapyadenine (28.2 min), 8-hydroxyadenine (32.2 min), fapyguanine (39.2 min), and 8-hydroxyguanine (44.5 min). We did not quantify modified thymine because 5, 6-dihydroxythymine was below the minimum detection limit (Gabbita *et al*. 1998).

Three replicates were performed to determine the dynamic range of internal standards. Results show that all internal standards had a large dynamic range. 5-

hydroxyuracil showed a linear range from 6 pmol to 130 nmol (r = 0.9992) (Figure 3-6 b). 5-hydroxyuracil has three active hydrogen atoms from -NH and -OH groups, which are replaced with -Si(CH_3) from BSTFA during derivatization (Table 3-1). The resulting molecular ion (M^+) of the BSTFA derivative is 350 amu. With a loss of a CH_3 group, the daughter ion is observed at 335 amu (Figure 3-6 a). Similarly, three active hydrogen atoms of 5-hydroxycytosine are replaced by –Si(CH_3) during derivatization, resulting in m/z values of 346 and 331 amu (Table 3-1, Figure 3-7 a). The linear range (r = 0.9995) of 5-hydroxycytosine is from 2 pmol to 40 nmol (Figure 3-7 b). Three –Si(CH_3) groups replace three hydrogen atoms in fapyadenine, which results in m/z values of 372 amu for the molecular ion and 357 amu for the daughter ion resulting from a loss of CH_3 (Table 3-1, Figure 3-8 a). The linear dynamic range for fapyadenine is from 6 pmol to 120 nmol (r = 0.9993) (Figure 3-8 b). 8-hydroxyadenine has three replaceable hydrogens during derivatization by BSTFA, which results in m/z values of 370 amu (parent ion) and 355 amu (daughter ion) (Table 3-1, Figure 3-9 a). The standard curve of 8-hydroxyadenine showed a wide dynamic range from 4 pmol to 90 nmol with an r of 0.9985 (Figure 3-9 b). Four –Si(CH_3) are added to fapyguanine in derivatization. The resulting mass of M^+ is 460 amu. With a loss of CH_3, the mass is 445 amu (Table 3-1, Figure 3-10 a). The linear range of fapyguanine is from 7 pmol to 150 nmol (r = 0.9974) (Figure 3-10 b). Similar to fapyguanine, 8-hydroxyganine has 4 replaceable hydrogen atoms, resulting in ions with m/z values of 458 amu and 443 amu (Table 3-1, Figure 3-11 a). A linear response was observed from 7 pmol to 130 nmol (Figure 3-11 b) for 8-hydroxyguanine.

To address the concern that artifactual oxidation of DNA occurred during phenol extraction, we used DNA Extractor WB and mtDNA Extractor CT kits (Wako Chemicals USA, Inc.) that use non-organic solutions and NaI precipitation. Table 3-2 shows that levels of oxidized bases measured in DNA samples isolated using the two different methods were similar, although levels of fapyguanine ($p < 0.02$) and fapyadenine ($p < 0.01$) were significantly reduced in DNA isolated using the DNA Extractor WB kit and levels of fapyadenine ($p < 0.02$) were significantly reduced with the mtDNA Extractor CT kit. In contrast, levels of 5-hydroxycytosine ($p < 0.02$) were significantly increased in DNA samples prepared using the mtDNA Extractor CT kit. Levels of 8-hydroxyguanine and 8-hydroxyadenine showed no significant differences between the

two methods. Based on these data, DNA samples used for statistical comparisons were isolated using phenol/chloroform extraction.

Eight AD and eight age-matched control DNA samples as previously described were used in GC/MS-SIM analysis and six modified bases quantified using stable isotope-labeled internal standards. There were no significant differences in age or postmortem interval (PMI) between LAD and age-matched control subjects (Table 3-3). There was a significant difference in median Braak score between AD (VI) and age-matched control subjects (I) (Table 3-3). The amount of each modified base is expressed as mean ± SEM number of modified lesions per million DNA bases (Halliwell and Dizdaroglu 1992) as shown in Table 3-4. Table 3-5 shows a comparison of levels of oxidized bases in terms of lesions/10^6 DNA bases, lesions/unmodified DNA bases, percentage of lesions, and nmol/mg DNA. Levels of modified bases in mtDNA were statistically significantly ($p < 0.01$) higher than in nDNA for both LAD and control subjects for each region. Comparison of the ratio of mitochondrial to nuclear DNA oxidation showed no significant differences between LAD and control subjects due to considerable subject to subject variability. In LAD samples, the damage was consistently higher than controls. The absolute amount of 8-hydroxyadenine was the lowest among the modified bases, whereas 8-hydroxyguanine was the highest.

Hydroxyl radical attack on the C8 of adenine leads to the production of 8-hydroxyadenine. Mean levels of 8-hydroxyadenine were approximately twofold higher in AD than in the controls, and mtDNA had approximately eightfold higher levels than the nDNA. Significant differences were found in nDNA in the frontal lobe ($p < 0.03$) and parietal lobe ($p < 0.04$), and nDNA ($p < 0.001$) and mtDNA ($p < 0.04$) of temporal lobe in LAD. The absolute amount of 8-hydroxyadenine in LAD mtDNA of the temporal lobe was the highest (Figure 3-12).

One electron reduction followed by ring opening of 8-hydroxyadenine leads to formation of fapyadenine. Significant elevations of fapyadenine were present in mtDNA of LAD parietal lobe ($p < 0.05$), nDNA ($p < 0.001$) and mtDNA ($p < 0.05$) of AD temporal lobe, and nDNA of cerebellum (Figure 3-13).

5-Hydroxycytosine is formed by dehydration of cytosine glycol and 5-hydroxyuracil by dehydration and deamination of cytosine glycol, the oxidation product

of cytosine. Our data show that 5-hydroxycytosine was significantly elevated in AD samples in nDNA ($p < 0.01$) and mtDNA ($p < 0.01$) of frontal lobe, mtDNA ($p < 0.01$) of parietal lobe and nDNA ($p < 0.001$) and mtDNA ($p < 0.05$) of temporal lobe (Figure 3-14). 5-Hydroxyuracil levels were significantly elevated in mtDNA of parietal ($p < 0.05$) and temporal ($p < 0.04$) lobes, and nDNA in temporal lobe of AD ($p < 0.05$) (Figure 3-15).

In our study, we observed levels of 8-hydroxyguanine considerably higher than any of the other bases. Statistical comparison showed significant elevations of 8-hydroxyguanine in nDNA in the frontal ($p < 0.03$) and parietal ($p < 0.01$) lobes of AD subjects and in mtDNA of parietal ($p < 0.05$) and temporal ($p < 0.05$) lobes in AD (Figure 3-16). Fapyguanine, which results from a one electron reduction and ring opening product of 8-hydroxyguanine, was significantly elevated in mtDNA of cerebellum ($p < 0.04$), and parietal ($p < 0.05$) lobe in AD (Figure 3-17).

Statistical results from two-way ANOVA showed that 8-hydoxyadenine ($p < 0.02$) and 8-hydroxyguanine ($p < 0.04$) in AD nDNA were significantly increased in neocortical regions compared to cerebellum (Table 3-4). In order to compare our results easily to previous studies, a units conversion table is provided (Table 3-5).

Table 3-1. m/z values of BSTFA derivatives of internal standards

Internal Standards	Molecular weight	Addition of – $Si(CH_3)$ groups	m/z of M^+	m/z for $M^+ - CH_3$
5-hydroxyuracil	134	3	350	335
5-hydroxycytosine	130	3	346	331
fapyadenine	156	3	372	357
8-hydroxyadenine	154	3	370	355
fapyguanine	172	4	460	445
8-hydroxyguanine	170	4	458	443

Table 3-2. Comparison of two different DNA extraction methods

	Level of modified bases (Lesions/10^6 DNA Bases, mean ± SEM)			
	Nuclear DNA		Mitochondrial DNA	
	Phenol-Chloroform	WB kit (NaI)	Phenol-Chloroform	CT kit(NaI)
Frontal lobe				
8-OH-guanine	50.4 ± 7.8	61.9 ± 21.6	262.7 ± 64.9	223.7 ± 53.4
Fapyguanine	20.5 ± 2.3	12.1 ± 1.0*	187.2 ± 75.1	154.5 ± 48.6
5-OH-cytosine	8.2 ± 1.0	26.2 ± 9.5	78.0 ± 15.9	158.2 ± 21.9*
8-OH-adenine	12.2 ± 2.3	19.0 ± 7.0	42.5 ± 12.5	22.0 ± 10.1
Fapyadenine	12.9 ± 1.3	4.6 ± 0.5*	72.6 ± 16.7	7.3 ± 1.9*

* $p < 0.05$ phenol-chloroform vs. NaI precipitation

Table 3-3. Demographic data for control and LAD subjects

	Number and sex	Age (yr) (mean ± SEM)	PMI (hr) (mean ± SEM)	Braak Score (median)
Control	N=8 (4F, 4M)	84.3 ± 3.4	2.9 ± 0.2	I
LAD	N=8 (4F, 4M)	85.1 ± 1.6	3.3 ± 0.2	VI*

* $p < 0.05$ control vs. LAD

Table 3-4. Levels of markers of DNA oxidation in nuclear and mitochondrial DNA from late stage Alzheimer's disease and age-matched control subjects.

	Level of modified bases (Lesions/10^6 DNA Bases, mean ± SEM)			
	Nuclear DNA		Mitochondrial DNA	
	control	LAD	control	LAD
Cerebellum				
8-OH-adenine	13.0 ± 2.2	*18.0 ± 2.1*	96.1 ± 13.4	136.9 ± 17.8
Fapyadenine	7.2 ± 1.4	13.2 ± 1.9*	81.5 ± 13.1	114.4 ± 14.4
5-OH-cytosine	9.9 ± 1.1	14.9 ± 1.9	90.0 ± 18.5	226.6 ± 58.0
5-OH-uracil	6.9 ± 0.8	9.6 ± 2.1	52.8 ± 12.3	95.1 ± 21.9
8-OH-guanine	36.3 ± 4.9	*49.4 ± 8.7*	205.0 ± 35.1	439.6 ± 115.7
Fapyguanine	14.8 ± 2.1	21.5 ± 3.2	144.9 ± 23.2	344.8 ± 70.5*
Frontal lobe				
8-OH-adenine	11.8 ± 2.0	28.3 ± 4.1*#	92.6 ± 8.9	124.9 ± 16.9
Fapyadenine	12.8 ± 1.2	16.4 ± 3.2	73.1 ± 12.2	101.7 ± 23.2
5-OH-cytosine	9.4 ± 1.4	16.6 ± 2.4*	93.7 ± 19.8	223.9 ± 22.4*
5-OH-uracil	8.7 ± 1.4	10.9 ± 2.5	39.4 ± 4.8	70.8 ± 21.5
8-OH-guanine	49.4 ± 5.8	133.9 ± 25.8*#	407.9 ± 70.7	568.5 ± 140.2
Fapyguanine	20.7 ± 2.1	22.3 ± 5.0	238.7 ± 59.7	532.2 ± 131.4
Parietal lobe				
8-OH-adenine	12.5 ± 1.6	23.3 ± 3.9*#	86.8 ± 10.4	119.3 ± 15.4
Fapyadenine	12.7 ± 1.8	15.7 ± 1.9	71.7 ± 10.0	108.1 ± 9.2*
5-OH-cytosine	10.5 ± 1.3	15.2 ± 1.8	95.4 ± 12.6	217.7 ± 31.0*
5-OH-uracil	9.8 ± 1.2	13.9 ± 2.3	27.3 ± 4.0	68.4 ± 14.3*
8-OH-guanine	46.6 ± 4.9	84.4 ± 10.4*#	271.6 ± 34.1	646.9 ± 175.3*
Fapyguanine	17.0 ± 1.5	38.7 ± 11.4	178.5 ± 33.7	370.8 ± 84.8*
Temporal lobe				
8-OH-adenine	12.7 ± 1.5	35.7 ± 4.9 *#	77.8 ± 10.4	210.8 ± 48.6*
Fapyadenine	10.2 ± 1.3	18.1 ± 1.1*	79.4 ± 15.9	126.0 ± 13.6*
5-OH-cytosine	7.6 ± 0.6	15.5 ± 1.2*	102.3 ± 22.4	315.5 ± 95.1*
5-OH-uracil	6.5 ± 0.6	11.3 ± 2.0*	30.5 ± 4.4	87.8 ± 19.8*
8-OHguanine	72.8 ± 17.1	142.5 ± 31.5#	350.1 ± 81.8	610.6 ± 158.9*
Fapyguanine	23.3 ± 3.6	41.6 ± 8.5	178.4 ± 49.2	257.5 ± 31.6

* $p < 0.05$ significant elevations in LAD DNA compared to age matched control subjects
# $p < 0.05$ significant elevations in DNA from frontal, parietal and temporal lobes compared to cerebellum.

Table 3-5. Comparison of levels of DNA damage in terms of lesions/10^6 total DNA bases, ratio of lesion/unmodified DNA base, percentage of lesions, and nmol/mg of DNA

lesions/10^6 total DNA bases	1	10	20	50	100	250	500
lesion:unmodified DNA base	1:250,000	1:25,000	1:12,500	1:5,000	1:2,500	1:1,000	1:500
% of lesions	0.0004%	0.004%	0.008%	0.02%	0.04%	0.1%	0.2%
nmol lesions/mg of DNA	0.003	0.031	0.063	0.159	0.300	0.796	1.592

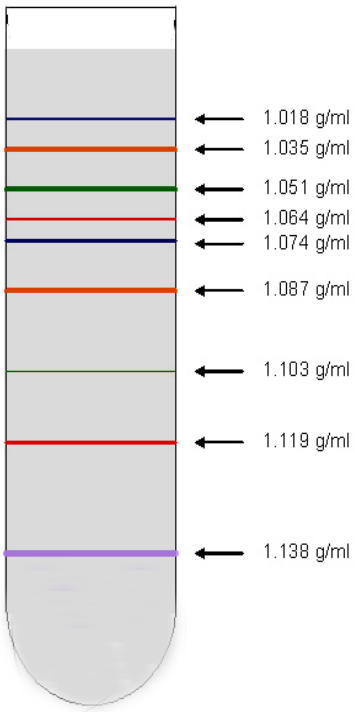

Figure 3-1. Mitochondrial density was measured using density marker beads. Mitochondria were positioned at a density of 1.035 g/ml during centrifugation through a Percoll gradient.

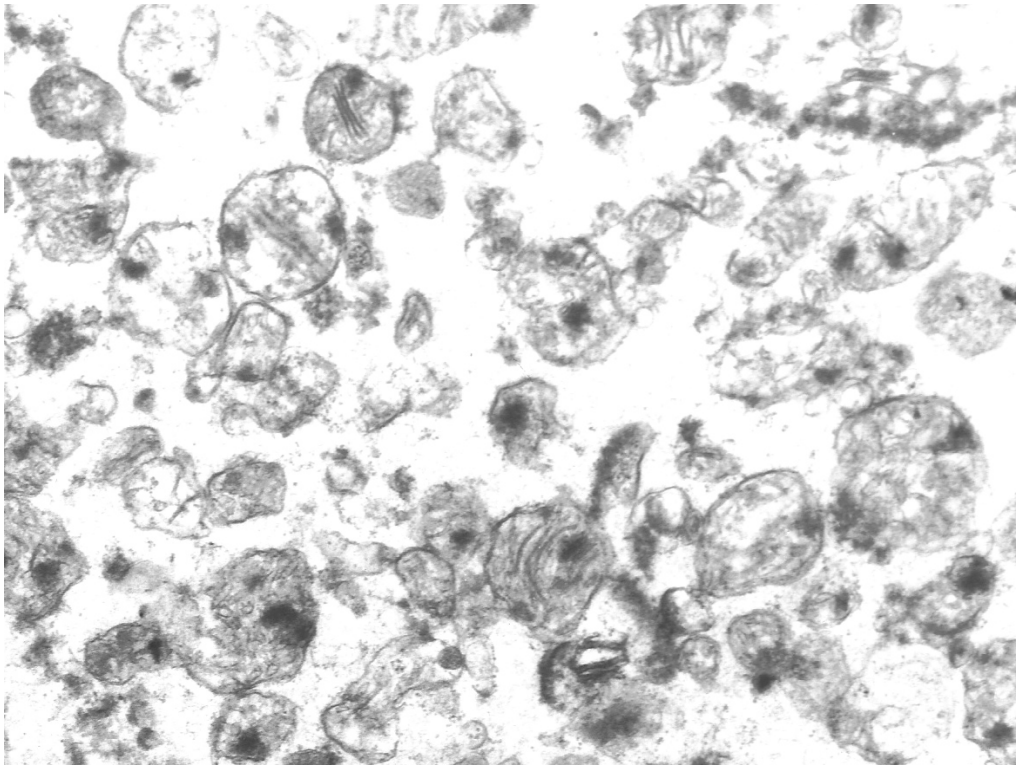

Figure 3-2. Electron micrograph of a representative mitochondrial preparation after centrifugation through Percoll gradients. Final magnitude is 32,500 X.

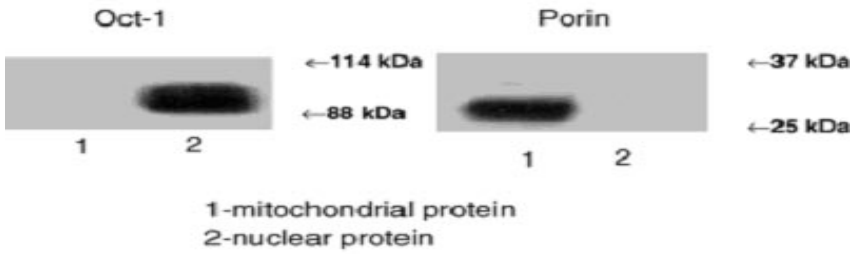

Figure 3-3. Western blot analysis of protein from nuclei and mitochondria using antibodies against Oct-1(a nuclear protein) and porin (a mitochondrial protein). The blots show there was no cross contamination between nuclear and mitochondrial preparations.

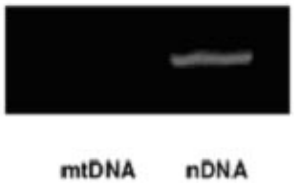

Figure 3-4. Two percent low-melt agarose gel of PCR amplified nDNA and mtDNA for APOE, a nuclear encoded protein. It showed that there was no cross contamination between nDNA and mtDNA.

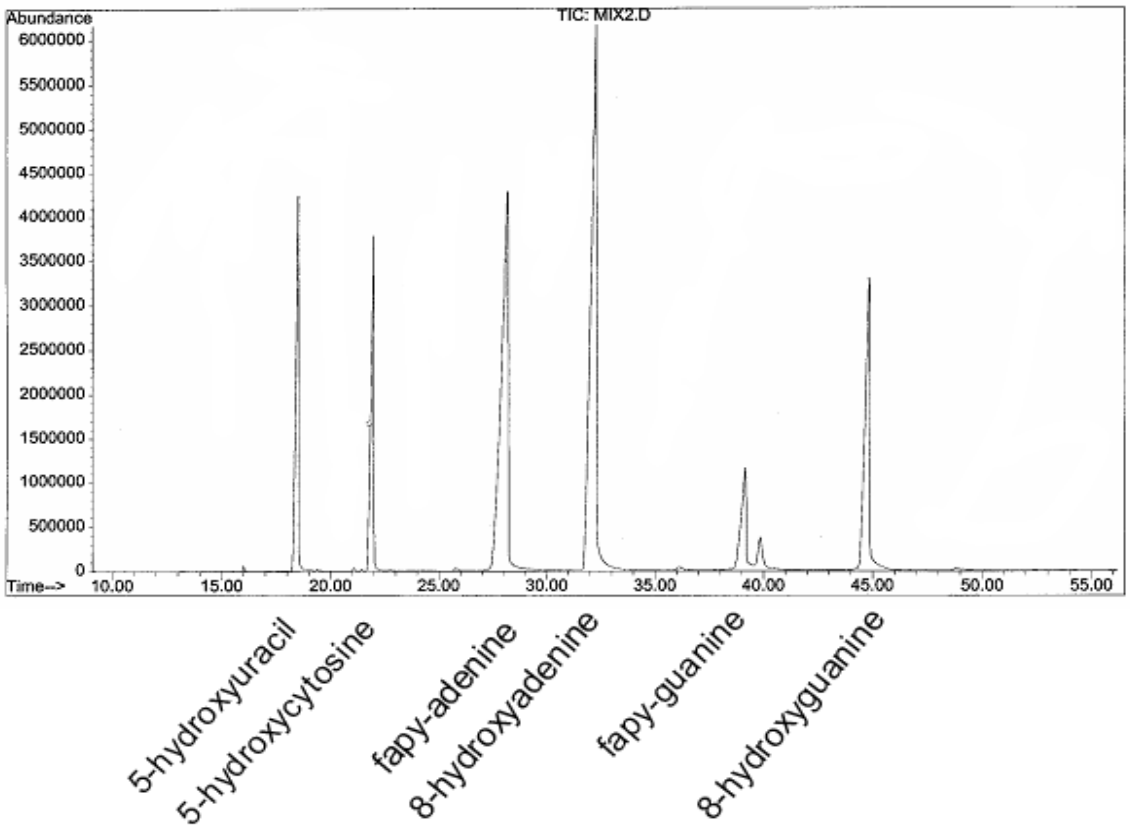

Figure 3-5. A representative gas chromatogram of a DNA sample with stable isotope - labeled internal standards.

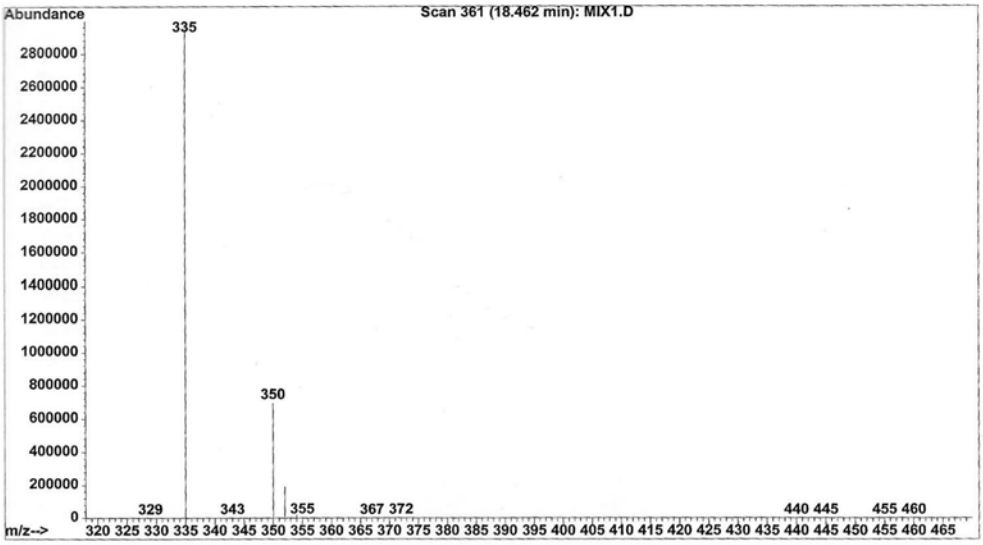

(a)

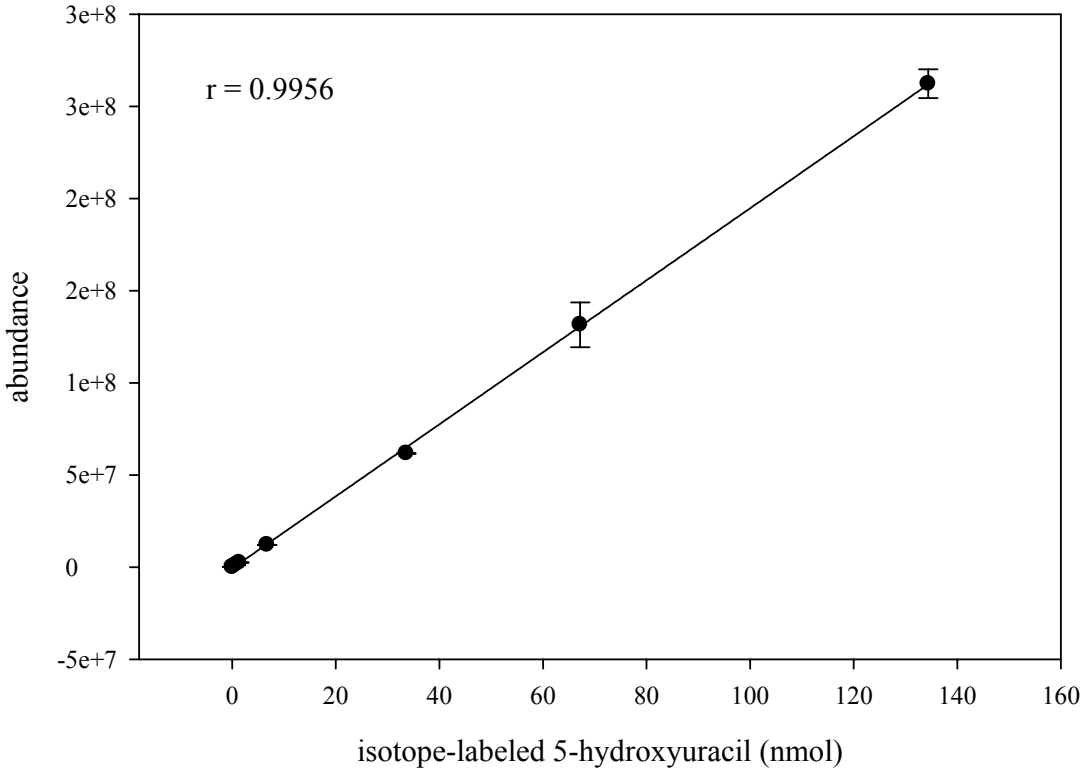

(b)

Figure 3-6. (a) A representative mass spectrum of isotope-labeled 5-hydroxyuracil (retention time 18.2 min). Figure (b) shows a standard curve of isotope-labeled 5-hydroxyuracil, which has a good dynamic range from 6 pmol to 130 nmol.

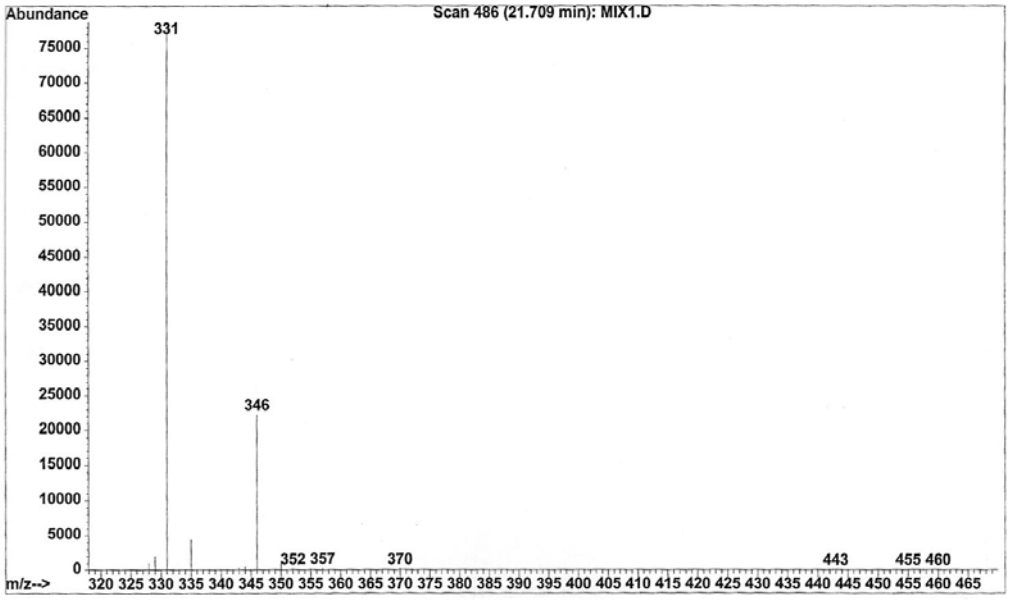

(a)

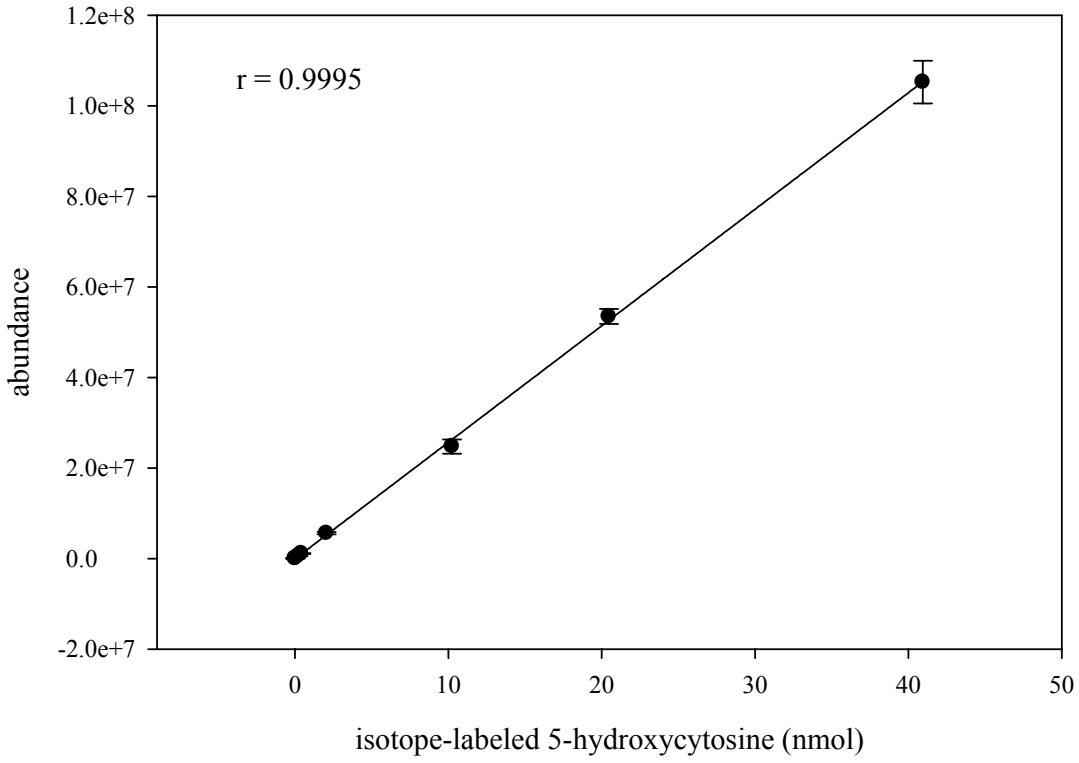

(b)

Figure 3-7. (a) A representative mass spectrum of isotope-labeled 5-hydroxycytosine (retention time 21.7 min). Figure (b) shows a standard curve of isotope-labeled 5-hydroxycytosine, which has a wide dynamic range from 2 pmol to 40 nmol.

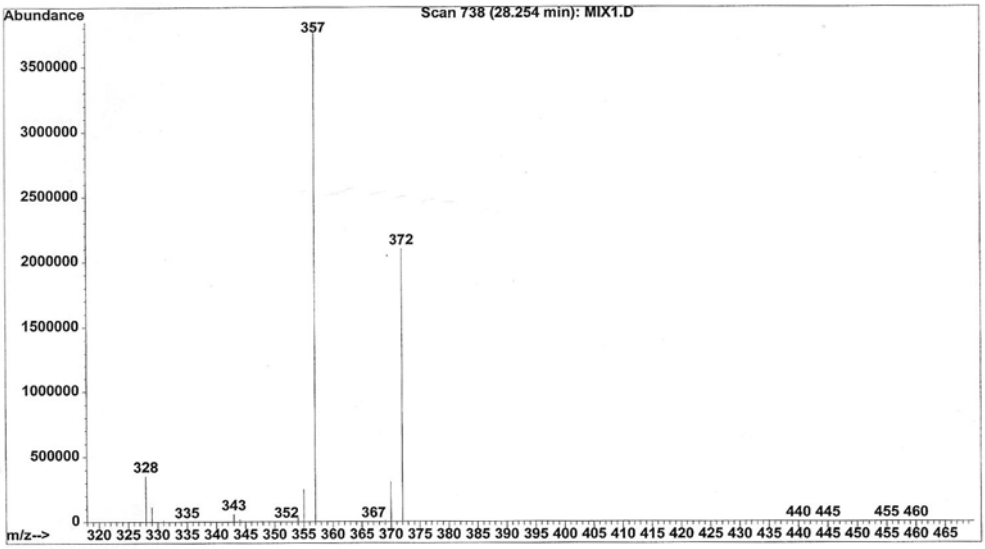

(a)

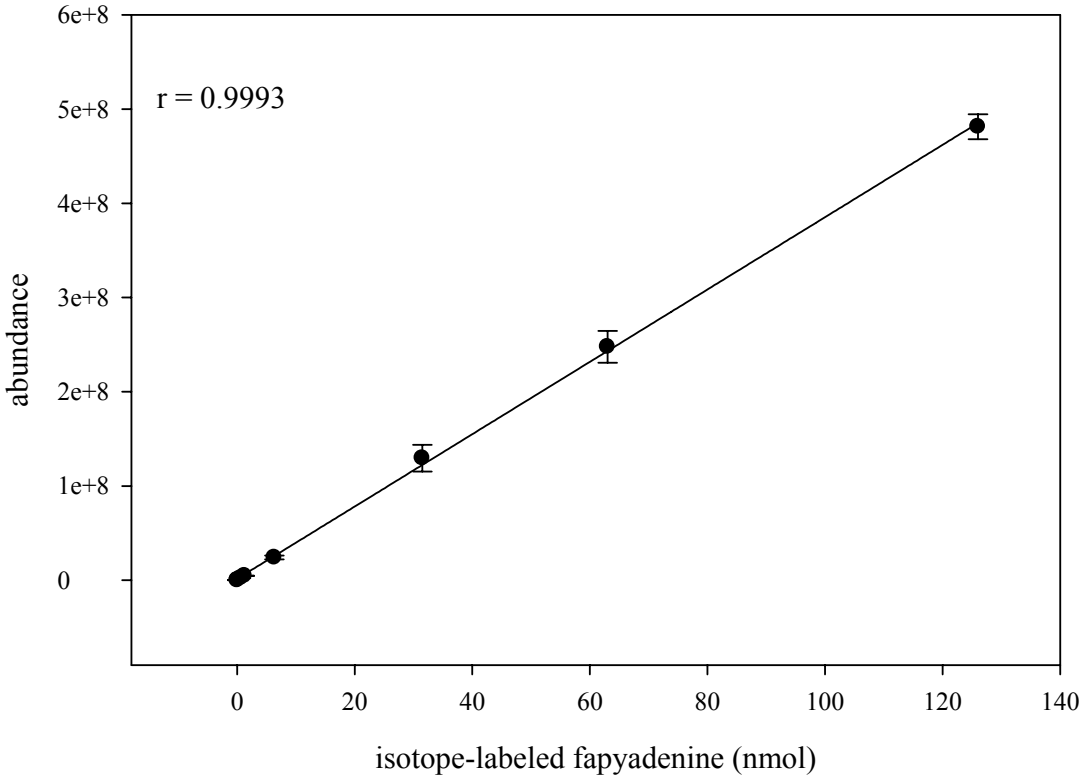

(b)

Figure 3-8. (a) A representative mass spectrum of isotope-labeled fapyadenine (retention time 28.2 min). Figure (b) shows standard curve of isotope-labeled fapyadenine, which has a wide dynamic range from 6 pmol to 120 nmol.

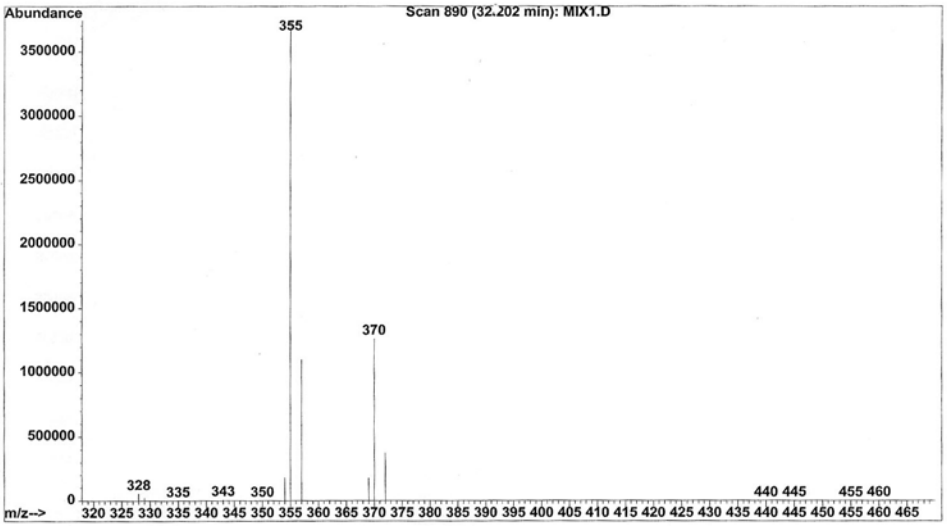

(a)

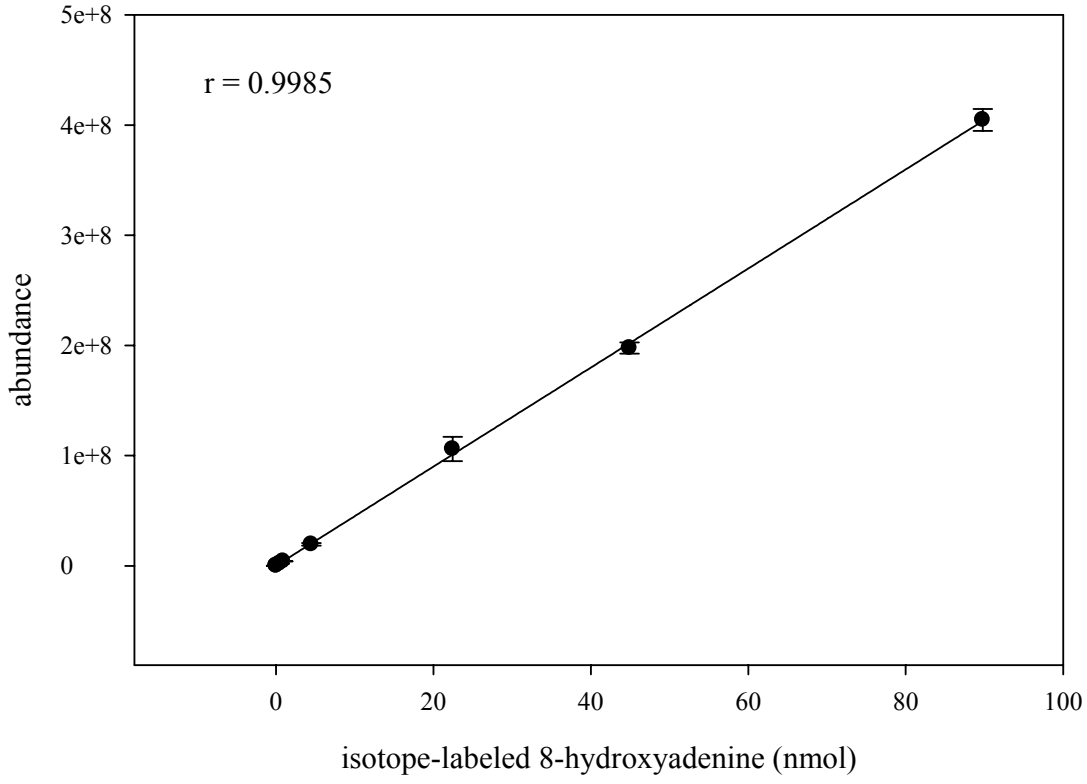

(b)

Figure 3-9. (a) A representative mass spectrum of isotope-labeled 8-hydroxyadenine (retention time 32.2 min). Figure (b) shows a standard curve of isotope-labeled 8-hydroxyadenine, which has a wide dynamic range from 4 pmol to 90 nmol.

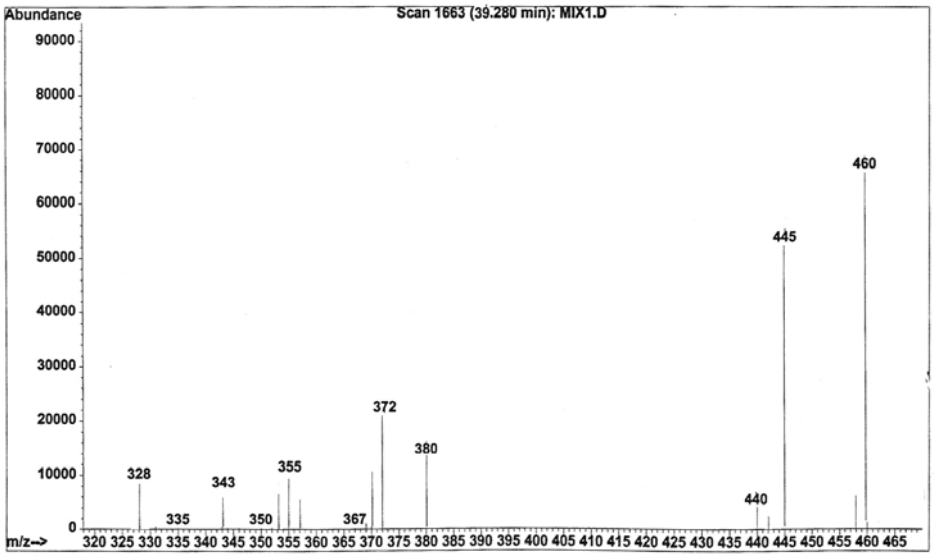

(a)

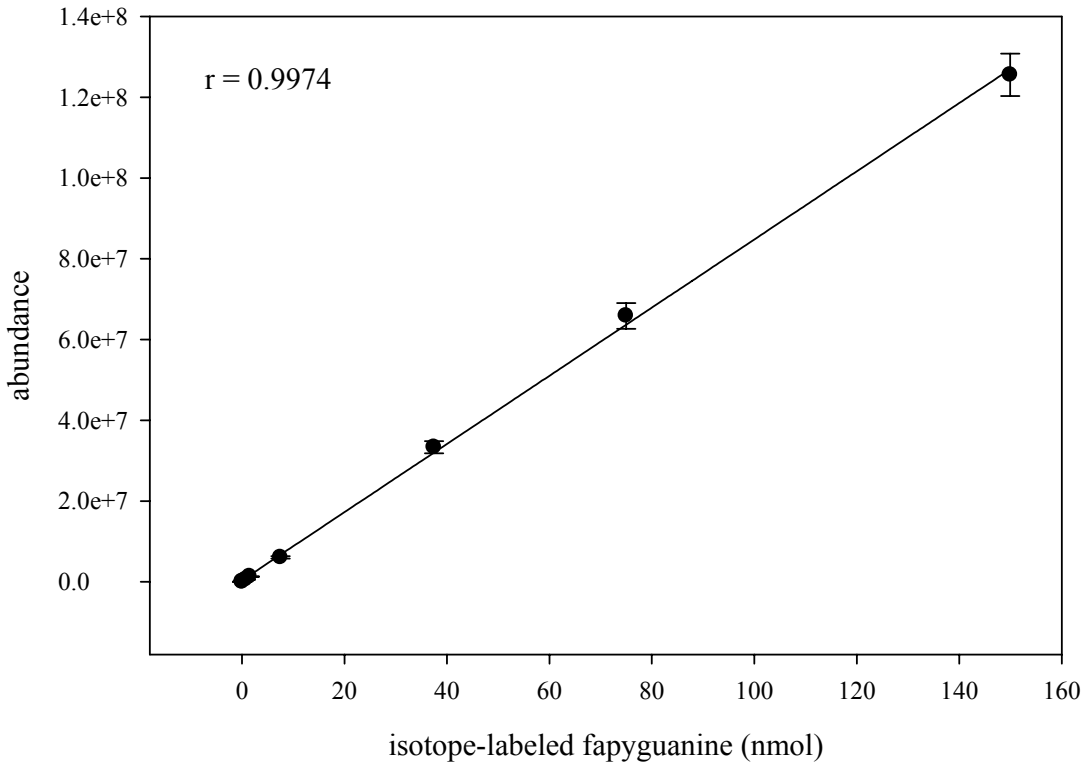

(b)

Figure 3-10. (a) A representative mass spectrum of isotope-labeled fapyguanine (retention time at 39.2 min). Figure (b) shows a standard curve of isotope-labeled fapyguanine, which has a dynamic range from 7 pmol to 150 nmol.

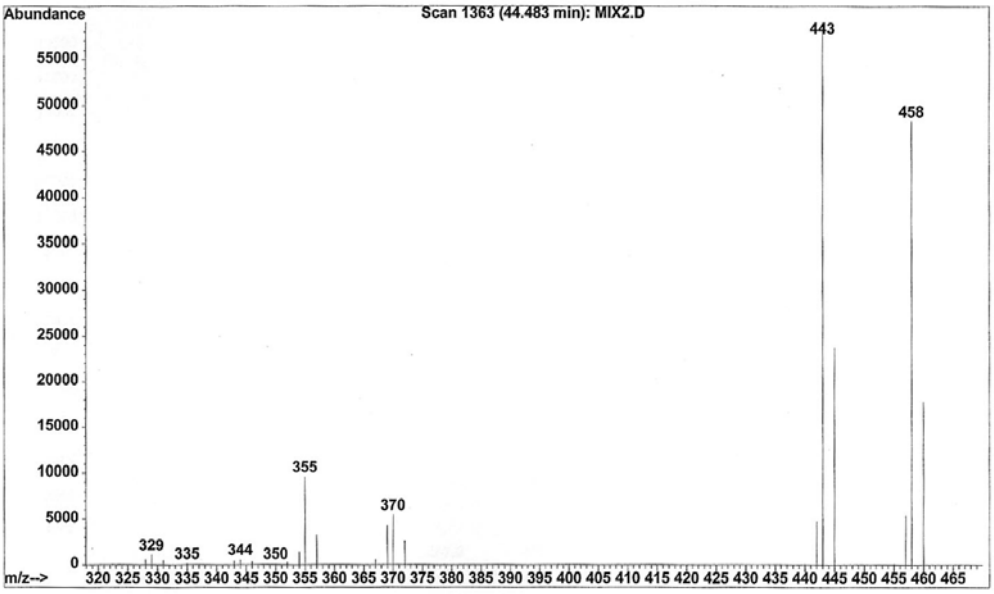

(a)

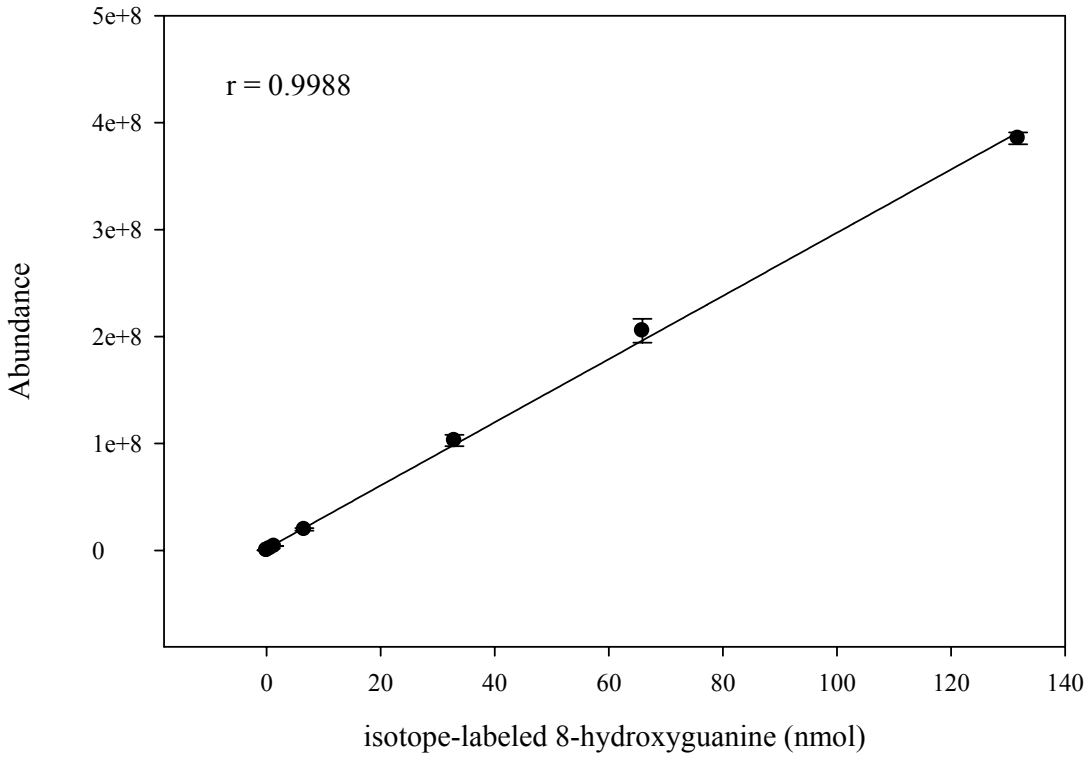

(b)

Figure 3-11. (a) A representative mass spectrum of isotope-labeled 8-hydroxyguanine (retention time 44.5 min). Figure (b) shows a standard curve of isotope-labeled 8-hydroxyguanine, which has a dynamic range from 7 pmol to 130 nmol.

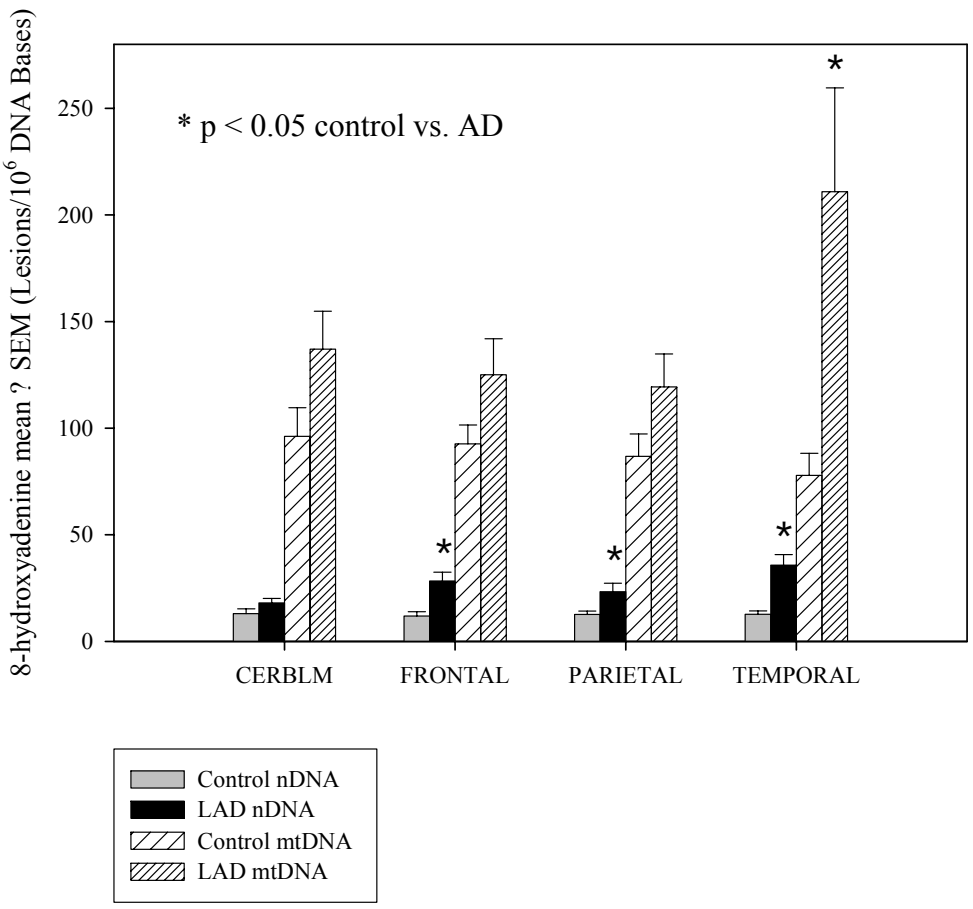

Figure 3-12. Mean regional differences in levels of 8-hydroxyadenine. Significant elevations were observed in nDNA of frontal ($p < 0.03$) and parietal ($p < 0.04$) lobes, and nDNA ($p < 0.01$) and mtDNA ($p < 0.04$) of temporal lobe. Results are expressed as mean ± SEM altered bases/10^6 bases. * $p < 0.05$

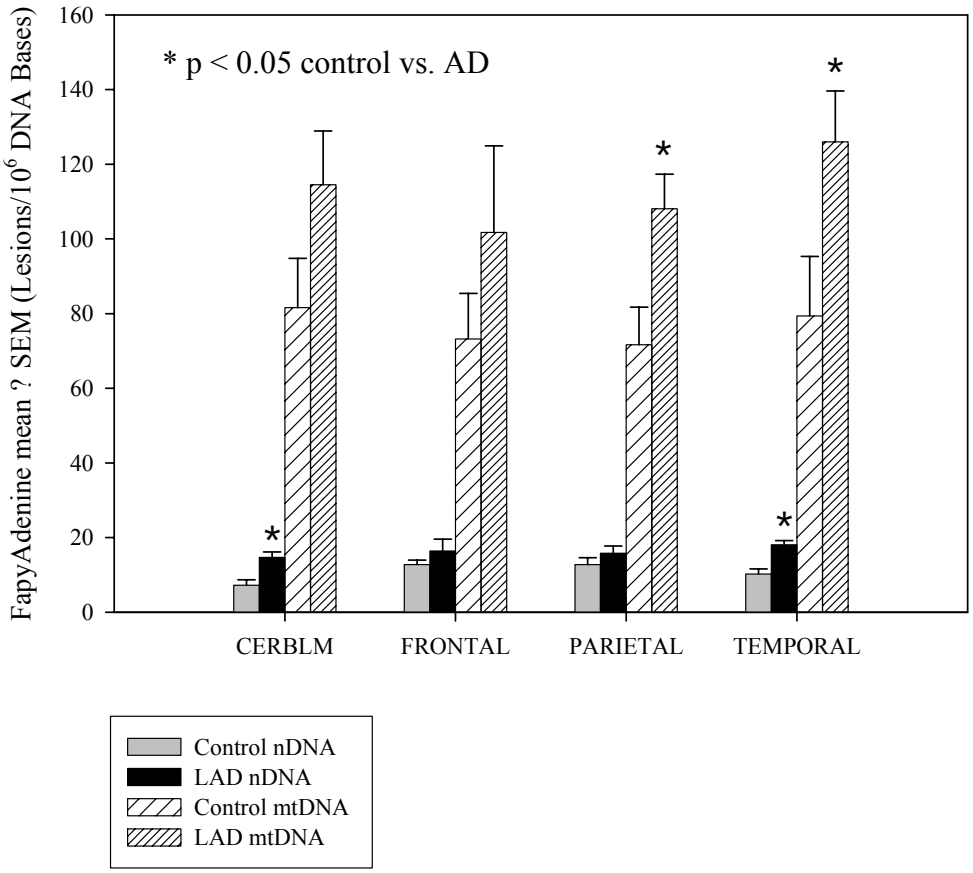

Figure 3-13. Mean regional differences in levels of fapyadenine. Significant elevations were observed in nDNA of cerebellum ($p < 0.02$), mtDNA of parietal lobe ($p < 0.05$), and nDNA ($p < 0.001$) and mtDNA ($p < 0.05$) of temporal lobe. Results are expressed as mean ± SEM altered bases/10^6 bases. * $p < 0.05$

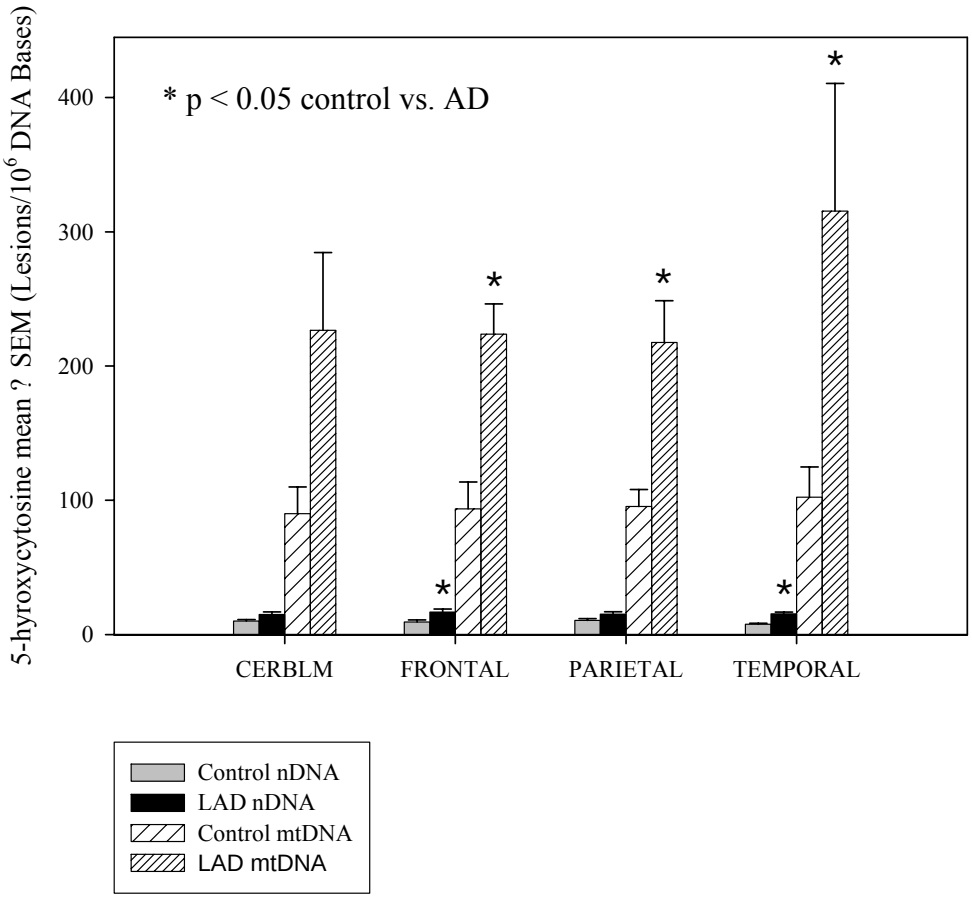

Figure 3-14. Mean regional differences in levels of 5-hydroxycytosine. 5-hydroxycytosine was significantly elevated in AD samples in nDNA ($p < 0.01$) and mtDNA ($p < 0.01$) of frontal lobe, mtDNA ($p < 0.01$) of parietal lobe and nDNA ($p < 0.001$) and mtDNA ($p < 0.05$) of temporal lobe. Results are expressed as mean ± SEM altered bases/10^6 bases. * $p < 0.05$

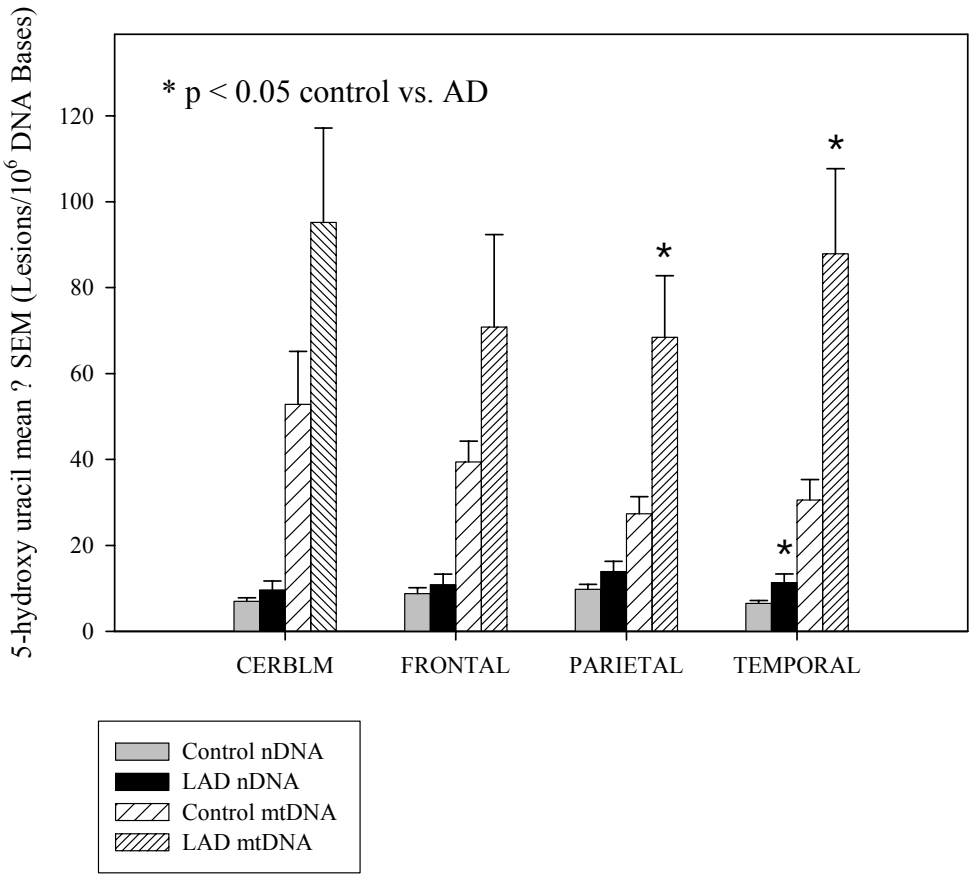

Figure 3-15. Mean regional differences in the levels of 5-hydroxyuracil. 5-hydroxyuracil was significantly elevated in mtDNA from parietal ($p < 0.05$) and temporal ($p < 0.04$) lobe of AD subjects. Results are expressed as mean ± SEM altered bases/10^6 bases. * $p < 0.05$

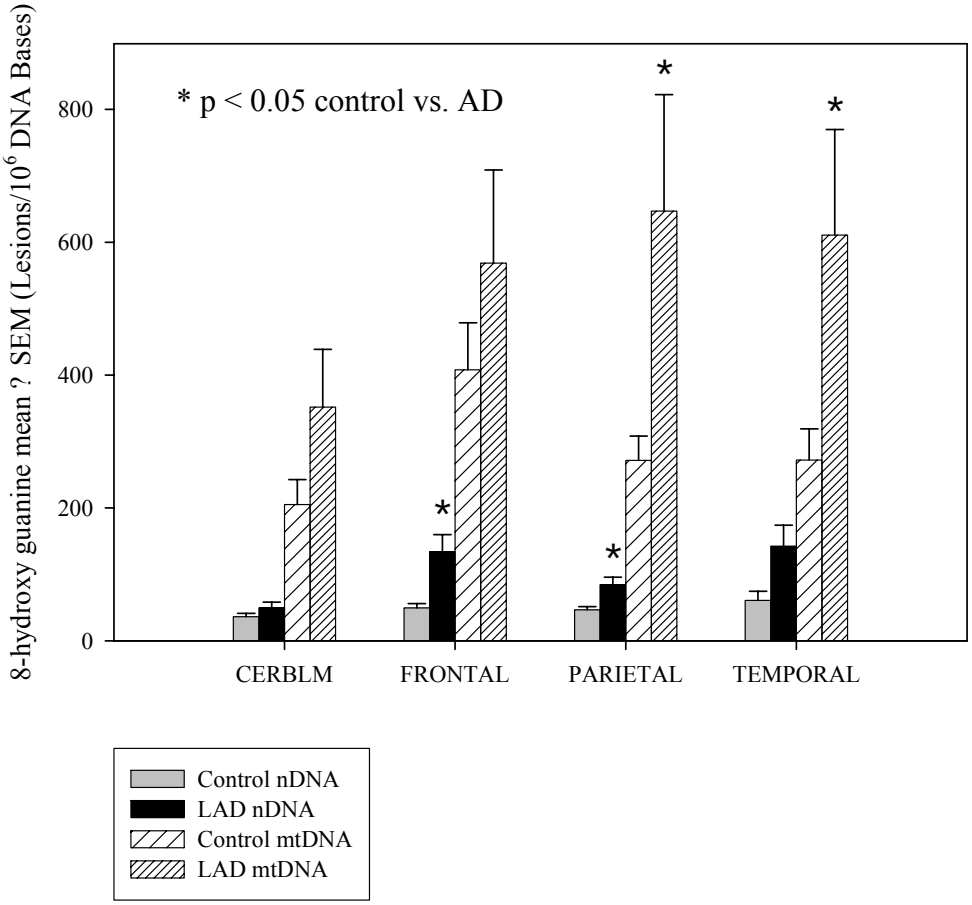

Figure 3-16. Mean regional differences in the levels of 8-hydroxyguanine. There were significant elevations of 8-hydroxyguanine in nDNA of frontal ($p < 0.03$) and parietal ($p < 0.01$) lobes and in mtDNA of parietal ($p < 0.05$) and temporal ($p < 0.05$) lobes of AD subjects. Results are expressed as mean ± SEM altered bases/10^6 bases. * $p < 0.05$

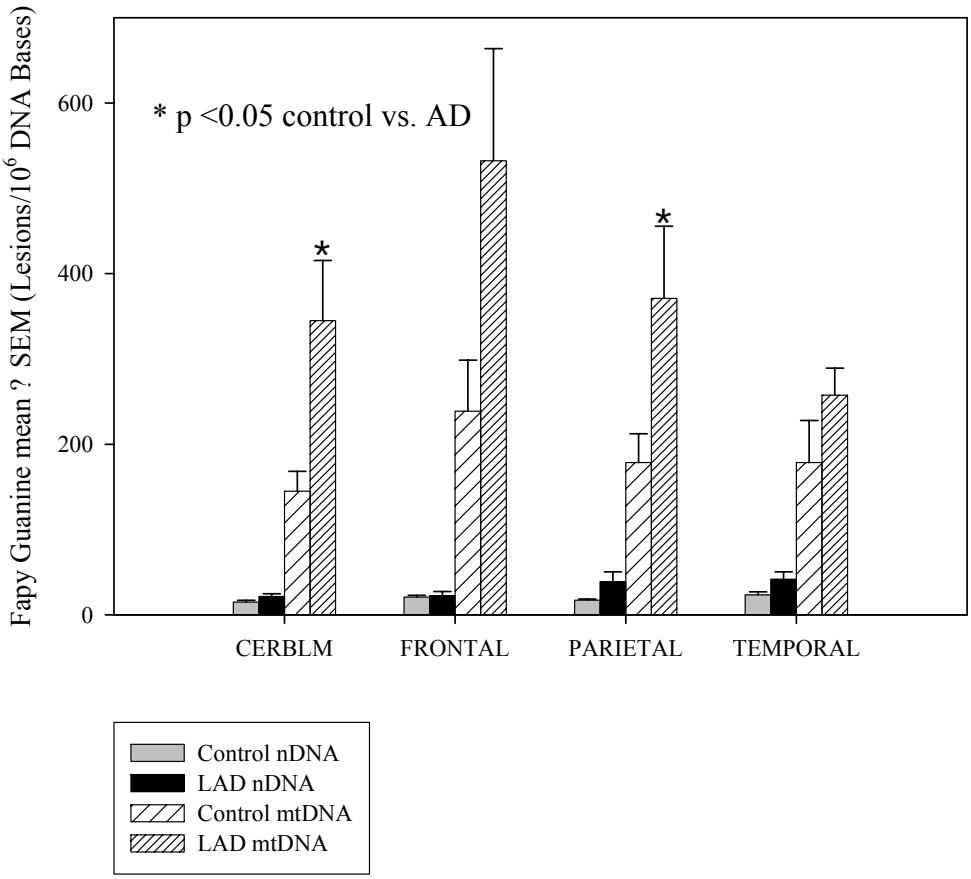

Figure 3-17. Mean regional differences in the levels of fapyguanine. Fapyguanine was significantly increased in mtDNA of cerebellum ($p < 0.04$) and parietal ($p < 0.05$) lobe of AD brain. Results are expressed as mean ± SEM altered bases/10^6 bases. * $p < 0.05$

3.2 **Increased oxidative damage in nuclear and mitochondrial DNA in Mild Cognitive Impairment**

Subject demographic data are shown in Table 3-6. There were no significant differences for age or PMI, although there was a significant difference in median Braak staging scores between control (I) and MCI (III) ($p < 0.001$) subjects.

Table 3-7 shows levels of all five base adducts expressed as the mean ± SEM number of modified bases per million DNA bases. Two-way ANOVA showed that 8-hydroxyguanine ($p < 0.04$), fapyadenine ($p < 0.001$) and 5-hydroxycytosine ($p < 0.004$) in mtDNA were significantly increased in neocortical regions compared with cerebellum in MCI (Table 3-7) but not in control subjects. A similar comparison of data for nDNA showed no significant differences between cerebellum and neocortical regions for either MCI or control subjects.

Hydroxyl radicals can adduct to C8 and C5 of guanine. The C8 attack is predominant and leads to formation of 8-hydroxyguanine. Significant elevations of 8-hydroxyguanine were observed in nDNA from frontal and parietal ($p < 0.04$) lobes and mtDNA of temporal lobe ($p < 0.05$) in MCI (Figure 3-18). Comparison of 8-hydroxyguanine in MCI mtDNA showed no significant differences between MCI and LAD subjects from our previous study (Wang *et al*. 2005) suggesting that oxidative DNA damage occurs early in the progression of AD. Fapyguanine is produced by ring opening of 8-hydroxyguanine followed by one electron reduction and was not significantly altered in mtDNA or nDNA of any MCI brain region studied compared with control subjects (Figure 3-17).

5-Hydroxycytosine, produced by free radical attack on C5 of cytosine followed by dehydration of cytosine glycol, was significantly elevated in nDNA of frontal ($p < 0.01$), parietal ($p < 0.05$) and temporal ($p < 0.01$) lobes and mtDNA of frontal lobe ($p < 0.003$) in MCI (Figure 3-18). Comparison of levels of 5-hydroxycytosine in MCI with those in late-stage AD (Wang *et al*. 2005) showed no significant differences suggesting that oxidative damage to cytosine is an early event in the pathogenesis of AD.

As shown in Figure 3-19, levels of 8-hydroxyadenine were significantly increased in MCI nDNA from frontal ($p < 0.05$), parietal ($p < 0.02$) and temporal ($p < 0.007$) lobes consistent with our observations in late-stage AD (Wang *et al*. 2005). However, no

significant differences in levels of 8-hydroxyadenine were observed in mtDNA between MCI and control subjects. These data are in contrast to our previous study of late-stage AD subjects that showed a significant elevation of 8-hydroxyadenine in mtDNA from late-stage AD temporal lobe (Wang *et al*. 2005). Figure 3-20 shows that levels of fapyadenine were significantly elevated in both nDNA and mtDNA of frontal, parietal and temporal lobes in MCI compared with age-matched control subjects. Levels of 8-hydroxyadenine and fapyadenine in MCI were not significantly different from those observed in our previous study of late-stage AD brain (Wang *et al*. 2005).

Table 3-6. Demographic data for control and MCI subjects

	Number and sex	Age (yr) (mean ± SEM)	PMI (hr) (mean ± SEM)	Braak Score (median)	ApoE genotype
Control	N=6 (3F, 3M)	81.0 ± 3.8	3.0 ± 0.4	I	E3/E3, N=6
MCI	N=8 (6F, 2M)	89.5 ± 4.8	4.0 ± 0.9	III*	E3/E3, N=6 E4/E4, N=2

* $p < 0.05$ control vs. MCI

Table 3-7. Levels of DNA oxidation in nuclear and mitochondrial DNA in MCI and age-matched control subjects

	Level of modified bases (Lesions/10^6 DNA Bases, mean ± SEM)			
	Nuclear DNA		Mitochondrial DNA	
	control	MCI	control	MCI
Cerebellum				
8-OH-guanine	40.8 ± 6.9	95.2 ± 38.0	227.1 ± 35.5	307.2 ± 75.9
Fapyguanine	6.5 ± 1.8	21.0 ± 9.6	131.2 ± 33.2	133.4 ± 9.6
5-OH-cytosine	11.6 ± 1.2	20.7 ± 4.9	92.5 ± 23.2	124.2 ± 4.8
8-OH-adenine	12.9 ± 2.5	16.7 ± 5.9	50.8 ± 11.2	47.2 ± 4.9
Fapyadenine	14.9 ± 2.6	20.8 ± 4.5	75.3 ± 17.1	72.2 ± 5.3
Frontal lobe				
8-OH-guanine	50.4 ± 7.8	143.8 ± 53.4*	262.7 ± 64.9	329.4 ± 128.6$^{\#}$
Fapyguanine	20.5 ± 2.3	19.9 ± 1.2	187.2 ± 75.1	237.3 ± 48.5
5-OH-cytosine	8.2 ± 1.0	32.8 ± 6.6*	78.0 ± 15.9	257.8 ± 37.4*$^{\#}$
8-OH-adenine	12.2 ± 2.3	24.1 ± 4.9*	42.5 ± 12.5	53.1 ± 15.4
Fapyadenine	12.9 ± 1.3	27.8 ± 5.2*	72.6 ± 16.7	158.1 ± 9.6*$^{\#}$
Parietal lobe				
8-OH-guanine	46.4 ± 6.0	149.1 ± 41.4*	293.0 ± 45.0	343.0 ± 63.9$^{\#}$
Fapyguanine	16.6 ± 1.5	18.3 ± 0.9	158.8 ± 41.3	158.5 ± 20.1
5-OH-cytosine	10.0 ± 1.3	35.3 ± 9.9*	88.1 ± 13.4	92.7 ± 23.2$^{\#}$
8-OH-adenine	12.5 ± 1.6	26.2 ± 4.3*	64.4 ± 18.3	74.6 ± 9.2
Fapyadenine	12.5 ± 1.7	40.7 ± 9.1*	77 ± 12.6	158.8 ± 10.4*$^{\#}$
Temporal lobe				
8-OH-guanine	69.0 ± 18.4	135.1 ± 22.7	271.5 ± 46.9	460.3 ± 83.5*$^{\#}$
Fapyguanine	22.0 ± 4.5	21.4 ± 1.4	127.4 ± 50.4	159.6 ± 16.9
5-OH-cytosine	8.1 ± 0.9	24.5 ± 4.6*	107.0 ± 29.6	187.4 ± 50.5$^{\#}$
8-OH-adenine	14.2 ± 1.6	25.8 ± 2.9*	48.8 ± 10.0	66.5 ± 9.9
Fapyadenine	10.3 ± 1.6	29.1 ± 5.5*	69.8 ± 19.7	177.1 ± 10.8*$^{\#}$

* $p < 0.05$ significant elevation in MCI DNA compared to age matched control subjects
$^{\#}$ $p < 0.05$ significant elevations in DNA from frontal, parietal and temporal lobes compared to cerebellum.

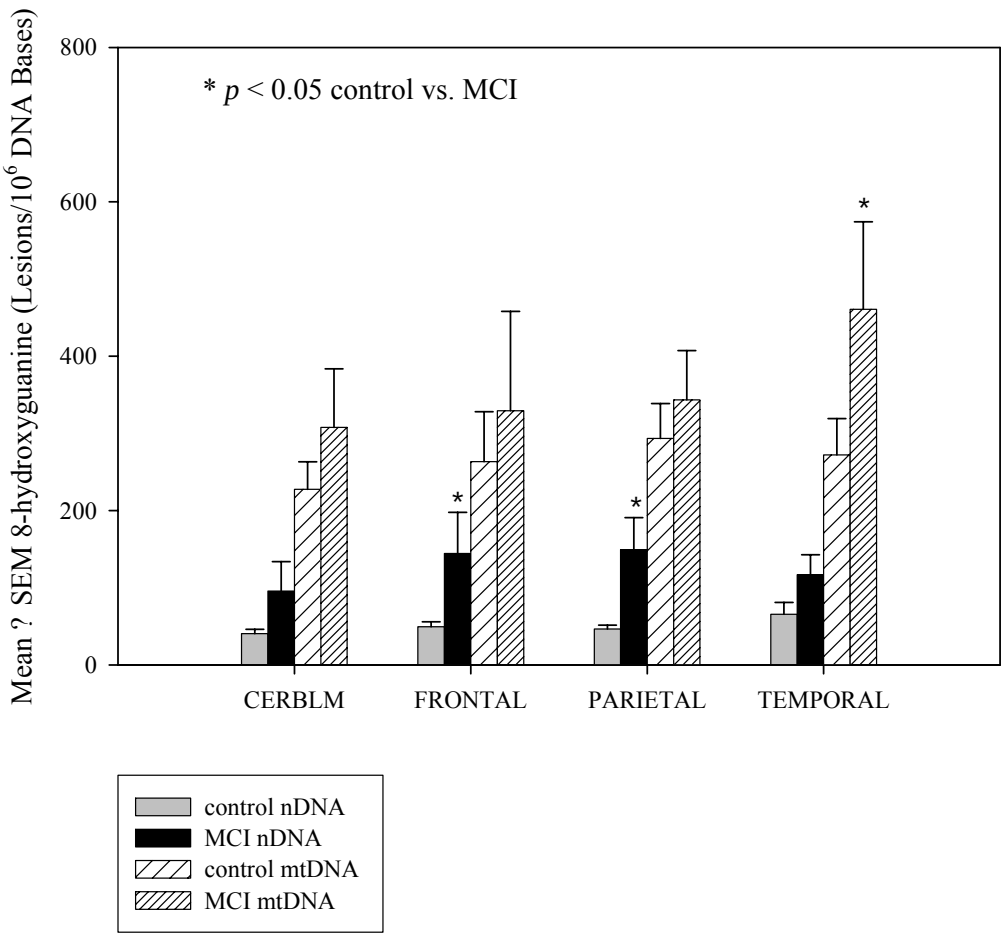

Figure 3-18. Mean regional levels of 8-hydroxyguanine. There was a statistically significant elevation of 8-hydroxyguanine in MCI in nDNA of frontal ($P < 0.05$) and parietal ($P < 0.04$) lobes, and mtDNA of temporal lobe ($P < 0.05$). Results are expressed as mean ± SEM altered bases/10^6 bases. * $P < 0.05$

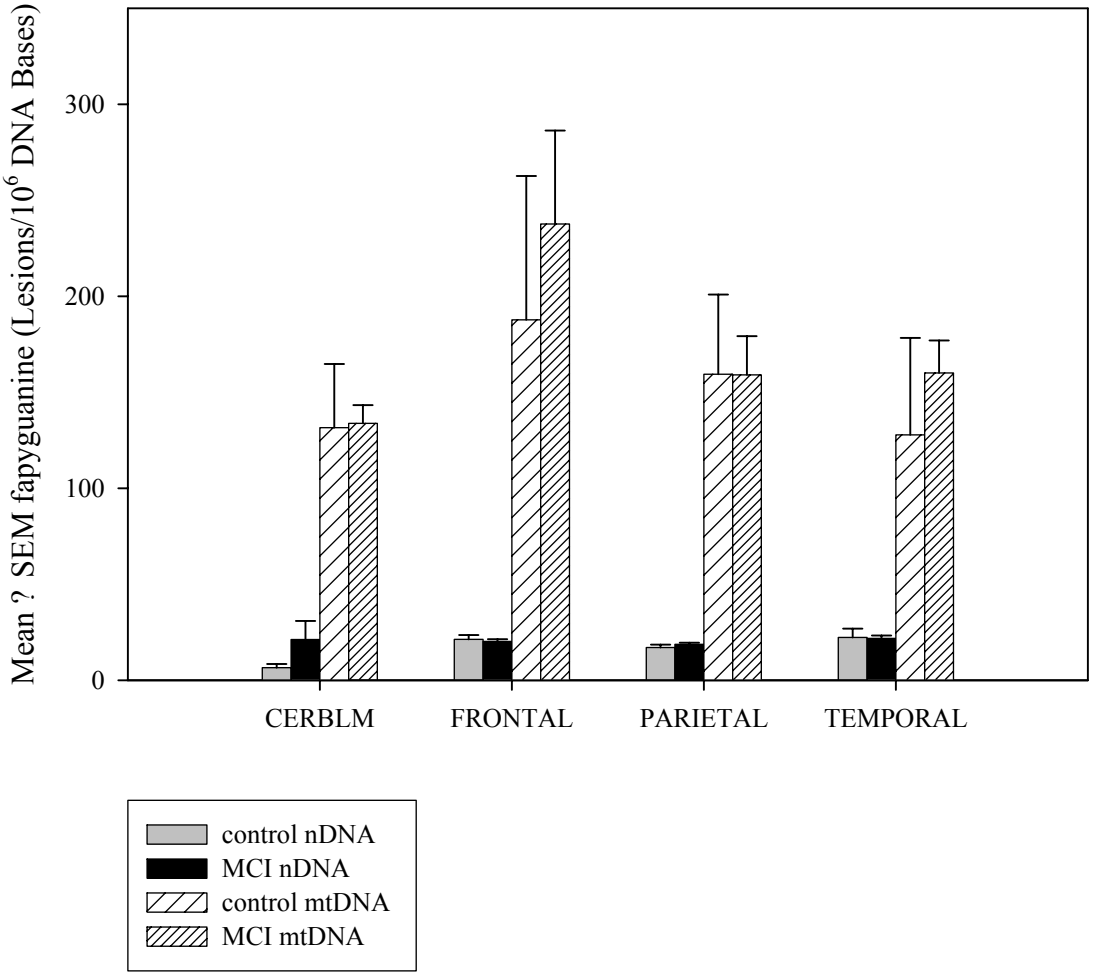

Figure 3-19. Mean regional differences in levels of fapyguanine. Results are expressed as mean ± SEM altered bases/10^6 bases. * $P < 0.05$

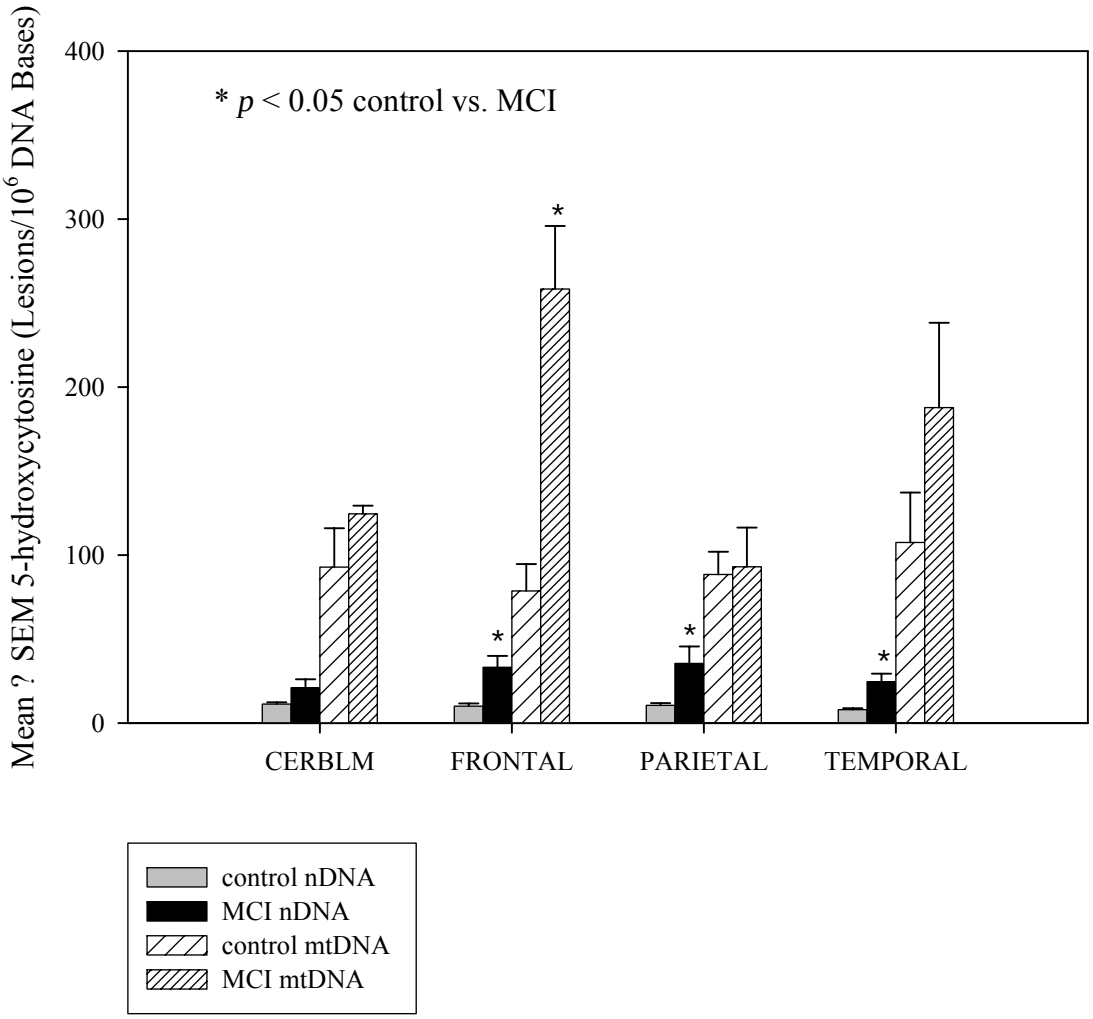

Figure 3-20. Mean regional differences in levels of 5-hydroxycytosine. There were significant elevations in MCI in nDNA of frontal ($P < 0.01$), parietal ($P < 0.05$) and temporal ($P < 0.01$) lobes, and mtDNA of frontal lobe ($P < 0.003$) compared to age-matched control subjects. Results are expressed as mean ± SEM altered bases/10^6 bases. * $P < 0.05$

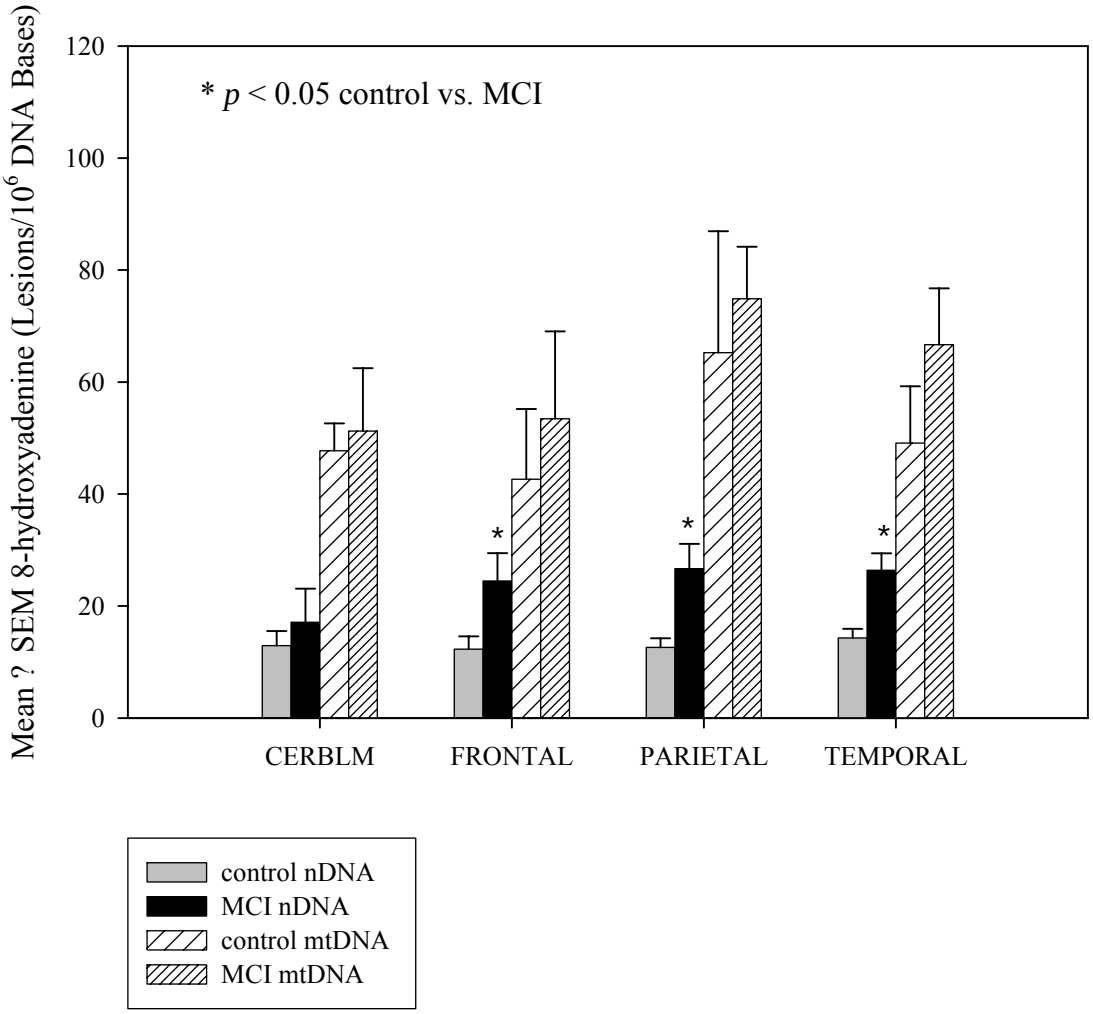

Figure 3-21. Mean regional levels of 8-hydroxyadenine. There were significant elevations in nDNA of frontal ($P < 0.05$), parietal ($P < 0.02$), and temporal ($P < 0.007$) lobes. Results are expressed as mean ± SEM altered bases/10^6 bases. * $P < 0.05$

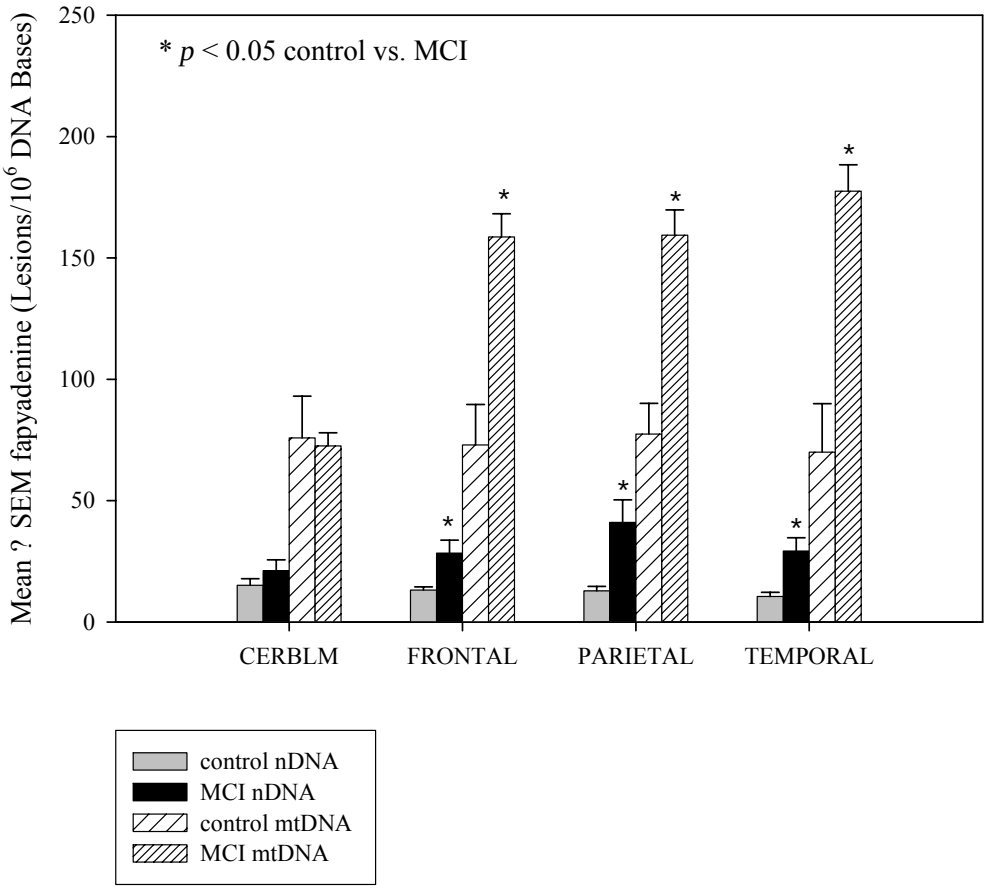

Figure 3-22. Mean regional differences in levels of fapyadenine. There were significant elevations in MCI in nDNA of frontal ($P < 0.02$), parietal ($P < 0.02$) and temporal ($P < 0.02$) lobes, and mtDNA of frontal ($P < 0.0007$), parietal ($P < 0.0002$) and temporal ($P < 0.0002$) lobes. Results are expressed as mean ± SEM altered bases/10^6 bases. * $P < 0.05$

3.3 Increased oxidative damage in nuclear DNA in APP/PS1 transgenic mice

To evaluate the effects of Aβ deposition on DNA oxidation, one third of cortex from APP/PS1 (ages 3, 6, 9, 12 months) and wild type mice were used for the analysis of oxidative damage to nDNA. Each group consisted of 8 to 10 mice. Damage to nDNA was quantified in this study because the brain tissue was too small to get enough mtDNA for GC/MS-SIM analysis. Phenol-chloroform extraction was used in nDNA extraction as previously described.

Figure 3-23 shows amounts of oxidized DNA base adducts expressed as the mean ± SEM number of modified bases per million DNA bases. Levels of 8-hydroxyguanine were consistently higher than the levels of 8-hydroxyadenine both in wild type and APP / PS1 mice ($p < 0.001$).

C8 attack on guanine by hydroxyl radicals leads to formation of 8-hydroxyguanine, the most studied adduct in DNA oxidation. Significant elevations of 8-hydroxyguanine in 12-month old APP / PS1 mice ($p < 0.05$) compared to 12-month WT were observed (Figure 3-23). Hydroxyl radical attack on C8 of adenine leads to production of 8-hydroxyadenine. No significant change was observed between wild type and APP / PS1 mice at any age (Figure 3-23). Using ANOVA there was no significant age-dependent changes observed.

Aβ plaque counts were performed by Dr. WR Markesbery's laboratory (Table 3-8). A statistically significant positive correlation between plaque counts and the levels of 8-hydroxyguanine in APP / PS1 mice was observed (r = 0.90).

Table 3-8. Aβ plaque burden of WT and APP/PS1 mice

	3 month	6 month	9 month	12 month
WT	0	0	0	0
APP/PS1	0	0.81 ± 0.12*	1.37 ± 0.13*	1.88 ± 0.13*

* $p < 0.05$ WT vs. APP/PS1

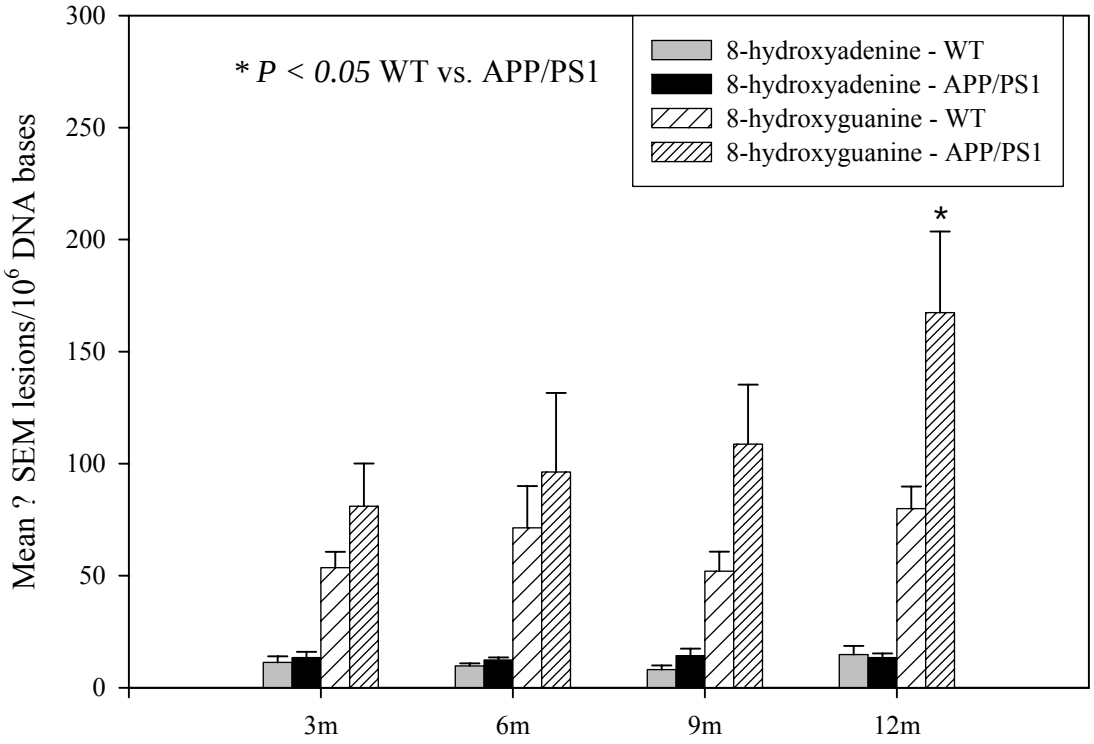

Figure 3-23. Mean levels of 8-hydroxyadenine and 8-hydroxyguanine in APP/PS1 and WT mice. There was significant elevations in the level of 8-hydroxyguanine in APP/PS1 in nDNA of 12-month mice compared to wild type. Results are expressed as mean ± SEM altered bases/10^6 bases. No significant difference was observed in levels of 8-hydroxyadenine. * $P < 0.05$

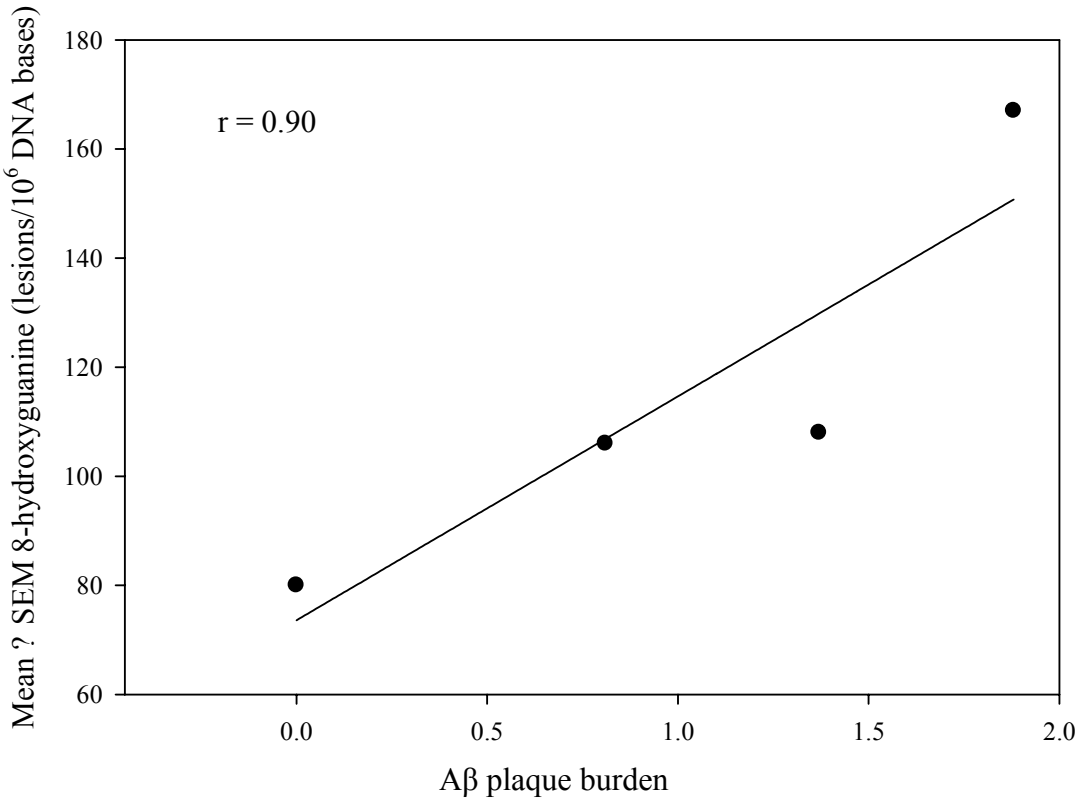

Figure 3-24. A positive correlation between plaque counts and the levels of 8-hydroxyguanine in APP/PS1 mice (r = 0.90)

3.4 Proteomic studies of mitochondria in Alzheimer's disease

Based on our previous DNA studies, protein expression in mitochondria was expected to be altered in LAD. Proteomics is an efficient way to study these changes. In this study, mitochondrial proteins from temporal pole specimens of 5 LAD (3 female, 2 male) and 4 (2 female, 2 male) age-matched control subjects were analyzed. Subject demographic data are shown in Table 3-9. There were no significant differences in age or PMI between LAD and control subjects using Student's *t*-test. There was a significant difference in median Braak staging scores between control (I) and LAD (VI) ($p < 0.001$) subjects.

Mitochondrial protein was isolated using Percoll gradient centrifugation as previously described. 500 μg protein was used for 2D gel electrophoresis. After Sypro ruby staining, ~650 protein spots on each gel were detected by PDQuest software. A representative gel is shown in figure 3-24. An IPG strip (pH 3-10 nonlinear) was used in the first dimension and an 8-16% SDS gel was used to separate proteins in the second dimension. Proteins identified were labeled on gel (Figure 3-24). Molecular weights of mitochondrial proteins detected ranged from 10 to 80 kDa.

A MALDI mass spectrum for a representative protein spot is shown in figure 3-25. Every peak in the spectrum represents a specific peptide which was characterized by its m/z value. The mass of peptides in the mass spectrum ranged from 800 to 2,000 Da. MS data were submitted to the Mascot database in the form of peptide mass fingerprint (PMF). By comparing these experimental data to the existing calculated peptide mass, the matched proteins were identified. Only proteins with the lowest probability were assigned as the best match. In this study, a Mowse score $\geqslant$ 52 was considered a significant match ($p < 0.05$). Figure 3-26 shows the probability based Mowse score of ATP synthase beta chain protein. 176 spots were identified and listed alphabetically in Table 3-10 out of ~250 intense spots excised manually and analyzed. 116 out of 176 spots were unique proteins (Table 3-10).

Of the spots identified as differentially expressed, 116 spots representing 67 proteins were mitochondrial proteins. 23 spots were cytoplasmic proteins which represent 18 different proteins. 10 spots represented 7 endoplasmic reticulum proteins. 6

spots were 6 nuclear proteins. 2 spots were 1 lysosomal protein. Results were expressed based on protein's subcellular locations (Figure 3-27).

The 66 mitochondrial proteins were classified into 11 categories based on function (Figure 3-28). 70% of these proteins were involved in oxidative phosphorylation (OXPHOS), redox, tricarboxylic acid (TCA) cycle, carbohydrate metabolism, nucleotide metabolism, lipid metabolism and glycolysis. The remaining 30% were involved in DNA/RNA/protein synthesis, signaling proteins, targeting proteins, and transporter proteins.

Student's *t* test was used to compare alterations in protein expression. 10 of 116 proteins were found to be significantly different in LAD brain ($p < 0.05$) (Table 3-11). Two cytoplasmic proteins were significantly increased in LAD. Five mitochondrial proteins were significantly decreased in LAD, in which 2 mitochondria-encoded proteins from mitochondrial inner membrane were highlighted. One nuclear, one ER, and one cytoplasmic protein were significantly decreased in LAD brain.

Western blots were used to verify proteomics results for representative proteins. Because no commercial antibodies were available for the significantly altered proteins, we used rabbit anti-VDAC and rabbit anti-CNPase for Western analysis. No significant difference was observed in Western blots for either protein, which were consistent with our findings using 2D gel analysis (Figure 3-29).

Table 3-9**.** Demographic data of LAD and control subjects

	Number and sex	Age (mean ± SEM)	PMI (mean ± SEM)	Braak Score (median)
Control	N=4 (2F, 2M)	82.8 ± 3.9	2.9 ± 0.5	I
LAD	N=5 (3F, 2M)	88.2 ± 3.6	3.8 ± 0.9	VI*

* $p < 0.05$ control vs. LAD

Table 3-10. Protein spots identified with MALDI-TOF MS in two-dimensional gels

Spot #	Protein name	Acce-ssion Number	Mowse score	Sequen-ce Covera-ge (%)	M.W (Da)	PI	Subcellular Location
4403	26S protease regulatory subunit 8	P47210	52	20	45,597	7.11	Cytoplasmic and nuclear
6102	39S ribosomal protein L12, mitochondrial [Precursor]	P52815	55	19	21,335	9.04	Mitochondrial
7303	3-hydroxyacyl-CoA dehydrogenase type II	Q99714	95	43	26,906	7.66	Mitochondrial
7901 7902 7903	Aconitate hydratase, mitochondrial [Precursor]	Q99798	55 56 65	10 10 11	85372	7.36	Mitochondrial
1505 2502	Actin, cytoplasmic 1	P02570	123 129	32 33	41,710	5.29	Cytoplasmic
9304	Adenylate kinase isoenzyme 4, mitochondrial	P27144	76	33	25,252	8.47	Mitochondrial matrix
2806	Alanyl-tRNA synthetase	P49588	52	5	106734	5.31	Cytoplasmic
3808 4701 4702	Aldehyde dehydrogenase, mitochondrial [Precursor]	P05091	106 80 125	23 17 18	56,346	6.63	Mitochondrial matrix
5205	Alpha crystallin B chain	P02511	76	26	20,146	6.76	Unknown
6601	Alpha enolase	P06733	62	18	47,002	6.99	Cytoplasmic
1402	Annexin A5	P08758	212	47	35,783	4.94	Unknown
0805 5503 8702 8705 8706 9503 9504 1401 1701	ATP synthase alpha chain, mitochondrial [Precursor]	P25705	54 103 196 215 123 62 153 124 191	20 22 36 39 26 10 27 33 40	59,714	9.16	mitochondrial inner membrane

Table 3-10. (continued)

0206	ATP synthase D chain, mitochondrial	O75947	67	43	18,348	5.22	Mitochondrial
9008	ATP synthase E chain, mitochondrial	P56385	76	76	7,797	9.34	Mitochondrial
9205	ATP synthase O subunit, mitochondrial [Precursor]	P48047	121	52	23,263	9.97	Mitochondrial matrix
8102 8103	ATPase inhibitor, mitochondrial [Precursor]	Q9UII2	60 58	33 35	12,241	9.34	Mitochondrial
0804	Calreticulin [Precursor]	P27797	89	19	48,112	4.29	cytoplasmic
2402 2404	Cathepsin D [Precursor]	P07339	64 70	16 18	44,524	6.10	Lysosomal
2605	Creatine kinase B-type	P12277	107	27	42,617	5.34	Cytoplasmic
7501 7502 8501	Creatine kinase, ubiquitous mitochondrial [Precursor]	P12532	106 106 53	26 26 16	47,007	8.60	Mitochondrial inner membrane; outer side
7301	CTD small phosphatase-like protein	O15194	57	13	37,851	8.95	Nuclear
3603	cyclic-nucleotide 3'-phosphodiesterase	P09543	58	12	47,579	8.90	Mitochondrial
4004	Cytochrome c oxidase polypeptide VIb	P14854	55	47	10,055	6.78	Mitochondrial
6803 6804	Delta-1-pyrroline-5-carboxylate dehydrogenase, mitochondrial [Precursor]	P30038	73 181	7 33	61,713	8.25	Mitochondrial matrix
5804 6801 6802	Dihydrolipoyl dehydrogenase, mitochondrial [Precursor]	P09622	103 54 64	24 11 15	54,116	7.59	Mitochondrial matrix

Table 3-10. (continued)

4710	Dihydrolipoyllysine-residue succinyltransferase component of 2-oxoglutarate dehydrogenase complex, mitochondrial [Precursor]	P36957	131	25	48,609	9.01	Mitochondrial
3806	Dihydropyrimidinase related protein-2	Q16555	76	16	62,255	5.95	Cytoplasmic
3506	DNA topoisomerase I, mitochondrial [Precursor]	Q969P6	54	18	69,828	9.46	Mitochondrial
4402	Dolichyl-phosphate beta-glucosyltransferase	Q9Y673	56	10	36,922	9.34	Endoplasmic reticulum
7401	Electron transfer flavoprotein alpha-subunit, mitochondrial [Precursor]	P13804	60	17	35,058	8.62	Mitochondrial matrix
8304	Electron transfer flavoprotein beta-subunit	P38117	86	32	27,826	8.24	Mitochondrial matrix
5602 5604 5605	Elongation factor Tu, mitochondrial [Precursor]	P49411	80 156 215	20 35 41	49,510	7.26	Mitochondrial
4303	Endoplasmic reticulum protein ERp29 [Precursor]	P30040	84	33	28,975	6.77	Endoplasmic reticulum
0802	Endoplasmin [Precursor]	P14625	130	22	92,411	4.76	ER
0403	Fatty aldehyde dehydrogenase	P51648	53	12	54,813	7.98	cytoplasmic
7105	Fibroblast growth factor-20	Q9NP95	53	22	23,484	8.89	Secreted
3203	Fibroblast growth factor-8 [Precursor]	P55075	53	20	26,509	10.44	Unknown

Table 3-10. (continued)

8502	Fructose-bisphosphate aldolase	P04075	53	8	39,264	8.39	Mitochondrial
6501	Fructose-bisphosphate aldolase C	P09972	124	32	39,300	6.46	Mitochondrial
6602 6603 7601 7602	Fumarate hydratase, mitochondrial [Precursor]	P07954	63 52 167 167	18 12 30 30	54,602	8.85	Mitochondrial and cytoplasmic
1101	Galectin-1	P09382	53	38	14,575	5.34	Unknown
5702 5703 5704 7701	Glutamate dehydrogenase 1, mitochondrial [Precursor]	P00367	75 134 68 135	18 28 13 29	61,359	7.66	Mitochondrial matrix
6701 6703	Glutamate dehydrogenase 2, mitochondrial [Precursor]	P49448	52 114	10 20	61,395	8.63	Mitochondrial matrix
5805 5809	Glycerol-3-phosphate dehydrogenase, mitochondrial [Precursor]	P43304	90 33	16 11	80,764	6.98	Mitochondrial
9305	GTP:AMP phosphotransferase mitochondrial	Q9UIJ7	131	48	25,419	9.16	Mitochondrial matrix
4005	Guanine nucleotide-binding protein G(I)/G(S)/G(O) gamma-5 subunit	P63218	48	30	7,314	9.90	Mitochondrial
1504 3502	Guanine nucleotide-binding protein G(I)/G(S)/G(T) beta subunit 1	P62873	53 53	12 12	37,353	5.60	Mitochondrial
1403	Guanine nucleotide-binding protein G(I)/G(S)/G(T) beta subunit 2	P62879	61	17	37,307	5.60	Mitochondrial
1501	Heat shock cognate 71 kDa protein	P11142	76	10	70,898	7.80	Cytoplasmic

Table 3-10. (continued)

9004	heat shock protein (10 kDa), mitochondrial	Q04984	95	59	10,794	8.91	Mitochondrial matrix
1801 2801 2802 2803 2808	heat shock protein (60 kDa), mitochondrial [Precursor]	P10809	79 199 82 129 199	16 34 18 22 26	61,016	5.70	Mitochondrial matrix
7004	heat shock protein1 (10 kDa), mitochondrial	P61604	87	39	10,794	8.91	Mitochondrial matrix
1901	Huntingtin interacting protein 1	O00291	53	7	115404	5.20	Cytoplasmic
4807	Hypothetical protein KIAA0555	Q96AA8	58	7	94,875	5.88	Unknown
0107	hypothetical RNA-binding protein	P42696	54	21	25,187	9.75	nuclear
9007	Hypoxia-inducible gene protein 2	Q9Y5L2	52	31	6,946	6.72	Unknown
3604	Inositol 1,4,5-trisphosphate receptor type 1	Q14643	73	6	313945	7.20	Endoplasmic reticulum
8604	Isocitrate dehydrogenase [NADP], mitochondrial [Precursor]	P48735	52	16	50,877	8.88	Mitochondrial
5701	Lipoamide acyltransferase component of branched-chain alpha-keto acid dehydrogenase complex, mitochondrial [Precursor]	P11182	122	26	53,453	8.71	Mitochondrial matrix

Table 3-10. (continued)

6805	Methylcrotonoyl-CoA carboxylase beta chain, mitochondrial [Precursor]	Q9HCC0	112	20	61,294	7.57	Mitochondrial matrix
7801 8801 8802	Methylmalonate-semialdehyde dehydrogenase [acylating], mitochondrial [Precursor]	Q02252	93 57 109	15 10 21	57,803	8.72	Mitochondrial
5504	Mitochondrial 28S ribosomal protein S22	P82650	159	34	41,254	7.70	Mitochondrial
5501	Mitochondrial import inner membrane translocase subunit TIM9 A	Q9Y5J7	52	47	10,371	6.71	Mitochondrial inner membrane
2506	Myosin Id	O94832	55	12	78740	9.58	Unknown
7102	NADH-ubiquinone oxidoreductase 13 kDa-A subunit, mitochondrial [Precursor]	O75380	53	34	13,703	8.59	inner membrane
3102	NADH-ubiquinone oxidoreductase 13 kDa-B subunit	Q16718	68	40	13,327	5.70	Mitochondrial inner membrane
1204	NADH-ubiquinone oxidoreductase 23 kDa subunit, mitochondrial [Precursor]	P80269	105	23	23,690	6.00	mitochondrial inner membrane
4201	NADH-ubiquinone oxidoreductase 24 kDa subunit, mitochondrial [Precursor]	P19404	62	27	27,374	8.22	mitochondrial inner membrane

Table 3-10. (continued)

2302	NADH-ubiquinone oxidoreductase 30 kDa subunit, mitochondrial [Precursor]	O75489	52	16	30,223	6.69	Mitochondrial inner membrane
5603	NADH-ubiquinone oxidoreductase 39 kDa subunit, mitochondrial [Precursor]	Q16795	52	14	42,483	9.81	Mitochondrial matrix
8601	NADH-ubiquinone oxidoreductase 51 kDa subunit, mitochondrial [Precursor]	P49821	57	11	50,817	8.29	Matrix side of the mitochondrial inner membrane.
2902	NADH-ubiquinone oxidoreductase 75 kDa subunit, mitochondrial [Precursor]	P28331	175	27	79,523	5.80	mitochondrial inner membrane
9006	NADH-ubiquinone oxidoreductase 9 kDa subunit, mitochondrial [Precursor]	P56181	64	24	11,933	9.72	Mitochondrial inner membrane; matrix side
9201	NADH-ubiquinone oxidoreductase PDSW subunit	O96000	67	26	20,632	8.77	Mitochondrial inner membrane; matrix side
9303	NipSnap1 protein	Q9BPW8	91	22	33,289	9.35	Unknown
3505	Nucleoprotein TPR	P12270	54	6	265441	5.1	nuclear pore complex
6103	Origin recognition complex subunit 6	Q9Y5N6	52	18	28,089	8.91	Nuclear

Table 3-10. (continued)

8108	Peptidyl-prolyl cis-trans isomerase A	P05092	67	26	17,870	7.82	Cytoplasmic
9103	Peptidyl-prolyl cis-trans isomerase B [Precursor]	P23284	103	39	22,728	9.33	Endoplasmic reticulum
3201	Peroxiredoxin 2	P32119	67	27	21,878	5.66	Cytoplasmic
4401	Peroxiredoxin 6	P30041	51	20	24,888	6.02	Cytoplasmic
7101 8201	Phosphatidylethanolamine-binding protein	P30086	55 75	27 37	20,913	7.42	Cytoplasmic
3304	Potential phospholipid-transporting ATPase IIA	O75110	56	7	118506	8.00	Integral membrane protein
2403 3301 3303	Prohibitin	P35232	152 53 59	45 12 15	29,786	5.57	Cytoplasmic
0602 0803	Protein disulfide-isomerase [Precursor]	P07237	65 87	15 21	57,081	4.76	Endoplasmic reticulum
3809 3901 4803	Protein disulfide-isomerase A3 [Precursor]	P30101	115 77 93	25 17 20	56,747	5.98	Endoplasmic reticulum
0501	Protein NipSnap3A	Q9UFN0	53	19	28,449	9.21	Unknown
9102	Putative RNA-binding protein 3	P98179	64	26	17,160	8.86	Mitochondrial
5501	Pyruvate dehydrogenase E1 component alpha subunit, somatic form, mitochondrial [Precursor]	P08559	133	26	43,268	8.35	Mitochondrial matrix
3401	Pyruvate dehydrogenase E1 component beta subunit, mitochondrial [Precursor]	P11177	53	25	3,1949	6.20	Mitochondrial matrix

Table 3-10. (continued)

4709	Pyruvate dehydrogenase protein X component, mitochondrial [Precursor]	O00330	67	14	54,089	8.80	Mitochondrial matrix
2508 3302	Ras-related protein Rab-17	Q9H0T7	53 57	16 29	23,460	7.70	Mitochondrial
6301	Ras-related protein Rab-39A	Q14964	52	22	24,854	6.90	Mitochondrial
1201	Rho GDP-dissociation inhibitor 1	P52565	83	29	23,195	5.02	Cytoplasmic
8106	Single-stranded DNA-binding protein, mitochondrial [Precursor]	Q04837	65	45	17,870	9.59	Mitochondrial
1104 1202	Sorcin	P30626	97 117	37 31	21,662	5.32	Cytoplasmic
5301	SSX5 protein	O60225	53	20	21,615	9.45	Unknown
2804 3801 3803	Stress-70 protein, mitochondrial [Precursor]	P38646	53 229 252	12 32 38	73,635	5.87	Mitochondrial
9302	Succinate dehydrogenase [ubiquinone] iron-sulfur protein, mitochondrial [Precursor]	P21912	62	27	31,609	9.03	Mitochondrial inner membrane
4804 4805 5801	Succinyl-CoA:3-ketoacid-coenzyme A transferase 1, mitochondrial [Precursor]	P55809	67 87 54	10 21 14	56,112	7.14	Mitochondrial matrix
6202	Superoxide dismutase [Mn], mitochondrial [Precursor]	P04179	58	11	24,707	8.35	Mitochondrial matrix
4502 5505	Synaptotagmin-1	P21579	61 95	16 23	47,543	8.26	Synaptic vesicles and chromaffin granules

Table 3-10. (continued)

4601	Transmembrane glycoprotein NMB [Precursor]	Q14956	58	5	62,603	6.17	Type I membrane protein
4708	Tryptophan 5-hydroxylase 1	P17752	59	8	50,972	6.97	Mitochondrial
0701 1404 1406	Tubulin beta-2 chain	P07437	72 54 63	13 9 15	49,727	4.75	Unknown
0402	Tubulin beta-4q chain	Q99867	64	14	48,403	5.11	Unknown
5203 5206 5208	Ubiquinol-cytochrome c reductase iron-sulfur subunit, mitochondrial [Precursor]	P47985	83 104 52	17 34 11	29,633	8.55	Mitochondrial inner membrane
8602	Ubiquinol-cytochrome-c reductase complex core protein 2, mitochondrial [Precursor]	P22695	79	23	48,413	8.74	Mitochondrial inner membrane; matrix side
3602	Ubiquinol-cytochrome-c reductase complex core protein I, mitochondrial [Precursor]	P31930	105	22	52,585	5.94	Mitochondrial inner membrane
2303	Ubiquitin carboxyl-terminal hydrolase isozyme L1	P09936	72	31	24,808	5.33	Cytoplasmic
2807 3805	Vacuolar ATP synthase catalytic subunit A, ubiquitous isoform	P38606	186 67	17 14	68260	5.35	Mitochondrial
7304	Vacuolar ATP synthase subunit E	P36543	56	24	26,129	7.71	Unknown

Table 3-10. (continued)

5302 5401 6401 8403 9401	Voltage-dependent anion-selective channel protein 1	P21796	61 88 102 77 139	19 30 31 25 30	30,623	8.63	Outer membrane of mitochondria and plasma membrane
5402 6403 6404 8402	Voltage-dependent anion-selective channel protein 2	P45880	83 59 62 84	22 20 17 23	38,069	6.32	Outer mitochondrial membrane
2104	Wilms' tumor 1-associating protein	Q15007	60	11	44,244	5.20	Nuclear
5802	Zinc finger protein 169	Q14929	54	11	57,615	9.61	Nuclear

Table 3-11. Proteins with significant alterations in AD brain (Bold proteins are encoded by mitochondrial DNA)

Protein name	Accession Number	P Value	Ratio of expression (AD/Control)	Subcellular Location
Calreticulin [Precursor]	P27797	0.03	3.2	cytoplasmic
CTD small phosphatase-like protein	O15194	0.02	0.58	Nuclear
Delta-1-pyrroline-5-carboxylate dehydrogenase, mitochondrial [Precursor]	P30038	0.01	0.18	Mitochondrial matrix
Fumarate hydratase, mitochondrial [Precursor]	P07954	0.02	0.47	Mitochondrial and cytoplasmic
Methylmalonate-semialdehyde dehydrogenase [acylating], mitochondrial [Precursor]	Q02252	0.02	0.52	Mitochondrial
NADH-ubiquinone oxidoreductase 13 kDa-B subunit	Q16718	0.01	0.71	mitochondrial inner membrane
Peroxiredoxin 2	P32119	0.05	0.3	Cytoplasmic
Prohibitin	P35232	0.01	2.17	cytoplasmic
Protein disulfide-isomerase A3 [Precursor]	P30101	0.01	0.28	Endoplasmic reticulum
Ubiquinol-cytochrome c reductase iron-sulfur subunit, mitochondrial [Precursor]	P47985	0.03	0.47	mitochondrial inner membrane

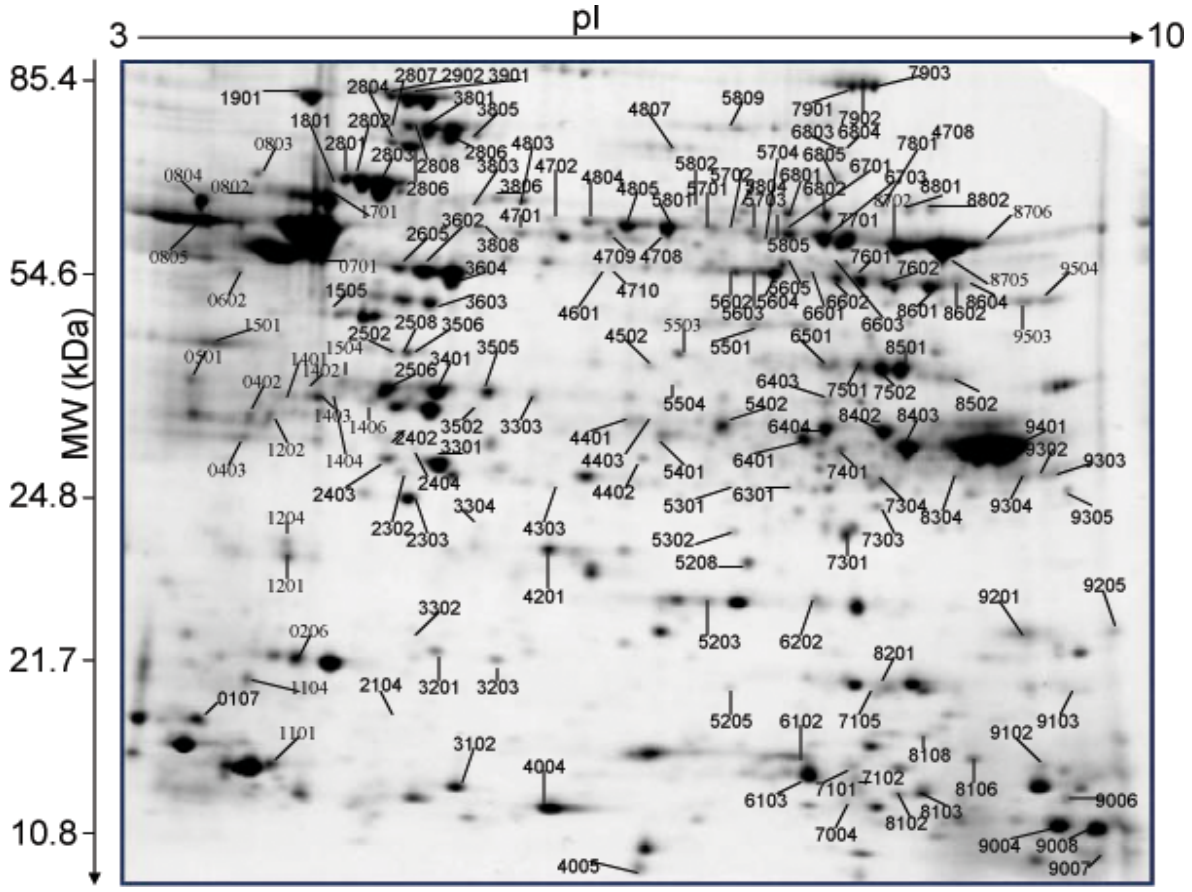

Figure 3-25. A representative 2-dimensional gel with 500 μg mitochondrial protein loaded. 8 – 16 % SDS gel was stained by Sypro Ruby and the pI of the IPG strip was from 3 to 10 (nonlinear).

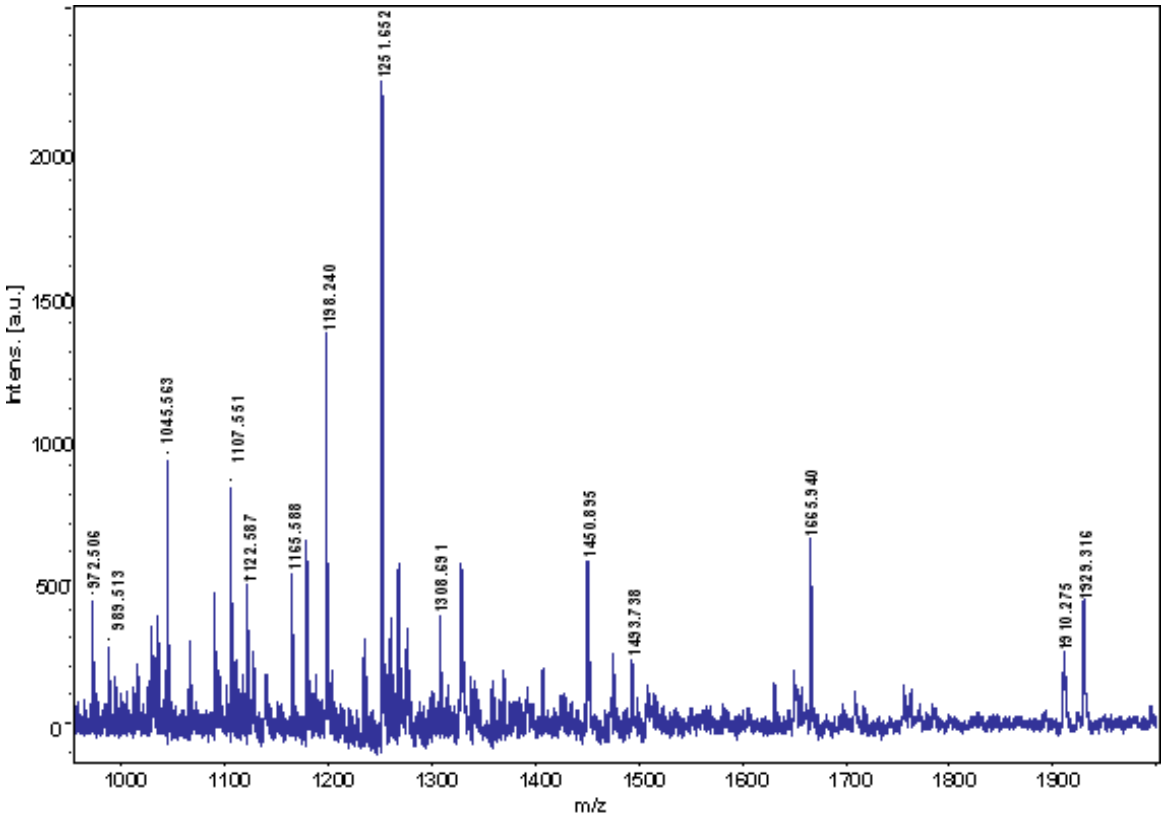

Figure 3-26. A representative MALDI / TOF mass spectrum. Each peak represents a unique peptide

Probability Based Mowse Score

Ions score is -10*Log(P), where P is the probability that the observed match is a random event. Protein scores greater than 52 are significant ($p<0.05$).

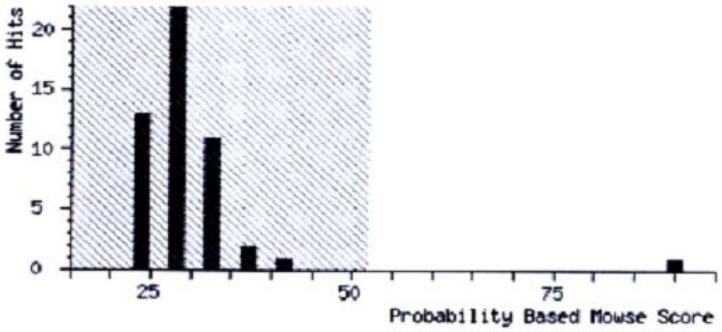

Figure 3-27. The probability based Mowse score. Protein scores greater than 52 were considered significant.

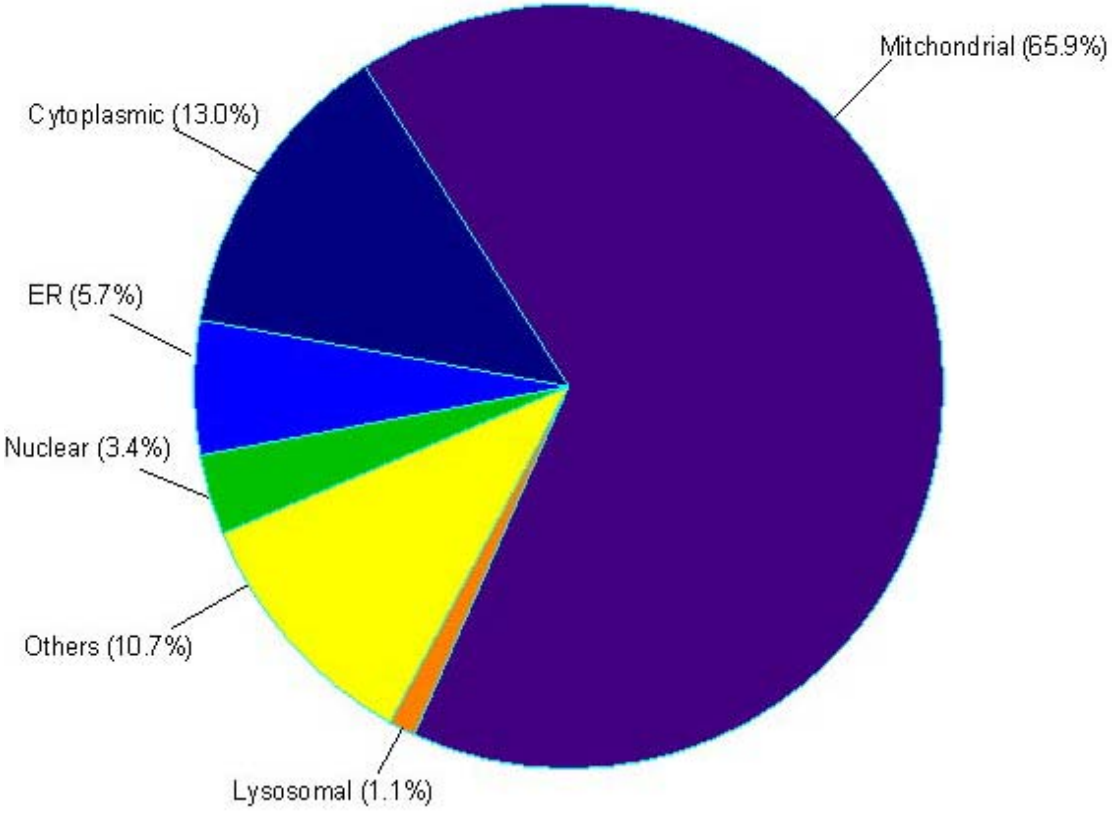

Figure 3-28. Proteins from the mitochondrial fraction classified by subcellular locations

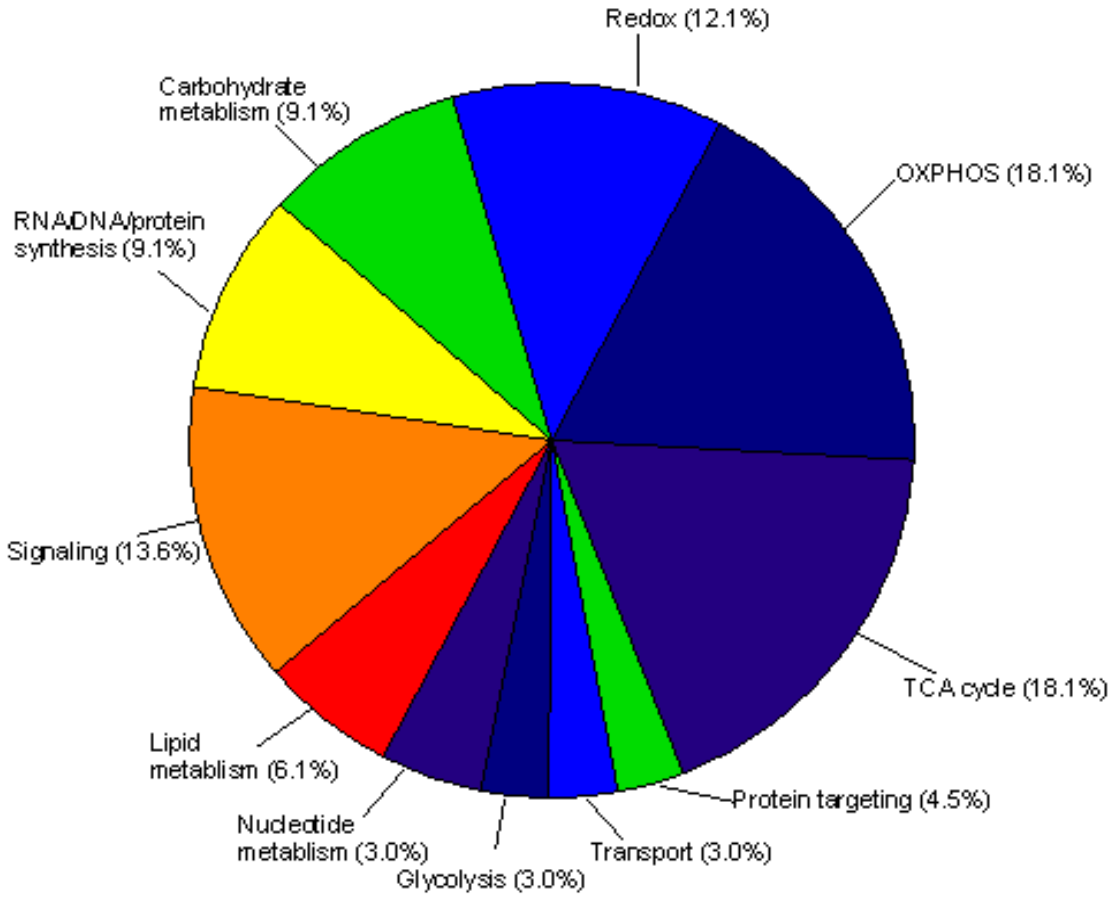

Figure 3-29. Mitochondrial proteins classified by cellular function

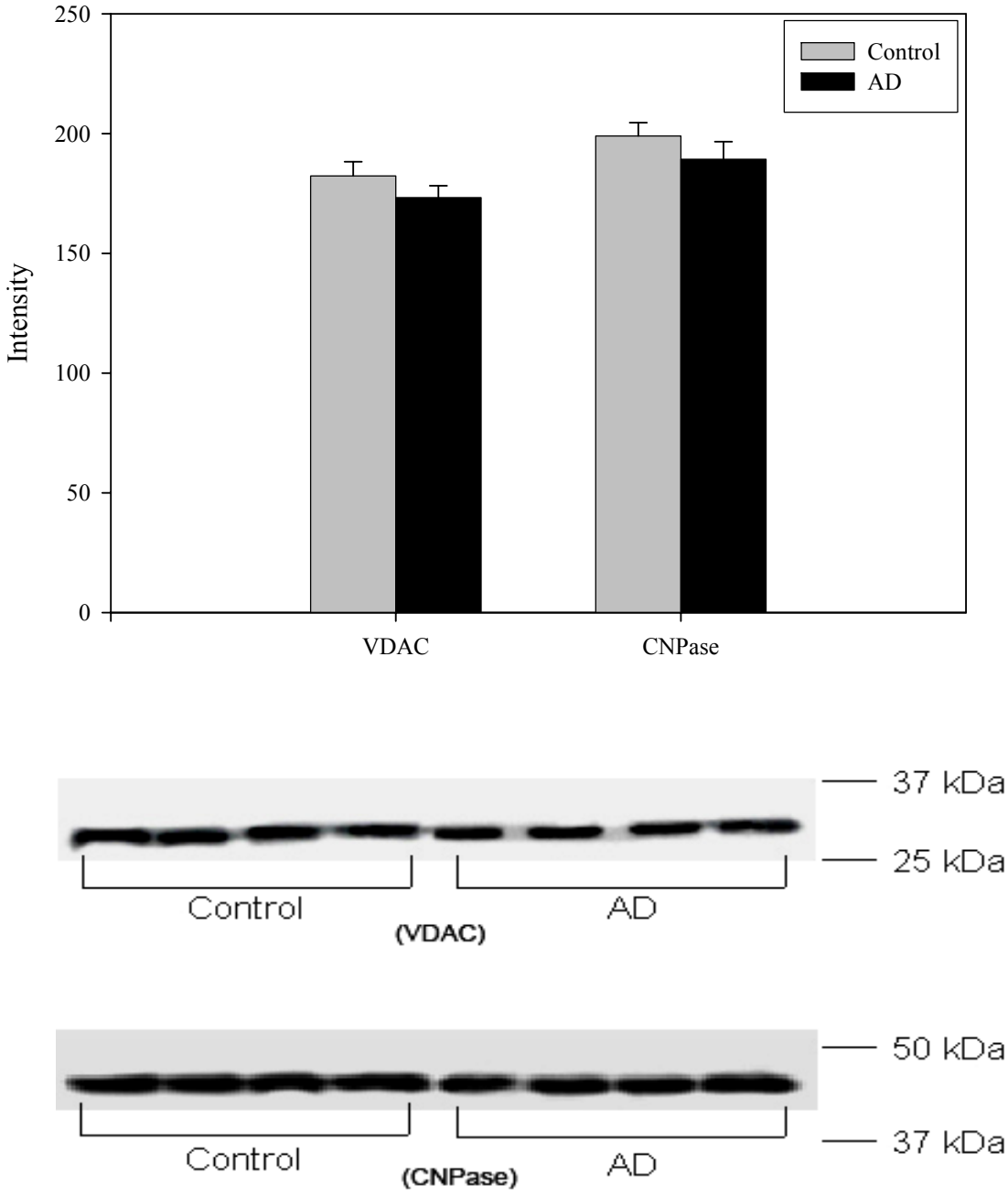

Figure 3-30. Western blots of VDAC and CNPase. No significant difference was observed in Western blots for both of proteins, which were consistent with what we got from 2D gel analysis. * $p < 0.05$

CHAPTER FOUR

Discussion

4.1 Increased oxidative damage in nuclear and mitochondrial DNA in late stage Alzheimer's disease

Oxidative stress to neurons may play an important role in the pathogenesis of AD (Marletta 1993; Lyras et al. 1997; Markesbery 1997; Marcus et al. 1998; Markesbery and Lovell 1998; Markesbery and Carney 1999; Martin 1999; Lovell et al. 2000, 2001). This increased oxidative damage includes elevated levels of oxidized DNA bases (Mecocci et al. 1994; Gabbita et al. 1998; Wang et al. 2005; Wang et al. 2006), lipid peroxidation (Lovell et al. 1995; Markesbery and Lovell 1998), and protein oxidation in AD brain (Butterfield et al. 2003) and increased lipid oxidation in ventricular CSF (Lovell et al. 1997; Montine et al. 2001, 2002). Because of the critical role of DNA in cellular function, oxidative damage to DNA may be one of the most important factors in neuron degeneration in AD. mtDNA may be more easily oxidized than nDNA due to its proximity to free radical species and the lack of histone protection.

This study is the first to use GC/MS-SIM to quantify multiple oxidized base adducts associated with mtDNA damage in LAD brain. Because of the large amounts of tissue required to isolate sufficient amounts of mtDNA for GC/MS-SIM, our results likely reflect a global measure of DNA oxidation from neurons and glia. Although there is increased astrocytosis in the brain in AD, Nunomura et al. (1999) showed a significant increase in 8-hydroxyguanine immunoreactivity in neuron cytoplasm in AD hippocampal neurons, but little to no reactivity in glia, suggesting that DNA oxidation is predominantly associated with neurons.

To verify that extracted mitochondria were pure, representative samples were analyzed by electron microscopy and Western blot analysis. Both showed the mitochondria isolated were ~95% pure after centrifugation through two Percoll gradients. PCR amplification of APOE, a gene coded by nDNA, showed that mtDNA was not

contaminated by nDNA. A previous study (Mecocci et al. 1994) demonstrated elevated 8-hydroxyguanisine in AD mtDNA; however, this is the first study to measure multiple base adducts and provide a more comprehensive measure of DNA oxidation. Although 8-hydroxyguanine is the predominate marker of oxidative damage, our results indicate several other base adducts were significantly increased in nDNA and mtDNA of LAD patients compared to age-matched controls subjects.

GC/MS-SIM is a highly selective and sensitive method that can monitor a wide range of bases simultaneously and unequivocally in a single run. Detection limits can approach 5 fmol (Halliwell and Dizdaroglu 1992), whereas the detection limit of HPLC-ECD is about 20 fmol. The major disadvantage in the use of GC/MS-SIM is the potential for artifactual oxidation during hydrolysis and derivatization (Douki et al. 1996). However, under proper processing, formic acid hydrolysis and derivatization do not induce artifacts (Dizdaroglu 1998). In our study, we excluded oxygen during these two steps, and used 8-hydroxyquinoline as an antioxidant to prevent artifactual DNA oxidation during extraction.

During DNA isolation, Na_2EDTA was added to complex trace metals that could catalyze oxidation. Prolonged PMIs could also contribute to artifactual oxidation and, in most other studies, tissue samples with PMIs longer than 6 hr were used. In contrast, we used brain specimens with short PMI (2.9 ± 0.2 hr for control and 3.3 ± 0.2 hr for LAD). Calculation of correlation coefficients between PMI and levels of oxidized bases showed no significant correlation for any of the oxidized base adducts ($r < 0.5$).

In order to verify that phenol extraction does not induce artifactual oxidation, the NaI 'salting out' method was used to isolate nDNA and mtDNA from representative tissues. Our results show that levels of DNA oxidation from representative brain specimens processed using the two methods are similar. Levels of 8-hydroxyguanine showed no significant difference between these two methods, although there was a decrease in fapyguanine and fapyadenine of nDNA and fapyadenine of mtDNA samples and an increase in 5-hydroxycytosine of mtDNA using NaI precipitation.

One concern in DNA isolation using phenol/chloroform extraction was the artifactual oxidation caused during isolation. Comparison of levels of base adducts in DNA isolated using either NaI precipitation or phenol/chloroform extraction suggests that phenol/chloroform extraction did not lead to artifactual oxidation. Therefore, all DNA samples used for statistical analyses in our studies were isolated using phenol/chloroform extraction.

Our data show significantly increased oxidative DNA damage in LAD subjects compared to age-matched controls with levels of damaged bases in mtDNA approximately 10-fold those of nDNA ($2.8 <$ ratio of mtDNA/nDNA < 23.8). Comparison of mtDNA and nDNA oxidative damage for each oxidized base showed statistically significantly increased oxidation in mtDNA for both LAD and control subjects for all base adducts analyzed. There were no significant differences in the ratio of mtDNA/nDNA oxidized bases between LAD and control subjects, which may be due to variability in the degree of oxidation between mitochondria and nuclei in LAD and aged control subjects.

In order to compare levels of oxidative damage in nDNA and mtDNA in the other way, we list oxidative levels in terms of lesions/10^6 total DNA bases, ratio of lesion/unmodified DNA base, percentage of lesions, and nmol/mg of DNA (Table 3-5). Due to the big size difference between nuclear genome (3.3 billion bp) and mitochondrial genome (16.6 kbp), the absolute value of oxidized bases in each nDNA molecule is much larger than in mtDNA. However, mtDNA have much higher mutation rate which is more important in protein synthesis ($2.8 <$ ratio of mtDNA/nDNA < 23.8). nDNA has ~10% protein coding genes, whereas 100% mtDNA are useful genes in protein synthesis. Considering above two facts, mutations in mtDNA cause far worse consequences than mutations in nDNA.

The absolute level of 8-hydroxyguanine is the highest of the damaged bases in both control and LAD subjects, which is consistent with previous studies (Mecocci et al. 1993, 1994; Lyras et al. 1997; Gabbita et al. 1998; Birincioglu et al. 2003), suggesting that guanine is the DNA base most vulnerable to oxidative damage (Aruoma et al. 1989;

Steenken 1989; Floyd et al. 1990; Halliwell and Dizdaroglu 1992; Gabbita et al. 1998; Dizdaroglu et al. 2002; Birincioglu et al. 2003; Musiek et al. 2004). In nDNA and mtDNA from temporal lobe, five of the six oxidized bases (except fapyguanine) were increased significantly in LAD. In mtDNA from parietal lobe, statistically significant increases in levels of 8-hydroxyguanine, fapyguanine, 5-hydroxyuracil, 5-hydroxycytosine, and fapyadenine were observed.

For different DNA bases, the variation in levels of oxidation may be due to their different structures and redox potentials (Steenken 1989). This is one reason why all adducts are not elevated in the same proportion, even in the same brain region. Also it is possible that a small variable amount of white matter was present in some specimens, which might alter the cellular makeup of the specimens. Our results show that there is more oxidative damage in neocortical regions in AD brain than cerebellum, which has minimal pathologic changes in AD and is consistent with previous studies (Mecocci et al. 1994; Hensley et al. 1995; Lovell et al. 1995; Lyras et al. 1997; Gabbita et al. 1998). The variation in levels of DNA damage in brain regions may be due to differences in trace metals, antioxidant levels, and repair mechanisms (Xie et al. 1996; Cornett et al. 1998; Lovell et al. 1998, 1999, 2002). The levels of oxidized bases per million DNA bases in our study are consistent with previous studies using HPLC (Mecocci et al. 1993, 1994) and GC/MS (Lyras et al. 1997; Dizdaroglu 1998; Dizdaroglu et al. 2002; Birincioglu et al. 2003).

High levels of free radical damage in mitochondria may cause impaired mitochondrial function, which may result in cellular dysfunction in neurons. Previous studies (Lustbader et al. 2004) demonstrated a link between Aβ and mitochondrial toxicity through Aβ binding to alcohol dehydrogenase. This interaction in mitochondria promotes increased ROS formation, mitochondrial dysfunction, and neuron death (Wallace 1992; Markesbery 1997). Thus, it is possible that the increase in Aβ in AD enhances mtDNA oxidation, which also might cause variable results from region to region. Oxidative damage to DNA may accelerate protein crosslinking and aggregation,

such as beta amyloid and tau protein (Dyrks et al. 1992, 1993; Butterfield et al. 1999; Varadarajan et al. 2000; Butterfield 2003).

The current study shows that the neuron degeneration in AD may be associated with oxidative damage to both nDNA and mtDNA, with more pronounced damage accumulating in mtDNA. In contrast to nDNA that contains ~10% protein coding genes, entire mtDNA encode 37 genes exclusively involved in respiratory chain. Accumulation of mitochondrial mutations could lead to energy deficiencies and eventually neuron death in the brain in AD.

4.2 Increased oxidative damage in nuclear and mitochondrial DNA in Mild Cognitive Impairment

This is the first study to quantify multiple oxidized DNA base adducts in MCI brain. Although the DNA in this study was isolated from a mixture of glia and neurons, previous immunohistochemical studies show that only neurons are immunopositive for 8-hydroxyguanine (Hirai et al. 2001; Aliyev et al. 2005), suggesting that the levels of oxidized bases which we measured represent neuronal DNA oxidation.

Our data showed significantly ($p < 0.05$) increased levels of all base adducts analyzed in mtDNA compared with nDNA for both MCI and control subjects. Comparison of MCI and control subjects shows significantly increased levels of oxidized base adducts in MCI subjects compared with control subjects in several brain regions. The absolute level of 8-hydroxyguanine was the highest among the five adducts analyzed, which is consistent with previous studies of LAD brain (Mecocci et al. 1993, 1994; Lyras et al. 1997; Gabbita et al. 1998; Birincioglu et al. 2003; Wang et al. 2005). Guanine is particularly vulnerable to oxidation by hydroxyl radicals because of its high electron density (Steenken 1989). Our data show significantly elevated 8-hydroxyguanine in nDNA from MCI frontal and parietal lobe but not temporal lobe or cerebellum. These data are consistent with our previous study of late-stage AD subjects that showed significantly elevated 8-hydroxyguanine in frontal and parietal lobe DNA but not temporal lobe (Wang et al. 2005).

In contrast to our study of LAD subjects that showed significantly elevated 8-hydroxyguanine in mtDNA from parietal and temporal lobe, our current data show a significant elevation in mtDNA from temporal lobe only. Our current data show no significant differences in levels of fapyguanine in nDNA or mtDNA between MCI and control subjects which is in contrast to our previous study of LAD subjects that showed a significant elevation of fapyguanine in mtDNA from parietal lobe and cerebellum (Wang et al. 2005).

Free radical attack of C8 of adenine leads to 8-hydroxyadenine radicals that result in 8-hydroxyadenine and fapyadenine in the presence and absence of oxygen,

respectively (Steenken 1989; Breen and Murphy 1995; Dizdaroglu et al. 2002). Our results show significantly elevated 8-hydroxyadenine in nDNA from frontal, temporal and parietal lobes and significant increases in fapyadenine in both nDNA and mtDNA from frontal, temporal and parietal lobes of MCI subjects. The significant elevation of fapyadenine raises the question of a hypoxic environment being present in MCI. Hypoxia can also increase the risk of AD (Tatemichi et al. 1994; Kokmen et al. 1996; Higashide et al. 2004; Smith et al. 2004). In a particular brain region, electrophilic free radicals have different reaction rate constants with different bases (Steenken 1989) which may be one reason why absolute levels of the five adducts studied here varied between brain regions in the same subject.

Statistical analysis using two-way ANOVA showed that 8-hydroxyguanine, fapyadenine and 5-hydroxycytosine were significantly elevated in mtDNA but not nDNA from neocortical regions compared with cerebellum in MCI subjects. In controls there were no significant differences in levels of any of the base adducts studied in mtDNA or nDNA from neocortical regions compared with cerebellum. These observations are consistent with minimal pathological changes in cerebellum in normal aging brain (Mecocci et al. 1994; Hensley et al. 1995; Lovell et al. 1995; Lyras et al. 1997; Gabbita et al. 1998) and with our previous studies of DNA adducts in LAD brain (Gabbita et al. 1998; Wang et al. 2005). Neocortex and cerebellum have different levels of trace metals, antioxidants and DNA repair capacities (Xie et al. 1996; Cornett et al. 1998; Lovell et al. 1998, 1999, 2002; Dizdaroglu et al. 2002; Hashiguchi et al. 2004; Stuart et al. 2005) which may contribute to the different yields and patterns of DNA modification observed here.

Comparison of levels of oxidized bases and the presence of Apolipoprotein-E4 (APOE-4) alleles showed no significant differences in levels of oxidized bases between subjects carrying an APOE-4 allele and subjects who carried no APOE-4 alleles (Table 3-6).

In this study, we used brain specimens with short post-mortem intervals (3.0 ± 0.4 h for control subjects and 4.0 ± 0.9 h for MCI subjects), which is important

because prolonged post-mortem interval may lead to artifactual oxidation. During DNA isolation, Na_2EDTA was added following homogenization to chelate trace metals that may catalyze oxidative reactions (Xie et al. 1996; Cornett et al. 1998; Lovell et al. 1998, 1999, 2002). In addition, 8-hydroxyquinoline was added to phenol to prevent artifactual oxidation during DNA extraction.

To limit the possibility of artifactual oxidation during processing of DNA for GC/MS-SIM, tubes containing DNA samples were fully evacuated during formic acid hydrolysis and N,O-bis(trimethylsilyl)trifluoroacetamide derivatization which was previously shown to limit artifactual oxidation during DNA derivatization (Dizdaroglu 1998). Levels of oxidative damage that we measured are similar to previous studies of DNA oxidation in AD brain using HPLC (Mecocci et al. 1993, 1994) and gas chromatography/mass spectrometry (Lyras et al. 1997; Dizdaroglu 1998; Dizdaroglu et al. 2002; Birincioglu et al. 2003; Wang et al. 2005)

Compared with our previous study of LAD (Wang et al. 2005), these data show that levels of oxidized bases, especially 8-hydroxyguanine, 8-hydroxyadenine and fapyguanine, were not significantly different in MCI compared with LAD subjects. These results suggest that both nDNA and mtDNA are oxidized early in the progression of MCI to advanced AD. Due to the crucial role DNA plays in cells, high levels of oxidation, particularly early in the progression of AD, may result in a decline of normal cell function through altered transcription, changes in protein expression or cross-linking with proteins. In all regions of both control and MCI subjects, there is significantly more mtDNA damage than in nDNA ($p < 0.02$). mtDNA is more susceptible to oxidation because of the proximity to ROS, lack of protective histones and relatively limited antioxidant capacities. Repair of 8-hydroxyguanine through base excision repair (BER) has been demonstrated in mitochondria (Stuart et al. 2005). Although there have been no studies of BER in mitochondria from AD, MCI or aged control subjects, previous studies showed decreased BER capacity in mitochondria of aged rats (Chen et al. 2002; Englander et al. 2002). Our previous study of AD and control subjects showed decreased BER in nuclei isolated from AD brain (Lovell et al. 2000b). However, we did not

compare BER activity in mitochondria from AD subjects but would anticipate that mitochondrial BER may be diminished consistent with decreased nuclear activity. It is possible that the combination of diminished repair capacity and accumulated DNA damage in nuclei and mitochondria may lead to neuron death (Wallace 1992; Hashiguchi et al. 2004; Stuart et al. 2005).

In summary, our data show elevated levels of oxidized base adducts in MCI compared with age-matched control subjects that are similar to levels observed in LAD subjects, which suggests that the oxidative damage to nDNA and particularly mtDNA occurs early in the course of AD and may contribute to the pathology of neurodegeneration.

4.3 Increased oxidative damage in nuclear DNA in APP/PS1 transgenic mice

This is the first study to quantify oxidized DNA base adducts in APP/PS1 mice with GC/MS-SIM. Our results show significantly increased levels of 8-hydroxyguanine in nDNA of 12 month old APP/PS1 mice compared to wild type mice. The absolute level of 8-hydroxyguanine is consistently higher than 8-hydroxyadenine, which is consistent with previous AD studies (Mecocci et al. 1993; Mecocci et al. 1994; Lyras et al. 1997; Gabbita et al. 1998; Birincioglu et al. 2003; Wang et al. 2005; Wang et al. 2006). Due to the electrophilic property, guanine is vulnerable to be oxidized by ROS. In the oxidative condition, the oxidation is in favor of the production of 8-hydroxyguanine (Steenken 1989a). This significant elevation of the levels of 8-hydroxyguanine is consistent with the previous studies which showed the early-onset increased Aβ production in APP/PS1 transgenic mice (Borchelt et al. 1996; Duff et al. 1996; Borchelt et al. 1997). The levels of oxidized base adducts are comparable to previous AD studies using HPLC (Mecocci et al. 1993; Mecocci et al. 1994) and GC/MS (Lyras et al. 1997; Dizdaroglu 1998; Dizdaroglu et al. 2002; Birincioglu et al. 2003; Wang et al. 2005; Wang et al. 2006).

Our results also show a positive correlation between the amyloid plaque burden and levels of 8-hydroxyguanine in APP/PS1 mice ($r = 0.90$). No positive correlation was observed between amyloid plaque burden and levels of 8-hydroxyadenine. Previous studies suggest that Aβ may accelerate the generation of free radicals, which may increase oxidative damage in cells (Hensley et al. 1994; Markesbery 1997; Butterfield and Boyd-Kimball 2005). Increasing evidence suggests that Aβ may cause mitochondrial dysfunction and apoptosis, and that normal mitochondrial respiration is diminished with Aβ and free radicals, such as nitric oxide (Casley et al. 2002; Reddy et al. 2004). Studies showed that PS1 alone did not induce amyloid pathology, while PS1 coexpressing with APP showed the early onset deposition of Aβ (Shen et al. 1997).

To avoid artifactual DNA oxidation during nDNA isolation and sample preparation before GC injection, Na_2EDTA was added during tissue homogenization, and glass tubes were fully evacuated in the steps of formic acid hydrolysis and BSTFA

derivatization (Dizdaroglu 1998); (Xie et al. 1996; Cornett et al. 1998; Lovell et al. 1998; Lovell et al. 1999a; Lovell et al. 2002; Wang et al. 2005; Wang et al. 2006).

DNA oxidation may accumulate without efficient DNA repair ability. DNA damage may result in decline in normal cell functions through blocking transcription, changing protein expression, or cross-linking with proteins (Wallace 1992). The increased early-onset Aβ deposition accelerates the free radical production and results in neuronal death because of the mitochondrial dysfunction (Reddy et al. 2004).

In summary, our data show significantly elevated 8-hydroxyguanine in APP/PS1 mice at the age of 12 month old, which is consistent with the increased Aβ production. This mouse model may provide an insight to study the mechanism of neuron death and pathology of AD.

4.4 Proteomic studies of mitochondria in Alzheimer's disease

This study is a comprehensive survey of mitochondrial proteins in AD brain, which may provide more information about mitochondrial dysfunction in neurodegenerative diseases.

On each gel, ~650 protein spots were visualized with Sypro ruby staining. Sypro ruby provided a wider dynamic range than silver staining and is more sensitive than Coomassie Blue Staining (Berggren et al. 2000). On these gels, the majority of proteins were mid-sized proteins (10 kDa < M.W. < 90kDa). This is consistent with previous studies that showed middle range molecular weight proteins dominated the mitochondrial proteome (Taylor et al. 2003).

Among 176 differentially expressed spots, ~66% were mitochondrial, which represent 67 unique proteins. The remaining spots mainly consisted of proteins from cytoplasm (13%), nuclei (3%), and ER (5%). ~11% of the identified proteins were uncertain in localization. The percentage of mitochondrial protein was higher than previous mitochondrial studies (~40%) (Mootha et al. 2003; Fukada et al. 2004; Jiang et al. 2005), consistent with our Western blot charactering mitochondrial fraction using Oct-1 immunochemistry.

Based on different functions annotated by GeneBank and EXPASY, the 67 mitochondrial proteins were classified into 11 categories (Taylor et al. 2003). About half of mitochondrial proteins were enzymes involved in redox, TCA cycles, and the respiratory chain. Results showed that the enzymes involved in TCA cycle were mainly in mitochondrial matrix which was consistent with a previous study (Wallace 1999). The majority of enzymes function in respiratory chain and redox reactions and are located in the inner membrane of mitochondria, where the main components of enzyme complexes I-V are located (Wallace 1999). ~20% of the identified mitochondrial proteins were involved in carbohydrate metabolism, lipid metabolism, nucleotide metabolism, and glycolysis. 13% of the proteins identified were signaling proteins, mainly isoforms and subunits of G protein, which function as modulators or transducers in various transmembrane signaling systems (Gao et al. 1987). The targeting proteins identified

were mainly heat shock proteins, which facilitate folding of imported proteins. Under stress conditions, they may prevent misfolding and promote refolding of proteins (Venner et al. 1990; Hansen et al. 2003). VDAC1 (porin) and VDAC2 were also identified, which function to form channels allowing diffusion of small hydrophilic molecules in mitochondrial membranes (Yu et al. 1995).

Due to the restrictions of 2D gel electrophoresis and staining methods, we can only quantify and identify proteins with high expression levels. 67 mitochondrial proteins out of ~2000 were identified, which represents a small percentage of total mitochondrial proteins. This may be the reason why we only see 2 out of 13 mitochondrial-encoded proteins in our study.

Student's *t*-test was applied to analyze the protein expression changes. The abundance of 10 proteins was significantly altered. They include 5 mitochondrial proteins, 3 cytoplasmic proteins, 1 ER protein, and 1 nuclear protein. However, as no commercial antibodies were available, we used rabbit anti-VDAC and rabbit anti-CNPase for Western analysis. No significant difference was observed in Western blots for both proteins, which were consistent with what we got from 2D gel analysis.

NADH-ubiquinone oxidoreductase 13 kDa-B subunit, a mitochondrial-encoded subunit of complex I localized in the matrix side of the mitochondrial inner membrane, was decreased significantly in LAD brain. The protein functions to transfer electrons from NADH to the respiratory chain. In this process, ubiquinone is electron acceptor and is reduced to ubiquinol (Pata et al. 1997; Tensing et al. 1999). Decreased expression of NADH-ubiquinone oxidoreductase 13 kDa-B subunit in mitochondrial complexes may reduce the capacity and efficiency of ATP synthesis in AD brain, which may cause neuron death because of the energy deficiency.

Ubiquinol-cytochrome c reductase iron-sulfur subunit is also significantly decreased in AD brain, and is one mitochondrial-encoded subunit of complex III, which is located on the mitochondrial inner membrane. It is involved in the respiratory chain which generates the electrochemical potential necessary to promote ATP synthesis (Nishikimi et al. 1990; Grimwood et al. 2004). The electron transfer may be affected

because of the lower expression of ubiquinol-cytochrome c reductase iron-sulfur subunit. Lower electrochemical potentials may lead to ATP deficiencies for neurons in AD brain. Two aldehyde dehydrogenases (Delta-1-pyrroline-5-carboxylate dehydrogenase and Methylmalonate-semialdehyde dehydrogenase) were decreased in AD.

Delta-1-pyrroline-5-carboxylate dehydrogenase is located in the mitochondrial matrix and catalyzes conversion of Delta-1-pyrroline-5-carboxylate to glutamate. It is an interconnecting step between urea and TCA cycles. The decreased expression was consistent with previous studies of mental retardation, and AD (Hu et al. 1996; Li et al. 1997; Geraghty et al. 1998). Glutamate is the major excitatory neurotransmitter. Low expression of delta-1-pyrroline-5-carboxylate may disturb glutamate transport in neurons. Glutamate transporter alterations may affect the APP expression and calcium influx in neuronal cells, which may induce neuronal damage and memory loss in AD brain (Greenamyre et al. 1988; Li et al. 1997; Burbaeva et al. 2005).

Methylmalonate-semialdehyde dehydrogenase is an enzyme which catalyzes the reaction of 2-methyl-3-oxopropanoate and NAD^+ to propanoyl-CoA and NADH which is used in ATP generation through the electron transport chain. It plays an important role in valine and pyrimidine metabolism (Chambliss et al. 2000).

Fumarate hydratase is involved in the TCA cycle. It catalyzes the conversion of fumarate to malate. Defects in fumarate hydratase may cause the fumarase deficiency characterized by progressive encephalopathy, developmental delay, and cerebral atrophy. It also acts as a tumor suppressor (Coughlin et al. 1998; Tomlinson et al. 2002). Fumarase deficiency will cause the disorders of pyruvate metabolism and the oxygen – dependent energy production (Pithukpakorn 2005). All the five enzymes discussed above are associated with mitochondrial energy production. The decrease in these protein expressions in AD brain may cause the energy deficiency leading to neuron cell death.

This study provides a proteome map of mitochondria in AD brain and several proteins with altered expression. It also suggests that proteomic study in mitochondria may provide an insight to study the pathogenesis of neuron degeneration in Alzheimer's disease.

CHAPTER FIVE

Conclusion

In summary, oxidative stress plays a crucial role in the development of AD. Numerous studies show that the oxidation levels of DNA, protein, and lipids are increased in Alzheimer's disease. Mitochondria are the main energy source in eukaryotic cells, and are the primary sites for endogenous ROS generation. Our studies suggest that mitochondrial dysfunction might be involved in the process of neuron degeneration in AD.

In the LAD study, our data showed significantly increased oxidative DNA damage in LAD subjects compared to age-matched control subjects with levels of damaged bases in mtDNA approximately 10-fold those of nDNA ($2.8 <$ ratio of mtDNA/nDNA < 23.8), which is consistent with the absence of histone protection and low level of repair capacity for mtDNA. Results also showed that there was more oxidative damage in neocortical regions in LAD brain than cerebellum, which is consistent with the minimal pathologic changes in cerebellum in AD. The level of 8-hydroxyguanine is constantly higher than other base adducts, consistent with the lowest oxidation potential of guanine which is the most vulnerable to oxidative damage. This study suggested that neuron degeneration in AD might be associated with oxidative damage to both nDNA and mtDNA, especially mtDNA. Previous immunohistochemical studies show that only neurons are immunopositive for 8-hydroxyguanine, suggesting that the levels of oxidized bases which we measured represent neuronal DNA oxidation. However, it is not clear whether these changes in LAD are primary or secondary to neurodegeneration.

In order to see when the oxidation begins, we carried out a study of MCI and age-matched control subjects. Statistical analysis showed that 8-hydroxyguanine, fapyadenine and 5-hydroxycytosine were significantly elevated in mtDNA but not nDNA from neocortical regions compared with cerebellum in MCI subjects. Compared to the

LAD study, the levels of oxidized base adducts in MCI are comparable to levels observed in late-stage AD subjects. The significant elevation of fapyadenine raises the question of a hypoxic environment being present in MCI. Previous studies showed that hypoxia can also increase the risk of AD (Tatemichi et al. 1994; Kokmen et al. 1996; Smith et al. 2004). This study suggests that the DNA oxidation occurs early in the course of AD and is less likely to be secondary to neurodegenerative alterations. It suggests that oxidative damage to DNA might play an important role in AD progression.

Senile plaques are one of the main pathological hallmarks of AD. To study the effect of Aβ plaques on DNA oxidation, nDNA from four age groups of APP/PS1 transgenic mice were analyzed. The amyloid cascade hypothesis states that Aβ processing and aggregation may contribute to the pathogenesis of AD. In the mouse model coexpressing mutant APP and PS1, the deposition of senile plaques was accelerated and the ratio of Aβ42/Aβ40 was increased in brain. Our results showed significantly increased levels of oxidized 8-hydroxyguanine in nDNA of 12 month old APP/PS1 mice compared to wild type and a positive correlation between amyloid plaque counts and levels of 8-hydroxyguanine in APP/PS1 mice. Oxidative damage to DNA may accelerate protein crosslinking and aggregation, such as beta amyloid and tau protein (Dyrks et al. 1992; Dyrks et al. 1993; Mark et al. 1997; Varadarajan et al. 2000; Butterfield and Castegna 2003). Aβ deposition in turn increases ROS production through peptide interactions with redox-active trace metal ions (Huang et al. 1999). A previous study (Lustbader et al. 2004) demonstrated a link between Aβ and mitochondrial toxicity through Aβ binding to alcohol dehydrogenase, which causes increased ROS production.

There are ~2000 mitochondrial proteins encoded by both nDNA and mtDNA. Based on the results from DNA studies, we expected to see altered expression of mitochondrial proteins in AD brain. Our study provided a proteome map of mitochondria in AD brain and showed 5 mitochondrial proteins related to energy production were significantly altered in LAD. The down-regulation of mitochondrial proteins in AD brain may affect ATP synthesis and cause the energy deficiency leading to neuronal death.

In contrast to the nuclear genome that contains ~10% protein coding genes, the entire mitochondrial genome is involved in coding for 37 genes including 13 proteins exclusively involved in the respiratory chain, 22 tRNAs and 2 rRNAs for translation machinery. Damage to mtDNA could be potentially more detrimental than alterations in nDNA. All mitochondrial coded proteins are involved in oxidative phosphorylation and ATP synthesis. Oxidative alterations of mtDNA could lead to synthesis of functionally altered enzyme subunits, which in turn further augment ROS production.

DNA oxidation may accumulate without efficient DNA repair ability. DNA damage may result in decline in normal cell functions through blocking transcription, changing protein expression, or cross-linking with proteins. Aβ deposition accelerates the free radical production and results in neuronal death because of the mitochondrial dysfunction. Mutations in DNA lead to errors in protein biosynthesis, which especially affects the high-energy consumptive neuronal cells. The defects of mitochondrial proteins may result from mutations of nDNA and mtDNA. Alterations in nDNA-encoded mitochondrial proteins that we observed may be due to mutations in nDNA, or due to interruption during transportation from cytoplasm into mitochondria. Our results show the decreased expression of 5 mitochondrial proteins. Two of them are encoded by mtDNA, which accounts for 15% among the 13 mitochondrial-encoded proteins. Due to the restriction of 2-D gel electrophoresis and gel staining methods, only proteins with high expression levels could be identified and quantified. In our study, we identified 67 out of ~2000 mitochondrial proteins. This may explain why only 2 mitochondrial proteins were identified.

Oxidative damage to mitochondria, especially to respiratory enzymes, triggers mitochondria to release more ROS from the respiratory chain, which would further damage DNA and proteins. This vicious circle eventually causes dysfunctional mitochondria which would accumulate in non-dividing cells, such as neurons. Several factors, including oxidative stress and calcium disruption, could induce apoptosis through formation of a non-specific permeability transition pore that allows small molecular solutes to swell the mitochondrial matrix, leading to rupture of outer membrane and

release of several proapoptotic factors, including cytochrome c, resulting in activation of cytosolic caspases and subsequent cell death. During mitochondrion-mediated apoptosis, cytochrome c is released from intermembrane space and binds to apoptotic protease-activating factor 1 and caspase-9. This caspase complex activates downstream capases, such as caspase 3, followed by further activation of capases and ultimately apoptosis. Defective mitochondria can have catastrophic consequences for cells, not only due to loss of ATP, but also due to the impairment of downstream functions, such as disruption of calcium homeostasis. Accumulation of defective mitochondria may lead to neuronal cell apoptosis.

What causes AD is not fully understood. Our results suggest ROS are involved, although we do not know whether ROS production is a primary or secondary event. Considerable evidence suggests there is increased oxidation of DNA, protein, lipid, and RNA in AD brain. Neuronal death can be caused by many factors, such as enzyme dysfunction, energy deficiency, etc. Removal of ROS seems like a potential way to slow AD progression. Commonly used antioxidants have effects on slowing progression of AD (Ames et al. 1993). The tolerance of neurons to oxidative stress is limited because neurons are non-replicating cells and contain relatively low levels of antioxidants. Once damaged, neurons are permanently dysfunctional or are committed to apoptosis.

Currently, definite AD only can be diagnosed at autopsy. Although memory and recall tests are used to diagnose probable AD or predict individuals with high risk of AD, considerable effort has been devoted to methods of early diagnosis. Our studies suggest oxidative stress plays an important role in the development of AD. As the main energy source of cell, mitochondria are the primary sites for endogenous ROS generation. Neuron degeneration in AD may be associated with oxidative damage to DNA, especially to mtDNA, which may lead to altered expression of proteins involved in ATP synthesis. Our studies suggest that mitochondrial dysfunction might be involved in the process of neuron degeneration in AD.

REFERENCES

Aebersold R. H., Pipes G., Hood L. E. and Kent S. B. (1988) N-terminal and internal sequence determination of microgram amounts of proteins separated by isoelectric focusing in immobilized pH gradients. *Electrophoresis* **9,** 520-530.

Alms G. R., Sanz P., Carlson M. and Haystead T. A. (1999) Reg1p targets protein phosphatase 1 to dephosphorylate hexokinase II in Saccharomyces cerevisiae: characterizing the effects of a phosphatase subunit on the yeast proteome. *Embo J* **18,** 4157-4168.

Alzheimer A. (1907) Uber eine eigenartige Erkankung der Hirnrinde. *Allg. Zschr. f Psychiatr. Psychisch-Gerichtl. Mediz.* **64,** 146-148.

Ames B. N., Shigenaga M. K. and Hagen T. M. (1993) Oxidants, antioxidants, and the degenerative diseases of aging. *Proc Natl Acad Sci U S A* **90,** 7915-7922.

Andersen J. S. and Mann M. (2000) Functional genomics by mass spectrometry. *FEBS Lett* **480,** 25-31.

Anderson N. G. and Anderson N. L. (1996) Twenty years of two-dimensional electrophoresis: past, present and future. *Electrophoresis* **17,** 443-453.

Andreasen N., Minthon L., Vanmechelen E., Vanderstichele H., Davidsson P., Winblad B. and Blennow K. (1999) Cerebrospinal fluid tau and Abeta42 as predictors of development of Alzheimer's disease in patients with mild cognitive impairment. *Neurosci Lett* **273,** 5-8.

Bayer F. L. (1986) Gas chromatographic equipment. *Journal of Chromatographic Science* **24,** 549.

Benedetti A., Comporti M. and Esterbauer H. (1980) Identification of 4-hydroxynonenal as a cytotoxic product originating from the peroxidation of liver microsomal lipids. *Biochim Biophys Acta* **620,** 281-296.

Benedetti A., Pompella A., Fulceri R., Romani A. and Comporti M. (1986) 4-Hydroxynonenal and other aldehydes produced in the liver in vivo after bromobenzene intoxication. *Toxicol Pathol* **14,** 457-461.

Berggren K., Chernokalskaya E., Steinberg T. H., Kemper C., Lopez M. F., Diwu Z., Haugland R. P. and Patton W. F. (2000) Background-free, high sensitivity staining of proteins in one- and two-dimensional sodium dodecyl sulfate-polyacrylamide gels using a luminescent ruthenium complex. *Electrophoresis* **21,** 2509-2521.

Beyer W., Imlay J. and Fridovich I. (1991) Superoxide dismutases. *Prog Nucleic Acid Res Mol Biol* **40,** 221-253.

Birincioglu M., Jaruga P., Chowdhury G., Rodriguez H., Dizdaroglu M. and Gates K. S. (2003) DNA base damage by the antitumor agent 3-amino-1,2,4-benzotriazine 1,4-dioxide (tirapazamine). *J Am Chem Soc* **125,** 11607-11615.

Bjellqvist B., Pasquali C., Ravier F., Sanchez J. C. and Hochstrasser D. (1993) A nonlinear wide-range immobilized pH gradient for two-dimensional electrophoresis and its definition in a relevant pH scale. *Electrophoresis* **14,** 1357-1365.

Blanchard V., Moussaoui S., Czech C., Touchet N., Bonici B., Planche M., Canton T., Jedidi I., Gohin M., Wirths O., Bayer T. A., Langui D., Duyckaerts C., Tremp G. and Pradier L. (2003) Time sequence of maturation of dystrophic neurites associated with Abeta deposits in APP/PS1 transgenic mice. *Exp Neurol* **184,** 247-263.

Blumberg L. M. (1997) Theory of fast capillary gas chromatography part. 2: Speed of analysis. *Journal of High Resolution Chromatography* **20**.

Borchelt D. R., Ratovitski T., van Lare J., Lee M. K., Gonzales V., Jenkins N. A., Copeland N. G., Price D. L. and Sisodia S. S. (1997) Accelerated amyloid deposition in the brains of transgenic mice coexpressing mutant presenilin 1 and amyloid precursor proteins. *Neuron* **19,** 939-945.

Borchelt D. R., Thinakaran G., Eckman C. B., Lee M. K., Davenport F., Ratovitsky T., Prada C. M., Kim G., Seekins S., Yager D., Slunt H. H., Wang R., Seeger M., Levey A. I., Gandy S. E., Copeland N. G., Jenkins N. A., Price D. L., Younkin S. G. and Sisodia S. S. (1996) Familial Alzheimer's disease-linked presenilin 1 variants elevate Abeta1-42/1-40 ratio in vitro and in vivo. *Neuron* **17,** 1005-1013.

Borenstein A. R., Copenhaver C. I. and Mortimer J. A. (2006) Early-life risk factors for Alzheimer disease. *Alzheimer Dis Assoc Disord* **20,** 63-72.

Borodovsky A., Ovaa H., Kolli N., Gan-Erdene T., Wilkinson K. D., Ploegh H. L. and Kessler B. M. (2002) Chemistry-based functional proteomics reveals novel members of the deubiquitinating enzyme family. *Chem Biol* **9,** 1149-1159.

Boyer P. D., Falcone A. B. and Harrison W. H. (1954) Reversal and mechanism of oxidative phosphorylation. *Nature* **174,** 401-402.

Bruce-Keller A. J., Li Y. J., Lovell M. A., Kraemer P. J., Gary D. S., Brown R. R., Markesbery W. R. and Mattson M. P. (1998) 4-Hydroxynonenal, a product of lipid peroxidation, damages cholinergic neurons and impairs visuospatial memory in rats. *J Neuropathol Exp Neurol* **57,** 257-267.

Burbaeva G., Boksha I. S., Tereshkina E. B., Savushkina O. K., Starodubtseva L. I. and Turishcheva M. S. (2005) Glutamate metabolizing enzymes in prefrontal cortex of Alzheimer's disease patients. *Neurochem Res* **30,** 1443-1451.

Burlingame A. L., Boyd R. K. and Gaskell S. J. (1998) Mass spectrometry. *Anal Chem* **70,** 647R-716R.

Bussiere T., Giannakopoulos P., Bouras C., Perl D. P., Morrison J. H. and Hof P. R. (2003) Progressive degeneration of nonphosphorylated neurofilament protein-enriched pyramidal neurons predicts cognitive impairment in Alzheimer's disease: stereologic analysis of prefrontal cortex area 9. *J Comp Neurol* **463,** 281-302.

Butterfield D. A. and Castegna A. (2003) Proteomic analysis of oxidatively modified proteins in Alzheimer's disease brain: insights into neurodegeneration. *Cell Mol Biol (Noisy-le-grand)* **49,** 747-751.

Butterfield D. A. and Boyd-Kimball D. (2005) The critical role of methionine 35 in Alzheimer's amyloid beta-peptide (1-42)-induced oxidative stress and neurotoxicity. *Biochim Biophys Acta* **1703,** 149-156.

Butterfield D. A., Boyd-Kimball D. and Castegna A. (2003) Proteomics in Alzheimer's disease: insights into potential mechanisms of neurodegeneration. *J Neurochem* **86,** 1313-1327.

Casley C. S., Land J. M., Sharpe M. A., Clark J. B., Duchen M. R. and Canevari L. (2002) Beta-amyloid fragment 25-35 causes mitochondrial dysfunction in primary cortical neurons. *Neurobiol Dis* **10,** 258-267.

Celis J. E. and Gromov P. (1999) 2D protein electrophoresis: can it be perfected? *Curr Opin Biotechnol* **10,** 16-21.

Celis J. E., Ratz G. P. and Celis A. (1987) Secreted proteins from normal and SV40 transformed human MRC-5 fibroblasts: toward establishing a database of human secreted proteins. *Leukemia* **1,** 707-717.

Chambliss K. L., Gray R. G., Rylance G., Pollitt R. J. and Gibson K. M. (2000) Molecular characterization of methylmalonate semialdehyde dehydrogenase deficiency. *J Inherit Metab Dis* **23,** 497-504.

Chapman P. F., White G. L., Jones M. W., Cooper-Blacketer D., Marshall V. J., Irizarry M., Younkin L., Good M. A., Bliss T. V., Hyman B. T., Younkin S. G. and Hsiao K. K. (1999) Impaired synaptic plasticity and learning in aged amyloid precursor protein transgenic mice. *Nat Neurosci* **2,** 271-276.

Chen Q., Ding Q., Thorpe J., Dohmen R. J. and Keller J. N. (2005) RNA interference toward UMP1 induces proteasome inhibition in Saccharomyces cerevisiae: evidence for protein oxidation and autophagic cell death. *Free Radic Biol Med* **38,** 226-234.

Cheng K. C., Cahill D. S., Kasai H., Nishimura S. and Loeb L. A. (1992) 8-Hydroxyguanine, an abundant form of oxidative DNA damage, causes G----T and A----C substitutions. *J Biol Chem* **267,** 166-172.

Chishti M. A., Yang D. S., Janus C., Phinney A. L., Horne P., Pearson J., Strome R., Zuker N., Loukides J., French J., Turner S., Lozza G., Grilli M., Kunicki S., Morissette C., Paquette J., Gervais F., Bergeron C., Fraser P. E., Carlson G. A., George-Hyslop P. S. and Westaway D. (2001) Early-onset amyloid deposition and cognitive deficits in transgenic mice expressing a double mutant form of amyloid precursor protein 695. *J Biol Chem* **276,** 21562-21570.

Choi J., Forster M. J., McDonald S. R., Weintraub S. T., Carroll C. A. and Gracy R. W. (2004) Proteomic identification of specific oxidized proteins in ApoE-knockout mice: relevance to Alzheimer's disease. *Free Radic Biol Med* **36,** 1155-1162.

Citron M., Diehl T. S., Gordon G., Biere A. L., Seubert P. and Selkoe D. J. (1996) Evidence that the 42- and 40-amino acid forms of amyloid beta protein are generated from the beta-amyloid precursor protein by different protease activities. *Proc Natl Acad Sci U S A* **93,** 13170-13175.

Clauser K. R., Baker P. and Burlingame A. L. (1999) Role of accurate mass measurement (+/- 10 ppm) in protein identification strategies employing MS or MS/MS and database searching. *Anal Chem* **71,** 2871-2882.

Collins A., Cadet J., Epe B. and Gedik C. (1997) Problems in the measurement of 8-oxoguanine in human DNA. Report of a workshop, DNA oxidation, held in Aberdeen, UK, 19-21 January, 1997. *Carcinogenesis* **18,** 1833-1836.

Cooke M. S., Evans M. D., Dizdaroglu M. and Lunec J. (2003) Oxidative DNA damage: mechanisms, mutation, and disease. *Faseb J* **17,** 1195-1214.

Cooks R. G., Glish G. L., McLuckey S. A. and Kaiser R. E. (1991) Ion trap mass spectrometry. *Chem Eng Newsl* **25,** 26-41.

Cornett C. R., Markesbery W. R. and Ehmann W. D. (1998) Imbalances of trace elements related to oxidative damage in Alzheimer's disease brain. *Neurotoxicology* **19,** 339-345.

Coughlin E. M., Christensen E., Kunz P. L., Krishnamoorthy K. S., Walker V., Dennis N. R., Chalmers R. A., Elpeleg O. N., Whelan D., Pollitt R. J., Ramesh V., Mandell R. and Shih V. E. (1998) Molecular analysis and prenatal diagnosis of human fumarase deficiency. *Mol Genet Metab* **63,** 254-262.

Crawford D. R., Suzuki T., Sesay J. and Davies K. J. (2002) Analysis of gene expression following oxidative stress. *Methods Mol Biol* **196,** 155-162.

Cruts M., van Duijn C. M., Backhovens H., Van den Broeck M., Wehnert A., Serneels S., Sherrington R., Hutton M., Hardy J., St George-Hyslop P. H., Hofman A. and Van Broeckhoven C. (1998) Estimation of the genetic contribution of presenilin-1 and -2 mutations in a population-based study of presenile Alzheimer disease. *Hum Mol Genet* **7,** 43-51.

Davies K. J. (1995) Oxidative stress: the paradox of aerobic life. *Biochem Soc Symp* **61,** 1-31.

de Leon M. J., Convit A., Wolf O. T., Tarshish C. Y., DeSanti S., Rusinek H., Tsui W., Kandil E., Scherer A. J., Roche A., Imossi A., Thorn E., Bobinski M., Caraos C., Lesbre P., Schlyer D., Poirier J., Reisberg B. and Fowler J. (2001) Prediction of cognitive decline in normal elderly subjects with 2-[(18)F]fluoro-2-deoxy-D-glucose/poitron-emission tomography (FDG/PET). *Proc Natl Acad Sci U S A* **98,** 10966-10971.

De Strooper B., Saftig P., Craessaerts K., Vanderstichele H., Guhde G., Annaert W., Von Figura K. and Van Leuven F. (1998) Deficiency of presenilin-1 inhibits the normal cleavage of amyloid precursor protein. *Nature* **391,** 387-390.

DeCarli C. (2003) Mild cognitive impairment: prevalence, prognosis, aetiology, and treatment. *Lancet Neurol* **2,** 15-21.

DeCarli C., Miller B. L., Swan G. E., Reed T., Wolf P. A. and Carmelli D. (2001) Cerebrovascular and brain morphologic correlates of mild cognitive impairment in the National Heart, Lung, and Blood Institute Twin Study. *Arch Neurol* **58,** 643-647.

DeKosky S. T. and Scheff S. W. (1990) Synapse loss in frontal cortex biopsies in Alzheimer's disease: correlation with cognitive severity. *Ann Neurol* **27,** 457-464.

Dizdaroglu M. (1998) Facts about the artifacts in the measurement of oxidative DNA base damage by gas chromatography-mass spectrometry. *Free Radic Res* **29,** 551-563.

Dizdaroglu M., Jaruga P. and Rodriguez H. (2001) Measurement of 8-hydroxy-2'-deoxyguanosine in DNA by high-performance liquid chromatography-mass spectrometry: comparison with measurement by gas chromatography-mass spectrometry. *Nucleic Acids Res* **29,** E12.

Dizdaroglu M., Jaruga P., Birincioglu M. and Rodriguez H. (2002) Free radical-induced damage to DNA: mechanisms and measurement. *Free Radic Biol Med* **32,** 1102-1115.

Duff K., Eckman C., Zehr C., Yu X., Prada C. M., Perez-tur J., Hutton M., Buee L., Harigaya Y., Yager D., Morgan D., Gordon M. N., Holcomb L., Refolo L., Zenk B.,

Hardy J. and Younkin S. (1996) Increased amyloid-beta42(43) in brains of mice expressing mutant presenilin 1. *Nature* **383,** 710-713.

Dyrks T., Dyrks E., Hartmann T., Masters C. and Beyreuther K. (1992) Amyloidogenicity of beta A4 and beta A4-bearing amyloid protein precursor fragments by metal-catalyzed oxidation. *J Biol Chem* **267,** 18210-18217.

Dyrks T., Dyrks E., Monning U., Urmoneit B., Turner J. and Beyreuther K. (1993) Generation of beta A4 from the amyloid protein precursor and fragments thereof. *FEBS Lett* **335,** 89-93.

Eckert A., Keil U., Marques C. A., Bonert A., Frey C., Schussel K. and Muller W. E. (2003) Mitochondrial dysfunction, apoptotic cell death, and Alzheimer's disease. *Biochem Pharmacol* **66,** 1627-1634.

Edman P. (1949) A method for the determination of the amino acid sequence of peptides. *Arch Biochem Biophys* **22,** 475-483.

Ehmann W. D., Markesbery W. R., Alauddin M., Hossain T. I. and Brubaker E. H. (1986) Brain trace elements in Alzheimer's disease. *Neurotoxicology* **7,** 195-206.

Esposito L., Gan L., Yu G. Q., Essrich C. and Mucke L. (2004) Intracellularly generated amyloid-beta peptide counteracts the antiapoptotic function of its precursor protein and primes proapoptotic pathways for activation by other insults in neuroblastoma cells. *J Neurochem* **91,** 1260-1274.

Ettre L. S. and March E. W. (1974) Efficiency, resolution and speed of open tubular columns as compared to packed columns. *Journal of Chromatography* **91,** 5.

Evans D. A., Beckett L. A., Field T. S., Feng L., Albert M. S., Bennett D. A., Tycko B. and Mayeux R. (1997) Apolipoprotein E epsilon4 and incidence of Alzheimer disease in a community population of older persons. *Jama* **277,** 822-824.

Evans D. A., Funkenstein H. H., Albert M. S., Scherr P. A., Cook N. R., Chown M. J., Hebert L. E., Hennekens C. H. and Taylor J. O. (1989) Prevalence of Alzheimer's disease in a community population of older persons. Higher than previously reported. *Jama* **262,** 2551-2556.

Fenn J. B., Mann M., Meng C. K., Wong S. F. and Whitehouse C. M. (1989) Electrospray ionization for mass spectrometry of large biomolecules. *Science* **246,** 64-71.

Fenton H. J. H. (1894) Oxidation of tartaric acid in presence of iron. *J Chem Soc* **65,** 899.

Floyd R. A. (1999) Neuroinflammatory processes are important in neurodegenerative diseases: an hypothesis to explain the increased formation of reactive oxygen and

nitrogen species as major factors involved in neurodegenerative disease development. *Free Radic Biol Med* **26,** 1346-1355.

French L. R., Schuman L. M., Mortimer J. A., Hutton J. T., Boatman R. A. and Christians B. (1985) A case-control study of dementia of the Alzheimer type. *Am J Epidemiol* **121,** 414-421.

Fukada K., Zhang F., Vien A., Cashman N. R. and Zhu H. (2004) Mitochondrial proteomic analysis of a cell line model of familial amyotrophic lateral sclerosis. *Mol Cell Proteomics* **3,** 1211-1223.

Gabbita S. P., Lovell M. A. and Markesbery W. R. (1998) Increased nuclear DNA oxidation in the brain in Alzheimer's disease. *J Neurochem* **71,** 2034-2040.

Gakh O., Cavadini P. and Isaya G. (2002) Mitochondrial processing peptidases. *Biochim Biophys Acta* **1592,** 63-77.

Games D., Adams D., Alessandrini R., Barbour R., Berthelette P., Blackwell C., Carr T., Clemens J., Donaldson T., Gillespie F. and et al. (1995) Alzheimer-type neuropathology in transgenic mice overexpressing V717F beta-amyloid precursor protein. *Nature* **373,** 523-527.

Gao B., Gilman A. G. and Robishaw J. D. (1987) A second form of the beta subunit of signal-transducing G proteins. *Proc Natl Acad Sci U S A* **84,** 6122-6125.

Geraghty M. T., Vaughn D., Nicholson A. J., Lin W. W., Jimenez-Sanchez G., Obie C., Flynn M. P., Valle D. and Hu C. A. (1998) Mutations in the Delta1-pyrroline 5-carboxylate dehydrogenase gene cause type II hyperprolinemia. *Hum Mol Genet* **7,** 1411-1415.

Gomez-Isla T., Hollister R., West H., Mui S., Growdon J. H., Petersen R. C., Parisi J. E. and Hyman B. T. (1997) Neuronal loss correlates with but exceeds neurofibrillary tangles in Alzheimer's disease. *Ann Neurol* **41,** 17-24.

Gorg A., Obermaier C., Boguth G., Harder A., Scheibe B., Wildgruber R. and Weiss W. (2000) The current state of two-dimensional electrophoresis with immobilized pH gradients. *Electrophoresis* **21,** 1037-1053.

Greenamyre J. T., Maragos W. F., Albin R. L., Penney J. B. and Young A. B. (1988) Glutamate transmission and toxicity in Alzheimer's disease. *Prog Neuropsychopharmacol Biol Psychiatry* **12,** 421-430.

Grimwood J., Gordon L. A., Olsen A., Terry A., Schmutz J., Lamerdin J., Hellsten U., Goodstein D., Couronne O., Tran-Gyamfi M., Aerts A., Altherr M., Ashworth L., Bajorek E., Black S., Branscomb E., Caenepeel S., Carrano A., Caoile C., Chan Y. M., Christensen M., Cleland C. A., Copeland A., Dalin E., Dehal P., Denys M., Detter J. C.,

Escobar J., Flowers D., Fotopulos D., Garcia C., Georgescu A. M., Glavina T., Gomez M., Gonzales E., Groza M., Hammon N., Hawkins T., Haydu L., Ho I., Huang W., Israni S., Jett J., Kadner K., Kimball H., Kobayashi A., Larionov V., Leem S. H., Lopez F., Lou Y., Lowry S., Malfatti S., Martinez D., McCready P., Medina C., Morgan J., Nelson K., Nolan M., Ovcharenko I., Pitluck S., Pollard M., Popkie A. P., Predki P., Quan G., Ramirez L., Rash S., Retterer J., Rodriguez A., Rogers S., Salamov A., Salazar A., She X., Smith D., Slezak T., Solovyev V., Thayer N., Tice H., Tsai M., Ustaszewska A., Vo N., Wagner M., Wheeler J., Wu K., Xie G., Yang J., Dubchak I., Furey T. S., DeJong P., Dickson M., Gordon D., Eichler E. E., Pennacchio L. A., Richardson P., Stubbs L., Rokhsar D. S., Myers R. M., Rubin E. M. and Lucas S. M. (2004) The DNA sequence and biology of human chromosome 19. *Nature* **428,** 529-535.

Grob K. (1982) "Band broadening in space" and the "retention gap" in capillary gas chromatography. *Journal of Chromatography* **237,** 15.

Gübitz G. and Schmid M. G. (2000) Recent progress in chiral separation principles in capillary electrophoresis. *Electrophoresis* **21,** 4112.

Gutteridge J. M. and Wilkins S. (1983) Copper salt-dependent hydroxyl radical formation. Damage to proteins acting as antioxidants. *Biochim Biophys Acta* **759,** 38-41.

Haass C. and Selkoe D. J. (1993) Cellular processing of beta-amyloid precursor protein and the genesis of amyloid beta-peptide. *Cell* **75,** 1039-1042.

Halász I. (1964) Concentration and Mass Flow Rate Sensitive Detectors in Gas Chromatography. *Analytical Chemistry* **36,** 1428.

Halfpenny E. and Robinson P. (1952) The nitration and hydroxylation of aromatic compounds by pernitrous acid. *J Am Chem Soc* **1952,** 939-946.

Halliwell B. and Dizdaroglu M. (1992) The measurement of oxidative damage to DNA by HPLC and GC/MS techniques. *Free Radic Res Commun* **16,** 75-87.

Hansen J. J., Bross P., Westergaard M., Nielsen M. N., Eiberg H., Borglum A. D., Mogensen J., Kristiansen K., Bolund L. and Gregersen N. (2003) Genomic structure of the human mitochondrial chaperonin genes: HSP60 and HSP10 are localised head to head on chromosome 2 separated by a bidirectional promoter. *Hum Genet* **112,** 71-77.

Harbor F. and Weiss J. (1934) The catalytic decomposition of hydrogen peroxide by iron. *Proc R Soc* **147,** 332.

Hardy J. (1997) Amyloid, the presenilins and Alzheimer's disease. *Trends Neurosci* **20,** 154-159.

Harman D. (1973) Free radical theory of aging. *Triangle* **12,** 153-158.

Harman D. (2003) The free radical theory of aging. *Antioxid Redox Signal* **5,** 557-561.

Harman D. (2006) Alzheimer's disease pathogenesis: role of aging. *Ann N Y Acad Sci* **1067,** 454-460.

Hashiguchi K., Bohr V. A. and de Souza-Pinto N. C. (2004) Oxidative stress and mitochondrial DNA repair: implications for NRTIs induced DNA damage. *Mitochondrion* **4,** 215-222.

Henderson A. S. (1986) The epidemiology of Alzheimer's disease. *Br Med Bull* **42,** 3-10.
Hensley K., Carney J. M., Mattson M. P., Aksenova M., Harris M., Wu J. F., Floyd R. A. and Butterfield D. A. (1994) A model for beta-amyloid aggregation and neurotoxicity based on free radical generation by the peptide: relevance to Alzheimer disease. *Proc Natl Acad Sci U S A* **91,** 3270-3274.

Hensley K., Hall N., Subramaniam R., Cole P., Harris M., Aksenov M., Aksenova M., Gabbita S. P., Wu J. F., Carney J. M. and et al. (1995) Brain regional correspondence between Alzheimer's disease histopathology and biomarkers of protein oxidation. *J Neurochem* **65,** 2146-2156.

Henzel W. J., Billeci T. M., Stults J. T., Wong S. C., Grimley C. and Watanabe C. (1993) Identifying proteins from two-dimensional gels by molecular mass searching of peptide fragments in protein sequence databases. *Proc Natl Acad Sci U S A* **90,** 5011-5015.

Herbert K. E., Evans M. D., Finnegan M. T., Farooq S., Mistry N., Podmore I. D., Farmer P. and Lunec J. (1996) A novel HPLC procedure for the analysis of 8-oxoguanine in DNA. *Free Radic Biol Med* **20,** 467-472.

Heyman A., Wilkinson W. E., Stafford J. A., Helms M. J., Sigmon A. H. and Weinberg T. (1984) Alzheimer's disease: a study of epidemiological aspects. *Ann Neurol* **15,** 335-341.

Holcomb L., Gordon M. N., McGowan E., Yu X., Benkovic S., Jantzen P., Wright K., Saad I., Mueller R., Morgan D., Sanders S., Zehr C., O'Campo K., Hardy J., Prada C. M., Eckman C., Younkin S., Hsiao K. and Duff K. (1998) Accelerated Alzheimer-type phenotype in transgenic mice carrying both mutant amyloid precursor protein and presenilin 1 transgenes. *Nat Med* **4,** 97-100.

Horst M., Azem A., Schatz G. and Glick B. S. (1997) What is the driving force for protein import into mitochondria? *Biochim Biophys Acta* **1318,** 71-78.

Hsiao K., Chapman P., Nilsen S., Eckman C., Harigaya Y., Younkin S., Yang F. and Cole G. (1996) Correlative memory deficits, Abeta elevation, and amyloid plaques in transgenic mice. *Science* **274,** 99-102.

Hu C. A., Lin W. W. and Valle D. (1996) Cloning, characterization, and expression of cDNAs encoding human delta 1-pyrroline-5-carboxylate dehydrogenase. *J Biol Chem* **271,** 9795-9800.

Huang X., Atwood C. S., Hartshorn M. A., Multhaup G., Goldstein L. E., Scarpa R. C., Cuajungco M. P., Gray D. N., Lim J., Moir R. D., Tanzi R. E. and Bush A. I. (1999) The A beta peptide of Alzheimer's disease directly produces hydrogen peroxide through metal ion reduction. *Biochemistry* **38,** 7609-7616.

Hurshman A. R. and Marletta M. A. (2002) Reactions catalyzed by the heme domain of inducible nitric oxide synthase: evidence for the involvement of tetrahydrobiopterin in electron transfer. *Biochemistry* **41,** 3439-3456.

Imlay J. A. and Linn S. (1988) DNA damage and oxygen radical toxicity. *Science* **240,** 1302-1309.

James P., Quadroni M., Carafoli E. and Gonnet G. (1993) Protein identification by mass profile fingerprinting. *Biochem Biophys Res Commun* **195,** 58-64.

Jaroszewski L., Rychlewski L., Reed J. C. and Godzik A. (2000) ATP-activated oligomerization as a mechanism for apoptosis regulation: fold and mechanism prediction for CED-4. *Proteins* **39,** 197-203.

Jaruga P., Birincioglu M., Rodriguez H. and Dizdaroglu M. (2002) Mass spectrometric assays for the tandem lesion 8,5'-cyclo-2'-deoxyguanosine in mammalian DNA. *Biochemistry* **41,** 3703-3711.

Jarvik J. W. and Telmer C. A. (1998) Epitope tagging. *Annu Rev Genet* **32,** 601-618.

Jiang X. S., Dai J., Sheng Q. H., Zhang L., Xia Q. C., Wu J. R. and Zeng R. (2005) A comparative proteomic strategy for subcellular proteome research: ICAT approach coupled with bioinformatics prediction to ascertain rat liver mitochondrial proteins and indication of mitochondrial localization for catalase. *Mol Cell Proteomics* **4,** 12-34.

Karas M. and Hillenkamp F. (1988) Laser desorption ionization of proteins with molecular masses exceeding 10,000 daltons. *Anal Chem* **60,** 2299-2301.

Katzman R. (1976) Editorial: The prevalence and malignancy of Alzheimer disease. A major killer. *Arch Neurol* **33,** 217-218.

Kim T. W., Pettingell W. H., Jung Y. K., Kovacs D. M. and Tanzi R. E. (1997) Alternative cleavage of Alzheimer-associated presenilins during apoptosis by a caspase-3 family protease. *Science* **277,** 373-376.

Kish S. J., Morito C. L. and Hornykiewicz O. (1986) Brain glutathione peroxidase in neurodegenerative disorders. *Neurochem Pathol* **4,** 23-28.

Kokmen E., Whisnant J. P., O'Fallon W. M., Chu C. P. and Beard C. M. (1996) Dementia after ischemic stroke: a population-based study in Rochester, Minnesota (1960-1984). *Neurology* **46,** 154-159.

Kril J. J., Hodges J. and Halliday G. (2004) Relationship between hippocampal volume and CA1 neuron loss in brains of humans with and without Alzheimer's disease. *Neurosci Lett* **361,** 9-12.

Kril J. J., Patel S., Harding A. J. and Halliday G. M. (2002) Neuron loss from the hippocampus of Alzheimer's disease exceeds extracellular neurofibrillary tangle formation. *Acta Neuropathol (Berl)* **103,** 370-376.

Laemmli U. K. (1970) Cleavage of structural proteins during the assembly of the head of bacteriophage T4. *Nature* **227,** 680-685.

Lemere C. A., Lopera F., Kosik K. S., Lendon C. L., Ossa J., Saido T. C., Yamaguchi H., Ruiz A., Martinez A., Madrigal L., Hincapie L., Arango J. C., Anthony D. C., Koo E. H., Goate A. M., Selkoe D. J. and Arango J. C. (1996) The E280A presenilin 1 Alzheimer mutation produces increased A beta 42 deposition and severe cerebellar pathology. *Nat Med* **2,** 1146-1150.

Li S., Mallory M., Alford M., Tanaka S. and Masliah E. (1997) Glutamate transporter alterations in Alzheimer disease are possibly associated with abnormal APP expression. *J Neuropathol Exp Neurol* **56,** 901-911.

Li X. and Greenwald I. (1996) Membrane topology of the C. elegans SEL-12 presenilin. *Neuron* **17,** 1015-1021.

Lieshout M., Derks R., Janssen H. G. and Cramers C. A. (1998) Fast Capillary Gas Chromatography: Comparison of Different Approaches. *Journal of High Resolution Chromatography* **21,** 583-586.

Liu X., Lovell M. A. and Lynn B. C. (2005) Development of a method for quantification of acrolein-deoxyguanosine adducts in DNA using isotope dilution-capillary LC/MS/MS and its application to human brain tissue. *Anal Chem* **77,** 5982-5989.

Loo D. T., Copani A., Pike C. J., Whittemore E. R., Walencewicz A. J. and Cotman C. W. (1993) Apoptosis is induced by beta-amyloid in cultured central nervous system neurons. *Proc Natl Acad Sci U S A* **90,** 7951-7955.

Lopez O. L., Jagust W. J., Dulberg C., Becker J. T., DeKosky S. T., Fitzpatrick A., Breitner J., Lyketsos C., Jones B., Kawas C., Carlson M. and Kuller L. H. (2003) Risk factors for mild cognitive impairment in the Cardiovascular Health Study Cognition Study: part 2. *Arch Neurol* **60,** 1394-1399.

Lovell M. A., Gabbita S. P. and Markesbery W. R. (1999a) Increased DNA oxidation and decreased levels of repair products in Alzheimer's disease ventricular CSF. *J Neurochem* **72,** 771-776.

Lovell M. A., Xie C. and Markesbery W. R. (1999b) Protection against amyloid beta peptide toxicity by zinc. *Brain Res* **823,** 88-95.

Lovell M. A., Xie C. and Markesbery W. R. (2000a) Acrolein, a product of lipid peroxidation, inhibits glucose and glutamate uptake in primary neuronal cultures. *Free Radic Biol Med* **29,** 714-720.

Lovell M. A., Xie C. and Markesbery W. R. (2000b) Decreased base excision repair and increased helicase activity in Alzheimer's disease brain. *Brain Res* **855,** 116-123.

Lovell M. A., Xie C. and Markesbery W. R. (2001) Acrolein is increased in Alzheimer's disease brain and is toxic to primary hippocampal cultures. *Neurobiol Aging* **22,** 187-194.

Lovell M. A., Ehmann W. D., Butler S. M. and Markesbery W. R. (1995) Elevated thiobarbituric acid-reactive substances and antioxidant enzyme activity in the brain in Alzheimer's disease. *Neurology* **45,** 1594-1601.

Lovell M. A., Ehmann W. D., Mattson M. P. and Markesbery W. R. (1997) Elevated 4-hydroxynonenal in ventricular fluid in Alzheimer's disease. *Neurobiol Aging* **18,** 457-461.

Lovell M. A., Xie C., Xiong S. and Markesbery W. R. (2003) Protection against amyloid beta peptide and iron/hydrogen peroxide toxicity by alpha lipoic acid. *J Alzheimers Dis* **5,** 229-239.

Lovell M. A., Xiong S., Markesbery W. R. and Lynn B. C. (2005) Quantitative proteomic analysis of mitochondria from primary neuron cultures treated with amyloid beta peptide. *Neurochem Res* **30,** 113-122.

Lovell M. A., Robertson J. D., Teesdale W. J., Campbell J. L. and Markesbery W. R. (1998) Copper, iron and zinc in Alzheimer's disease senile plaques. *J Neurol Sci* **158,** 47-52.

Lovell M. A., Robertson J. D., Buchholz B. A., Xie C. and Markesbery W. R. (2002) Use of bomb pulse carbon-14 to age senile plaques and neurofibrillary tangles in Alzheimer's disease. *Neurobiol Aging* **23,** 179-186.

Lyras L., Cairns N. J., Jenner A., Jenner P. and Halliwell B. (1997) An assessment of oxidative damage to proteins, lipids, and DNA in brain from patients with Alzheimer's disease. *J Neurochem* **68,** 2061-2069.

Mackey A. J., Haystead T. A. and Pearson W. R. (2002) Getting more from less: algorithms for rapid protein identification with multiple short peptide sequences. *Mol Cell Proteomics* **1,** 139-147.

Mann M. and Wilm M. (1994) Error-tolerant identification of peptides in sequence databases by peptide sequence tags. *Anal Chem* **66,** 4390-4399.

Marcus D. L., Thomas C., Rodriguez C., Simberkoff K., Tsai J. S., Strafaci J. A. and Freedman M. L. (1998) Increased peroxidation and reduced antioxidant enzyme activity in Alzheimer's disease. *Exp Neurol* **150,** 40-44.

Mark R. J., Lovell M. A., Markesbery W. R., Uchida K. and Mattson M. P. (1997) A role for 4-hydroxynonenal, an aldehydic product of lipid peroxidation, in disruption of ion homeostasis and neuronal death induced by amyloid beta-peptide. *J Neurochem* **68,** 255-264.

Markesbery W. R. (1997) Oxidative stress hypothesis in Alzheimer's disease. *Free Radic Biol Med* **23,** 134-147.

Markesbery W. R. and Lovell M. A. (1998) Four-hydroxynonenal, a product of lipid peroxidation, is increased in the brain in Alzheimer's disease. *Neurobiol Aging* **19,** 33-36.

Markesbery W. R. and Carney J. M. (1999) Oxidative alterations in Alzheimer's disease. *Brain Pathol* **9,** 133-146.

Marletta M. A. (1993) Nitric oxide synthase structure and mechanism. *J Biol Chem* **268,** 12231-12234.

Martin J. B. (1999) Molecular basis of the neurodegenerative disorders. *N Engl J Med* **340,** 1970-1980.

Matovská K. and Lehotay S. J. (2003) Practical approaches to fast gas chromatography–mass spectrometry. *Journal of Chromatography A* **1000,** 153-180.

Matsui N. M., Smith-Beckerman D. M. and Epstein L. B. (1999) Staining of preparative 2-D gels. Coomassie blue and imidazole-zinc negative staining. *Methods Mol Biol* **112,** 307-311.

McCormack A. L., Schieltz D. M., Goode B., Yang S., Barnes G., Drubin D. and Yates J. R., 3rd (1997) Direct analysis and identification of proteins in mixtures by LC/MS/MS and database searching at the low-femtomole level. *Anal Chem* **69,** 767-776.

Mecocci P., MacGarvey U. and Beal M. F. (1994) Oxidative damage to mitochondrial DNA is increased in Alzheimer's disease. *Ann Neurol* **36,** 747-751.

Mecocci P., MacGarvey U., Kaufman A. E., Koontz D., Shoffner J. M., Wallace D. C. and Beal M. F. (1993) Oxidative damage to mitochondrial DNA shows marked age-dependent increases in human brain. *Ann Neurol* **34,** 609-616.

Michalske T. A. and Freiman S. W. (1982) Molecular interpretation of stress corrosion in silica. *Nature* **295,** 511.

Migliore L., Fontana I., Trippi F., Colognato R., Coppede F., Tognoni G., Nucciarone B. and Siciliano G. (2005) Oxidative DNA damage in peripheral leukocytes of mild cognitive impairment and AD patients. *Neurobiol Aging* **26,** 567-573.

Miller P. E. and Denton M. B. (1986) The quadrupole mass filter: basic operating concepts. *J. Chem. Ed.* **63,** 617-622.

Milne G. L., Musiek E. S. and Morrow J. D. (2005) F2-isoprostanes as markers of oxidative stress in vivo: an overview. *Biomarkers* **10 Suppl 1,** S10-23.

Mitchell P. (1961) Coupling of Phosphorylation to Electron and Hydrogen Transfer by a Chemi-Osmotic type of Mechanism. *Nature* **191,** 144-148.

Montine T. J., Markesbery W. R., Morrow J. D. and Roberts L. J., 2nd (1998) Cerebrospinal fluid F2-isoprostane levels are increased in Alzheimer's disease. *Ann Neurol* **44,** 410-413.

Mootha V. K., Bunkenborg J., Olsen J. V., Hjerrild M., Wisniewski J. R., Stahl E., Bolouri M. S., Ray H. N., Sihag S., Kamal M., Patterson N., Lander E. S. and Mann M. (2003) Integrated analysis of protein composition, tissue diversity, and gene regulation in mouse mitochondria. *Cell* **115,** 629-640.

Morrow J. D., Awad J. A., Boss H. J., Blair I. A. and Roberts L. J., 2nd (1992a) Non-cyclooxygenase-derived prostanoids (F2-isoprostanes) are formed in situ on phospholipids. *Proc Natl Acad Sci U S A* **89,** 10721-10725.

Morrow J. D., Awad J. A., Kato T., Takahashi K., Badr K. F., Roberts L. J., 2nd and Burk R. F. (1992b) Formation of novel non-cyclooxygenase-derived prostanoids (F2-isoprostanes) in carbon tetrachloride hepatotoxicity. An animal model of lipid peroxidation. *J Clin Invest* **90,** 2502-2507.

Musiek E. S., Cha J. K., Yin H., Zackert W. E., Terry E. S., Porter N. A., Montine T. J. and Morrow J. D. (2004) Quantification of F-ring isoprostane-like compounds (F(4)-neuroprostanes) derived from docosahexaenoic acid in vivo in humans by a stable isotope dilution mass spectrometric assay. *J Chromatogr B Analyt Technol Biomed Life Sci* **799,** 95-102.

Nacmias B., Piccini C., Bagnoli S., Tedde A., Cellini E., Bracco L. and Sorbi S. (2004) Brain-derived neurotrophic factor, apolipoprotein E genetic variants and cognitive performance in Alzheimer's disease. *Neurosci Lett* **367,** 379-383.

NIA (1995) Progress report on Alzheimer's disease.
Nishikimi M., Hosokawa Y., Toda H., Suzuki H. and Ozawa T. (1990) The primary structure of human Rieske iron-sulfur protein of mitochondrial cytochrome bc1 complex deduced from cDNA analysis. *Biochem Int* **20,** 155-160.

O'Farrell P. H. (1975) High resolution two-dimensional electrophoresis of proteins. *J Biol Chem* **250,** 4007-4021.

Okamura N., Arai H., Maruyama M., Higuchi M., Matsui T., Tanji H., Seki T., Hirai H., Chiba H., Itoh M. and Sasaki H. (2002) Combined Analysis of CSF Tau Levels and [(123)I]Iodoamphetamine SPECT in Mild Cognitive Impairment: Implications for a Novel Predictor of Alzheimer's Disease. *Am J Psychiatry* **159,** 474-476.

Pandey A. and Mann M. (2000) Proteomics to study genes and genomes. *Nature* **405,** 837-846.

Pappin D. J., Hojrup P. and Bleasby A. J. (1993) Rapid identification of proteins by peptide-mass fingerprinting. *Curr Biol* **3,** 327-332.

Pappolla M. A., Omar R. A., Kim K. S. and Robakis N. K. (1992) Immunohistochemical evidence of oxidative [corrected] stress in Alzheimer's disease. *Am J Pathol* **140,** 621-628.

Parcher J. F. (1983) A review of vapor phase chromatography: gas chromatography with vapor carrier gases. *Journal of Chromatographic Science* **21,** 346.

Pata I., Tensing K. and Metspalu A. (1997) A human cDNA encoding the homologue of NADH: ubiquinone oxidoreductase subunit B13. *Biochim Biophys Acta* **1350,** 115-118.

Pedersen S. K., Harry J. L., Sebastian L., Baker J., Traini M. D., McCarthy J. T., Manoharan A., Wilkins M. R., Gooley A. A., Righetti P. G., Packer N. H., Williams K. L. and Herbert B. R. (2003) Unseen proteome: mining below the tip of the iceberg to find low abundance and membrane proteins. *J Proteome Res* **2,** 303-311.

Peng J. and Gygi S. P. (2001) Proteomics: the move to mixtures. *J Mass Spectrom* **36,** 1083-1091.

Perkins D. N., Pappin D. J., Creasy D. M. and Cottrell J. S. (1999) Probability-based protein identification by searching sequence databases using mass spectrometry data. *Electrophoresis* **20,** 3551-3567.

Pfanner N., Douglas M. G., Endo T., Hoogenraad N. J., Jensen R. E., Meijer M., Neupert W., Schatz G., Schmitz U. K. and Shore G. C. (1996) Uniform nomenclature for the

protein transport machinery of the mitochondrial membranes. *Trends Biochem Sci* **21,** 51-52.

Pike C. J., Burdick D., Walencewicz A. J., Glabe C. G. and Cotman C. W. (1993) Neurodegeneration induced by beta-amyloid peptides in vitro: the role of peptide assembly state. *J Neurosci* **13,** 1676-1687.

Pithukpakorn M. (2005) Disorders of pyruvate metabolism and the tricarboxylic acid cycle. *Mol Genet Metab* **85,** 243-246.

Poon H. F., Castegna A., Farr S. A., Thongboonkerd V., Lynn B. C., Banks W. A., Morley J. E., Klein J. B. and Butterfield D. A. (2004) Quantitative proteomics analysis of specific protein expression and oxidative modification in aged senescence-accelerated-prone 8 mice brain. *Neuroscience* **126,** 915-926.

Pratico D., Clark C. M., Liun F., Rokach J., Lee V. Y. and Trojanowski J. Q. (2002) Increase of brain oxidative stress in mild cognitive impairment: a possible predictor of Alzheimer disease. *Arch Neurol* **59,** 972-976.

Ravanat J. L., Duretz B., Guiller A., Douki T. and Cadet J. (1998) Isotope dilution high-performance liquid chromatography-electrospray tandem mass spectrometry assay for the measurement of 8-oxo-7,8-dihydro-2'-deoxyguanosine in biological samples. *J Chromatogr B Biomed Sci Appl* **715,** 349-356.

Reddy P. H., McWeeney S., Park B. S., Manczak M., Gutala R. V., Partovi D., Jung Y., Yau V., Searles R., Mori M. and Quinn J. (2004) Gene expression profiles of transcripts in amyloid precursor protein transgenic mice: up-regulation of mitochondrial metabolism and apoptotic genes is an early cellular change in Alzheimer's disease. *Hum Mol Genet* **13,** 1225-1240.

Richardson J. S. (1993) Free radicals in the genesis of Alzheimer's disease. *Ann N Y Acad Sci* **695,** 73-76.

Richter C., Park J. W. and Ames B. N. (1988) Normal oxidative damage to mitochondrial and nuclear DNA is extensive. *Proc Natl Acad Sci U S A* **85,** 6465-6467.

Roher A. E., Lowenson J. D., Clarke S., Wolkow C., Wang R., Cotter R. J., Reardon I. M., Zurcher-Neely H. A., Heinrikson R. L., Ball M. J. and et al. (1993) Structural alterations in the peptide backbone of beta-amyloid core protein may account for its deposition and stability in Alzheimer's disease. *J Biol Chem* **268,** 3072-3083.

Sampson J. B., Ye Y., Rosen H. and Beckman J. S. (1998) Myeloperoxidase and horseradish peroxidase catalyze tyrosine nitration in proteins from nitrite and hydrogen peroxide. *Arch Biochem Biophys* **356,** 207-213.

Santos F. J. and Galceran M. T. (2003) Modern developments in gas chromatography–mass spectrometry-based environmental analysis *Journal of Chromatography A* **1000,** 125-151.

Schatz G. (1996) The protein import system of mitochondria. *J Biol Chem* **271,** 31763-31766.

Scheele G. A. (1975) Two-dimensional gel analysis of soluble proteins. Charaterization of guinea pig exocrine pancreatic proteins. *J Biol Chem* **250,** 5375-5385.

Scheff S. W. and Price D. A. (1993) Synapse loss in the temporal lobe in Alzheimer's disease. *Ann Neurol* **33,** 190-199.

Scheuner D., Eckman C., Jensen M., Song X., Citron M., Suzuki N., Bird T. D., Hardy J., Hutton M., Kukull W., Larson E., Levy-Lahad E., Viitanen M., Peskind E., Poorkaj P., Schellenberg G., Tanzi R., Wasco W., Lannfelt L., Selkoe D. and Younkin S. (1996) Secreted amyloid beta-protein similar to that in the senile plaques of Alzheimer's disease is increased in vivo by the presenilin 1 and 2 and APP mutations linked to familial Alzheimer's disease. *Nat Med* **2,** 864-870.

Schleyer M., Schmidt B. and Neupert W. (1982) Requirement of a membrane potential for the posttranslational transfer of proteins into mitochondria. *Eur J Biochem* **125,** 109-116.

Schmitz C., Rutten B. P., Pielen A., Schafer S., Wirths O., Tremp G., Czech C., Blanchard V., Multhaup G., Rezaie P., Korr H., Steinbusch H. W., Pradier L. and Bayer T. A. (2004) Hippocampal neuron loss exceeds amyloid plaque load in a transgenic mouse model of Alzheimer's disease. *Am J Pathol* **164,** 1495-1502.

Schomburg G., Husmann H. and Rittmann R. (1981) "Direct" (on-column) sampling into glass capillary columns comparative investigations on split, splitless and on-column sampling. *Journal of Chromatography* **204,** 85.

Sclan S. G. and Kanowski S. (2001) Alzheimer's disease: stage-related interventions. *Lippincotts Case Manag* **6,** 48-60; quiz 61-43.

Selkoe D. J. (1999) Translating cell biology into therapeutic advances in Alzheimer's disease. *Nature* **399,** A23-31.

Selkoe D. J. (2001) Alzheimer's disease: genes, proteins, and therapy. *Physiol Rev* **81,** 741-766.

Selkoe D. J. and Schenk D. (2003) Alzheimer's disease: molecular understanding predicts amyloid-based therapeutics. *Annu Rev Pharmacol Toxicol* **43,** 545-584.

Serrano J., Palmeira C. M., Wallace K. B. and Kuehl D. W. (1996) Determination of 8-hydroxydeoxyguanosine in biological tissue by liquid chromatography/electrospray ionization-mass spectrometry/mass spectrometry. *Rapid Commun Mass Spectrom* **10,** 1789-1791.

Shen J., Bronson R. T., Chen D. F., Xia W., Selkoe D. J. and Tonegawa S. (1997) Skeletal and CNS defects in Presenilin-1-deficient mice. *Cell* **89,** 629-639.

Sherrington R., Rogaev E. I., Liang Y., Rogaeva E. A., Levesque G., Ikeda M., Chi H., Lin C., Li G., Holman K. and et al. (1995) Cloning of a gene bearing missense mutations in early-onset familial Alzheimer's disease. *Nature* **375,** 754-760.

Simard A. R., Soulet D., Gowing G., Julien J. P. and Rivest S. (2006) Bone marrow-derived microglia play a critical role in restricting senile plaque formation in Alzheimer's disease. *Neuron* **49,** 489-502.

Smith C. D., Carney J. M., Starke-Reed P. E., Oliver C. N., Stadtman E. R., Floyd R. A. and Markesbery W. R. (1991) Excess brain protein oxidation and enzyme dysfunction in normal aging and in Alzheimer disease. *Proc Natl Acad Sci U S A* **88,** 10540-10543.

Smith I. F., Boyle J. P., Green K. N., Pearson H. A. and Peers C. (2004) Hypoxic remodelling of Ca2+ mobilization in type I cortical astrocytes: involvement of ROS and pro-amyloidogenic APP processing. *J Neurochem* **88,** 869-877.

Smith M. A., Richey Harris P. L., Sayre L. M., Beckman J. S. and Perry G. (1997) Widespread peroxynitrite-mediated damage in Alzheimer's disease. *J Neurosci* **17,** 2653-2657.

Smith M. A., Vasak M., Knipp M., Castellani R. J. and Perry G. (1998) Dimethylargininase, a nitric oxide regulatory protein, in Alzheimer disease. *Free Radic Biol Med* **25,** 898-902.

Smith M. A., Nunomura A., Zhu X., Takeda A. and Perry G. (2000a) Metabolic, metallic, and mitotic sources of oxidative stress in Alzheimer disease. *Antioxid Redox Signal* **2,** 413-420.

Smith M. A., Rottkamp C. A., Nunomura A., Raina A. K. and Perry G. (2000b) Oxidative stress in Alzheimer's disease. *Biochim Biophys Acta* **1502,** 139-144.

Steenken S. (1989a) Purine Bases, Nucleosides, and Nucleotides: Aqueous Solution Redox Chemistry and Transformation Reaction of Their Radical Cations and e and OH Adducts. *Chem. Rev.* **89,** 503-520.

Steenken S. (1989b) Structure, acid/base properties and transformation reactions of purine radicals. *Free Radic Res Commun* **6,** 117-120.

Steenken S. (1989c) Purine Bases, Nucleosides, and Nucleotides: Aqueous Solution Redox Chemistry and Transformation Reaction of Their Radical Cations and e and OH Adducts. *Chem. Rev.* **89,** 503-520.

Stern E. A., Bacskai B. J., Hickey G. A., Attenello F. J., Lombardo J. A. and Hyman B. T. (2004) Cortical synaptic integration in vivo is disrupted by amyloid-beta plaques. *J Neurosci* **24,** 4535-4540.

Stock D., Gibbons C., Arechaga I., Leslie A. G. and Walker J. E. (2000) The rotary mechanism of ATP synthase. *Curr Opin Struct Biol* **10,** 672-679.

Storey E. and Cappai R. (1999) The amyloid precursor protein of Alzheimer's disease and the Abeta peptide. *Neuropathol Appl Neurobiol* **25,** 81-97.

Strittmatter W. J., Saunders A. M., Schmechel D., Pericak-Vance M., Enghild J., Salvesen G. S. and Roses A. D. (1993) Apolipoprotein E: high-avidity binding to beta-amyloid and increased frequency of type 4 allele in late-onset familial Alzheimer disease. *Proc Natl Acad Sci U S A* **90,** 1977-1981.

Stuart J. A., Mayard S., Hashiguchi K., Souza-Pinto N. C. and Bohr V. A. (2005) Localization of mitochondrial DNA base excision repair to an inner membrane-associated particulate fraction. *Nucleic Acids Res* **33,** 3722-3732.

Sullivan P., Petitti D. and Barbaccia J. (1987) Head trauma and age of onset of dementia of the Alzheimer type. *Jama* **257,** 2289-2290.

Tatemichi T. K., Paik M., Bagiella E., Desmond D. W., Pirro M. and Hanzawa L. K. (1994) Dementia after stroke is a predictor of long-term survival. *Stroke* **25,** 1915-1919.

Taylor R. W. and Turnbull D. M. (2005) Mitochondrial DNA mutations in human disease. *Nat Rev Genet* **6,** 389-402.

Taylor S. W., Fahy E., Zhang B., Glenn G. M., Warnock D. E., Wiley S., Murphy A. N., Gaucher S. P., Capaldi R. A., Gibson B. W. and Ghosh S. S. (2003) Characterization of the human heart mitochondrial proteome. *Nat Biotechnol* **21,** 281-286.

Tensing K., Pata I., Wittig I., Wehnert M. and Metspalu A. (1999) Genomic organization of the human complex I 13-kDa subunit gene NDUFA5. *Cytogenet Cell Genet* **84,** 125-127.

Tomlinson I. P., Alam N. A., Rowan A. J., Barclay E., Jaeger E. E., Kelsell D., Leigh I., Gorman P., Lamlum H., Rahman S., Roylance R. R., Olpin S., Bevan S., Barker K., Hearle N., Houlston R. S., Kiuru M., Lehtonen R., Karhu A., Vilkki S., Laiho P., Eklund C., Vierimaa O., Aittomaki K., Hietala M., Sistonen P., Paetau A., Salovaara R., Herva R., Launonen V. and Aaltonen L. A. (2002) Germline mutations in FH predispose to

dominantly inherited uterine fibroids, skin leiomyomata and papillary renal cell cancer. *Nat Genet* **30,** 406-410.

Travis J. (1993) New piece in Alzheimer's puzzle. *Science* **261,** 828-829.

Traykov L., Rigaud A. S., Baudic S., Smagghe A., Boller F. and Forette F. (2002) Apolipoprotein E epsilon 4 allele frequency in demented and cognitively impaired patients with and without cerebrovascular disease. *J Neurol Sci* **203-204,** 177-181.

Trojanowski J. Q. and Lee V. M. (1995) Phosphorylation of paired helical filament tau in Alzheimer's disease neurofibrillary lesions: focusing on phosphatases. *Faseb J* **9,** 1570-1576.

Unlu M., Morgan M. E. and Minden J. S. (1997) Difference gel electrophoresis: a single gel method for detecting changes in protein extracts. *Electrophoresis* **18,** 2071-2077.

Urwin V. E. and Jackson P. (1993) Two-dimensional polyacrylamide gel electrophoresis of proteins labeled with the fluorophore monobromobimane prior to first-dimensional isoelectric focusing: imaging of the fluorescent protein spot patterns using a cooled charge-coupled device. *Anal Biochem* **209,** 57-62.

Van den Driessche B., Esmans E. L., Van der Linden A., Van Dongen W., Schaerlaken E., Lemiere F., Witters E. and Berneman Z. (2005) First results of a quantitative study of DNA adducts of melphalan in the rat by isotope dilution mass spectrometry using capillary liquid chromatography coupled to electrospray tandem mass spectrometry. *Rapid Commun Mass Spectrom* **19,** 1999-2004.

Varadarajan S., Yatin S., Aksenova M. and Butterfield D. A. (2000) Review: Alzheimer's amyloid beta-peptide-associated free radical oxidative stress and neurotoxicity. *J Struct Biol* **130,** 184-208.

Vékey K. (2001) Mass spectrometry and mass-selective detection in chromatography. *Journal of Chromatography A* **921,** 227-236.

Venner T. J., Singh B. and Gupta R. S. (1990) Nucleotide sequences and novel structural features of human and Chinese hamster hsp60 (chaperonin) gene families. *DNA Cell Biol* **9,** 545-552.

von Heijne G., Steppuhn J. and Herrmann R. G. (1989) Domain structure of mitochondrial and chloroplast targeting peptides. *Eur J Biochem* **180,** 535-545.

Wadia J. S., Chalmers-Redman R. M., Ju W. J., Carlile G. W., Phillips J. L., Fraser A. D. and Tatton W. G. (1998) Mitochondrial membrane potential and nuclear changes in apoptosis caused by serum and nerve growth factor withdrawal: time course and modification by (-)-deprenyl. *J Neurosci* **18,** 932-947.

Wallace D. C. (1992) Mitochondrial genetics: a paradigm for aging and degenerative diseases? *Science* **256,** 628-632.

Wallace D. C. (1999) Mitochondrial diseases in man and mouse. *Science* **283,** 1482-1488.

Wang J., Markesbery W. R. and Lovell M. A. (2006) Increased oxidative damage in nuclear and mitochondrial DNA in mild cognitive impairment. *J Neurochem* **96,** 825-832.

Wang J., Xiong S., Xie C., Markesbery W. R. and Lovell M. A. (2005) Increased oxidative damage in nuclear and mitochondrial DNA in Alzheimer's disease. *J Neurochem* **93,** 953-962.

Wasinger V. C., Cordwell S. J., Cerpa-Poljak A., Yan J. X., Gooley A. A., Wilkins M. R., Duncan M. W., Harris R., Williams K. L. and Humphery-Smith I. (1995) Progress with gene-product mapping of the Mollicutes: Mycoplasma genitalium. *Electrophoresis* **16,** 1090-1094.

Watt J. A., Pike C. J., Walencewicz-Wasserman A. J. and Cotman C. W. (1994) Ultrastructural analysis of beta-amyloid-induced apoptosis in cultured hippocampal neurons. *Brain Res* **661,** 147-156.

Weidemann A., Konig G., Bunke D., Fischer P., Salbaum J. M., Masters C. L. and Beyreuther K. (1989) Identification, biogenesis, and localization of precursors of Alzheimer's disease A4 amyloid protein. *Cell* **57,** 115-126.

Weiler T., Sauder P., Cheng K., Ens W., Standing K. and Wilkins J. A. (2003) A proteomics-based approach for monoclonal antibody characterization. *Anal Biochem* **321,** 217-225.

Wengenack T. M., Whelan S., Curran G. L., Duff K. E. and Poduslo J. F. (2000) Quantitative histological analysis of amyloid deposition in Alzheimer's double transgenic mouse brain. *Neuroscience* **101,** 939-944.

West M. J., Coleman P. D., Flood D. G. and Troncoso J. C. (1994) Differences in the pattern of hippocampal neuronal loss in normal ageing and Alzheimer's disease. *Lancet* **344,** 769-772.

Wilkins M. R., Sanchez J. C., Gooley A. A., Appel R. D., Humphery-Smith I., Hochstrasser D. F. and Williams K. L. (1996) Progress with proteome projects: why all proteins expressed by a genome should be identified and how to do it. *Biotechnol Genet Eng Rev* **13,** 19-50.

Wilm M. (2000) Mass spectrometric analysis of proteins. *Adv Protein Chem* **54,** 1-30.
Wilm M. and Mann M. (1996) Analytical properties of the nanoelectrospray ion source. *Anal Chem* **68,** 1-8.

Wilm M., Shevchenko A., Houthaeve T., Breit S., Schweigerer L., Fotsis T. and Mann M. (1996) Femtomole sequencing of proteins from polyacrylamide gels by nano-electrospray mass spectrometry. *Nature* **379,** 466-469.

Wirths O., Weis J., Szczygielski J., Multhaup G. and Bayer T. A. (2006) Axonopathy in an APP/PS1 transgenic mouse model of Alzheimer's disease. *Acta Neuropathol (Berl)* **111,** 312-319.

Wolf H., Hensel A., Kruggel F., Riedel-Heller S. G., Arendt T., Wahlund L. O. and Gertz H. J. (2004) Structural correlates of mild cognitive impairment. *Neurobiol Aging* **25,** 913-924.

Xie C. X., Mattson M. P., Lovell M. A. and Yokel R. A. (1996) Intraneuronal aluminum potentiates iron-induced oxidative stress in cultured rat hippocampal neurons. *Brain Res* **743,** 271-277.

Xu H., Sweeney D., Wang R., Thinakaran G., Lo A. C., Sisodia S. S., Greengard P. and Gandy S. (1997) Generation of Alzheimer beta-amyloid protein in the trans-Golgi network in the apparent absence of vesicle formation. *Proc Natl Acad Sci U S A* **94,** 3748-3752.

Yates J. R., 3rd (1998) Mass spectrometry and the age of the proteome. *J Mass Spectrom* **33,** 1-19.

Yates J. R., 3rd, Speicher S., Griffin P. R. and Hunkapiller T. (1993) Peptide mass maps: a highly informative approach to protein identification. *Anal Biochem* **214,** 397-408.

Yates J. R., 3rd, Eng J. K., McCormack A. L. and Schieltz D. (1995) Method to correlate tandem mass spectra of modified peptides to amino acid sequences in the protein database. *Anal Chem* **67,** 1426-1436.

Youngman L. D., Park J. Y. and Ames B. N. (1992) Protein oxidation associated with aging is reduced by dietary restriction of protein or calories. *Proc Natl Acad Sci U S A* **89,** 9112-9116.

Yu W. H., Wolfgang W. and Forte M. (1995) Subcellular localization of human voltage-dependent anion channel isoforms. *J Biol Chem* **270,** 13998-14006.

Zawia N. H. and Basha M. R. (2005) Environmental risk factors and the developmental basis for Alzheimer's disease. *Rev Neurosci* **16,** 325-337.

Zhang M. Y., Katzman R., Salmon D., Jin H., Cai G. J., Wang Z. Y., Qu G. Y., Grant I., Yu E., Levy P. and et al. (1990) The prevalence of dementia and Alzheimer's disease in Shanghai, China: impact of age, gender, and education. *Ann Neurol* **27,** 428-437.

VITA

Jianquan Wang (Born: February 5, 1977 in Shandong, China)

Education and Awards

2001 - 2006 Thesis: Increased Oxidative Damage to DNA and The Effects On Mitochondrial Protein in Alzheimer's Disease
Advisor: Mark A Lovell
Department of Chemistry, University of Kentucky, Lexington, KY
Graduate School Travel Fellowship (2002-2004, 2006)
Research Scholarship (2002-2006)
Teaching Scholarship (2001-2002)

1995 - 1999 B.S. in Chemistry, Shandong University, Jinan, China
Panasonic Corporation Fellowship for Undergraduate in China (1997)
Excellent Students Fellowship at Shandong University (1995-1999)

Research and Teaching Experience

Research Assistant, 2002-2006**,** University of Kentucky, Lexington, KY
Teaching Assistant, 2001-2002, University of Kentucky, Lexington, KY
Research Assistant, 1999-2001**,** Shandong University, Jinan, China

Publications:

1. **Wang J.,** Xiong S., Xie C., Markesbery W.R., Lovell M.A., Increased oxidative damage in nuclear and mitochondrial DNA in Alzheimer's disease. *J Neurochem.,* 2005 May; 93(4): 953-62.

2. **Wang J.**, Markesbery W.R., Lovell M.A., Increased oxidative damage in nuclear and mitochondrial DNA in Mild Cognitive Impairment. *J Neurochem.,* 2006 Feb; 96(3):825-32

3. **Wang J.,** Lynn B.C., Markesbery W.R., Lovell M.A., Proteomic analysis of mitochondria in Alzheimer's disease. (in preparation)

4. **Wang J.**, Markesbery W.R., Lovell M.A., Increased oxidative damage in nuclear DNA in APP/PS1 transgenic mice. (in preparation)

5. Xie C., Xiong S., **Wang J.**, Smith J.L., Markesbery W.R., Lovell M.A., Huperzine A, an acetylcholinesterase inhibitor, protects primary hippocampal neurons against oxidative stress (Submitted to Free Radical Biology and Medicine)

6. Xiong S., Lovell M.A., Ashford J. W., Gorman L.S., Markesbery W.R., Xie C., **Wang J.**, Smith J.L., Gallicchio V.S, Lithium inhibits tau hyperphosphorylation mediated by glycogen synthase kinase 3 and protein phosphatase 2A in the hippocampus of eight week and 12 month old starved mice (in preparation)

Presentations:

1. **Wang J.**, Markesbery W.R., Lovell M.A., Increased oxidative damage in nuclear and mitochondrial DNA in Mild Cognitive Impairment. (Poster) 57th Pittsburg Conference on Analytical Chemistry and Applied Spectroscopy, Orlando, FL 2006

2. **Wang J.,** Xiong S., Xie C., Markesbery W.R., Lovell M.A., Increased oxidative damage in nuclear and mitochondrial DNA in Alzheimer's disease. (Poster) Society for Neuroscience, 35th Annual Meeting, San Diego, CA 2004

3. Xie C., Xiong S., **Wang J.**, Smith J.L., Markesbery W.R., Lovell M.A., Expression of Wilms' tumor (WT1) suppressor and caspase-3 in the isolated synaptosome from PS1 mutant knock-in mice following exposure to oxidative stresses. (Poster) Society for Neuroscience, 33th Annual Meeting, Orlando, FL 2002

4. Xiong S., Lovell M.A., Ashford J. W., Gorman L.S., Markesbery W.R., Xie C., **Wang J.**, Smith J.L., Gallicchio V.S, Lithium inhibits tau hyperphosphorylation mediated by glycogen synthase kinase 3 and protein phosphatase 2A in the hippocampus of eight week and 12 month old starved mice. (Book Chapter) *Macro and Trace Elements*, 2nd Volume, 2004, Page 1763-1799

Jianquan Wang

October 5, 2006